

# **Molecular Regulation of Life and Death Events During Plant Embryo Development**

Salim Hossain Reza

*Faculty of Natural Resources and Agricultural Sciences  
Department of Plant Biology  
Uppsala*

Doctoral thesis  
Swedish University of Agricultural Sciences  
Uppsala, 2017

Acta Universitatis agriculturae Sueciae  
2017:68

Cover: A schematic illustration of how subunits of the *Arabidopsis* cohesin complex might be arranged with cohesin loading complex

ISSN 1652-6880  
ISBN (print version) 978-91-7760-026-8  
ISBN (electronic version) 978-91-7760-027-5  
© 2017 Salim Hossain Reza, Uppsala  
Print: SLU Service/Repro, Uppsala 2017

# Molecular Regulation of Life and Death Events During Plant Embryo Development

## Abstract

The early plant embryo is divided into two domains with contrasting fates: apical embryo proper (in angiosperms) or embryonal mass (in gymnosperms) and basal suspensor. While apical domain is composed of proliferating cells and develops to plant, the suspensor consists of terminally-differentiated cells and functions as a conduit of growth factors to the growing apical domain followed by elimination through programmed cell death (PCD). The strict balance between cell division and PCD in the two domains is critical for correct embryo patterning and alteration of this balance can lead to lethality. The aim of this thesis was to identify and functionally characterize new molecular components participating in the regulation of cell division and death in plant embryo.

Cohesin is a multiprotein complex with important role in DNA replication and sister chromatid cohesion and separation. In non-plant species, cohesin is loaded on chromatin by the Scc2-Scc4 complex. *Arabidopsis thaliana* homologue of Scc4 (denoted AtSCC4) was identified and shown to form functional complex with AtSCC2. Knockout of *AtSCC4* induced inverse distribution of auxin response maxima in the embryos and ectopic cell division in the suspensor leading to developmental arrest and lethality. Split-nuclei iFRAP (inverse fluorescence recovery after photobleaching) assay revealed AtSCC2-independent immobilization of AtSCC4 on chromatin and critical requirement of AtSCC4 for nuclear immobilization of cohesin.

During anaphase, sister chromatid cohesion is released by evolutionary conserved protease separase (also called Extra Spindle Poles, ESP). Norway spruce (*Picea abies*) separase gene *PaESP* is highly expressed in the embryonal mass cells. *PaESP*-deficient embryos exhibited chromosome non-disjunction phenotype and perturbed anisotropic expansion of suspensor cells. Ectopic expression of PaESP could rescue chromosome non-disjunction phenotype of *Arabidopsis* ESP mutant (*rsw4*) but failed to rescue its root-swelling phenotype. This supports the notion of evolutionary conserved role of ESP in sister chromatid separation, but suggests that angiosperms and gymnosperms have evolved different molecular mechanisms of ESP-mediated regulation of cell expansion.

RNAseq analysis of transcriptomes of the Norway spruce embryo-suspensor *versus* embryonal mass established a set of potential regulators of suspensor PCD. Most of these regulators are conserved across various plant lineages and have been implicated in the control of developmental PCD in *Arabidopsis*. Interestingly, the suspensor cells showed transcriptional up-regulation of a key component of endoplasmic reticulum stress (ER)-induced PCD, PaBI-1 (*Picea abies* Bax inhibitor-1), suggesting that suspensor PCD may likewise implicate ER-stress. Silencing of *PaBI-1* induced necrotic cell death and abnormal suspensor phenotype leading to developmental arrest, thus establishing PaBI-1 as an indispensable component of the suspensor PCD.

**Keywords:** Cohesin loading, SCC4, cell division, auxin, separase, ESP, cell expansion, developmental PCD, RNAseq, Bax inhibitor-1.

**Author's address:** Salim Hossain Reza, SLU, Department of Plant Biology, P.O. Box 7080, 750 07 Uppsala, Sweden

## Molekylär reglering av liv och död under växtembryots utveckling

### Sammanfattning

Det tidiga växtembryot är uppdelat i två delar med olika öden: det apikala embryot ("apical embryo proper") (i angiospermer) eller embryonala embryot (i gymnospermer) och basala suspensorn. Medan den apikala delen består av växande celler som utvecklas till en planta, består suspensorn av differentierade celler som tillför tillväxtfaktorer till den växande apikala delen av embryot. När utvecklingen av embryot är färdig, avlägsnas suspensorn genom programmerad celldöd (PCD). Den strikta balansen mellan celldelning och PCD i de två delarna är kritisk för korrekt embryoutveckling, en störning kan vara dödlig. Målet med avhandlingen var att identifiera och funktionellt karakterisera nya molekyllära komponenter som deltar i reglering av celldelning och celldöd i växtembryot.

Kohesin är ett proteinkomplex med en viktig roll i DNA-replikation, kohesion och separation av systerkromatiderna. Inom andra arter utöver växter, är kohesin fäst till kromatin av Scc2-Scc4-komplexet. Homologen till Scc4 i *Arabidopsis thaliana*, AtSCC4, har identifierats och bildar ett funktionellt komplex med AtSCC2. Vid knockout av *AtSCC2* sker en omvänd distribuering av växthormonet auxin i embryona, vilket gör att suspensorn påbörjar celldelning och leder till en avbruten embryoutveckling och död. "Split-nuclei iFRAP" (inverse fluorescence recovery after photobleaching), visade att en AtSCC2-oberoende immobilisering av AtSCC4 på kromatin är nödvändig för den nukleära immobiliseringen av kohesin.

Separationen av systerkromatiderna under anafasen utförs av det evolutionärt bevarade "protease separase" (även kallat Extra Spindle Poles, ESP). Genen för separas, *PaESP*, i gran (*Picea abies*) är starkt uttryckt i cellerna i den embryonala massan. Otillräckligt uttryck av *PaESP* leder till embryon där kromosomerna inte delar sig och rubbad anisotropisk expanderings av suspensorcellerna. Ektopiskt uttryck av *PaESP* kunde upphäva kromosomernas ofullständiga separering i ESP-mutanter (*rsw4*) i *Arabidopsis* men hindrade inte den observerade fenotypen med uppsvällda rötter. Det här understödjer en evolutionärt välbevarad roll för ESP för separeringen av systerkromatiderna men föreslår att angiospermer och gymnospermer har utvecklat olika molekyllära mekanismer när det gäller ESP-förmedlad reglering av cellexpansion.

En RNAseq-analys av suspensorn *versus* den embryonala massan i granembryon fastställde en uppsättning av potentiella regulatoriska element av PCD i suspensorn. De flesta av dessa element är evolutionärt bevarade i flera växtfamiljer och har föreslagits delta i kontrollen av utvecklings-PCD i *Arabidopsis*. Intressant nog visade det sig att suspensorcellerna hade en transkriptionell uppreglering av en nyckelkomponent för stressinducerad PCD i det endoplasmatiska nätverket (ER), PaBI-1 (*Picea abies* Bax inhibitor-1) vilket föreslår att PCD i suspensorn lika gärna kan innebära stress i ER. Vid nedreglering av genen *PaBI-1* inducerades nekrotisk celldöd och en abnormal suspensorfenotyp vilket ledde till en avbruten utveckling som påvisar att PaBI-1 är nödvändig för PCD i suspensorn.

Nyckelord: Kohesion av systerkromatider, SCC4, celldelning, auxin, separase, ESP, cellexpansion, utvecklings-PCD, RNAseq, Bax inhibitor-1

*Author's address:* Salim Hossain Reza, SLU, Department of Plant Biology, P.O. Box 7080, 750 07 Uppsala, Sweden

## Dedication

To my beloved family (parents, brother, wife and son)



# Contents

<b>List of publications</b>	9
<b>1. Introduction</b>	11
1.1 Plant embryo development: balance of cell division and death	11
1.1.1 Development of <i>Arabidopsis</i> embryo: an angiosperm model	12
1.1.1.1 Developmental stages	12
1.1.1.2 Molecular regulation	13
1.1.2 Development of Norway spruce ( <i>Picea abies</i> ) embryo: a gymnosperm model	14
1.1.2.1 Developmental stages	14
1.1.2.2 Molecular regulation	16
1.2 Regulation of cell division	17
1.2.1 Cohesin	18
1.2.2 Loading of cohesin	18
1.2.3 Removal of cohesin	20
1.3 Regulation of programmed cell death	21
1.3.1 Regulation of developmental PCD	21
1.3.2 Norway spruce embryogenesis: a model system for developmental PCD	23
<b>2 Aims of this study</b>	25
<b>3 Results and Discussion</b>	27
3.1 AtSCC4 is required for cohesin loading and embryo development (Paper I)	27
3.1.1 Localization of AtSCC4	27
3.1.2 AtSCC4 is essential for embryonic cell fate determination	28
3.1.3 AtSCC4 and AtSCC2 act in same pathway	28
3.1.4 AtSCC4 is required for nuclear immobilization of cohesin	29
3.1.5 The role of AtSCC4 in post-embryonic development	29
3.2 <i>PaESP</i> controls cell expansion during Norway spruce embryo development (Paper II)	30
3.2.1 <i>PaESP</i> is required for cytoskeleton organization and cell division	30
3.2.2 <i>PaESP</i> is required for correct embryo patterning	30

3.3 RNA-seq analysis of embryonic domains in Norway spruce reveals new potential regulators of developmental cell death (Paper III)	31
3.3.1 Genes encoding flavonoid pathway enzymes are up-regulated in the EM	31
3.3.2 Genes related to cell differentiation and death are up-regulated in the suspensor	31
3.3.3 Cell-death components are largely conserved between angiosperms and gymnosperms	32
3.3.4 <i>PaBI-1</i> is involved in developmental PCD and embryo development	33
3.4 <i>Arabidopsis</i> metacaspases (unpublished experimental data not included in manuscripts)	33
3.4.1 Expression and localization analysis of <i>Arabidopsis</i> metacaspases	34
3.4.2 Single metacaspase knockout mutants exhibit low-frequency embryonic defects	34
3.4.3 <i>Arabidopsis</i> metacaspases may function redundantly in embryo development	35
3.4.4 Isolation of AtMC4 and AtMC5 interactors	35
<b>4. Conclusions</b>	<b>37</b>
<b>5. Future perspectives</b>	<b>39</b>
<b>References</b>	<b>41</b>
<b>Acknowledgements</b>	<b>47</b>

## List of publications

This thesis is based on the work contained in the following papers, referred to by Roman numerals in the text:

- I Panagiotis N. Moschou, Eugene I. Savenkov\*, Elena A. Minina\*, Kazutake Fukada\*, Salim Hossain Reza, Emilio Gutierrez-Beltran, Victoria Sanchez-Vera, Maria F. Suarez, Patrick J. Hussey, Andrei P. Smertenko and Peter V. Bozhkov (2016). EXTRA SPINDLE POLES (Separase) controls anisotropic cell expansion in Norway spruce (*Picea abies*) embryos independently of its role in anaphase progression. *New Phytologist*, 212, 232–243. \*These authors contributed equally.
- II Elena A. Minina\*, Salim Hossain Reza\*, Emilio Gutierrez-Beltran, Pernilla H. Elander, Peter V. Bozhkov and Panagiotis N. Moschou (2017). The Arabidopsis homolog of Scc4/MAU2 is essential for embryogenesis. *Journal of Cell Science*, 130, 1051-1063. \*The first two authors contributed equally.
- III Salim Hossain Reza\*, Nicolas Delhomme, Nathaniel R. Street, Prashanth Ramachandran, Ove Nilsson, Hannele Tuominen, Elena A. Minina and Peter V. Bozhkov. Transcriptome analysis of embryonic domains in Norway spruce reveals potential regulators of suspensor cell death (manuscript). \*Corresponding author.

Unpublished experimental data not included in manuscripts

- *Arabidopsis* metacaspases

Papers I and II are reproduced with the permission of the publishers.

The contribution Salim Hossain Reza to the papers included in this thesis was as follows:

- I. Planning, performing and data analysis of PaESP expression level in different spruce plant samples, somatic embryo domains and RNAi lines by qRT-PCR. Planning, performing and data analysis of CYCBL1, RBRL expression level in somatic embryo domains of PaESP RNAi lines by qRT-PCR.
- II. Initial discussion and planning, performing experiments, making some figures, reply to some reviewer comments with experiments and editing the text accordingly.
- III. Initial discussion and planning, sample preparation, data analysis except initial bioinformatics analysis of RNAseq raw data, performed all cloning and constructs preparation, all wet lab experiments, writing manuscript.

Unpublished experimental data not included in manuscripts

- *Arabidopsis* metacaspases: Highly involved in initial discussion and planning, metacaspase expression study; phenotyping of metacaspase knockout plants; constructs design, cloning and transformation of metacaspase RNAi; TAP-tag purification of metacaspase and sample preparation for mass spectroscopy, cloning of metacaspase interactors, COIP, localization study, wet lab experiments, compiling the results in written form.

# 1 Introduction

Most of the plants continue their life from one generation to next through producing seeds. Embryo forms within the seed and gives rise to the next plant generation upon germination. With the advancement of plant biotechnology, somatic embryos can be produced in laboratory in commercial scale for mass clonal propagation. Strict coordination of cell division and death is a prerequisite for successful embryo development both *in situ* and in laboratory conditions (Bozhkov et al., 2005a) and a failure to control this balance may affect embryo pattern formation, plant morphology and fitness. Our knowledge about regulation of cell division and death during plant embryogenesis is still scarce, especially in comparison with animal embryogenesis. This knowledge is however crucial for both mechanistic understanding of the precision of the earliest events in plant pattern formation, and biotechnological applications of plant embryos. This thesis highlights some of the molecular components that participate in the regulation of cell division and cell death during plant embryogenesis.

## 1.1 Plant embryo development: balance of cell division and death

Embryogenesis, the beginning of eukaryotic life starts with the fusion of egg cell with a sperm cell to form the zygote. In plants, the body axes and the body plan are already specified by establishment of apical-basal axis of the zygote, followed by establishment of radial axis and bilateral symmetry (De Smet et al., 2010). In both angiosperm and gymnosperm plants, asymmetric division perpendicular to the future apical-basal axis generates a small embryonic apical cell and a large extra-embryonic basal cell, giving rise to two structurally and functionally distinct domains: apical embryo proper (in angiosperms) or embryonal mass (EM, in gymnosperms) and basal suspensor, respectively (Smertenko and Bozhkov, 2014). Establishment of apical-basal polarity requires asymmetric distribution of auxin, which is in turn dictated by PIN proteins (Weijers et al., 2005).

Somatic embryogenesis is a process whereupon multiple genetically identical embryos develop from haploid or diploid cells without fusion of gametes (Williams and Maheswaran, 1986). The process begins with asymmetric distribution of auxin (De Smet et al., 2010) and both in angiosperms and gymnosperms and similar to zygotic embryogenesis, asymmetric cell divisions produce apical embryo proper or EM and basal suspensor (Smertenko and Bozhkov, 2014).

While the apical domain of the embryo develops to plant, the suspensor functions as a conduit of growth factors and nutrients to the apical domain and is gradually eliminated through programmed cell death (PCD) at later stages of embryogenesis. The balance between the cell division and death fates of two domains is crucial (Smertenko and Bozhkov, 2014) and alterations lead to embryo pattern abnormality and sometimes lethality. It has been shown that *Arabidopsis* embryo suspensor can also make embryo upon laser ablation of embryo proper and this potential of the suspensor is generally inhibited by the embryo proper (Liu et al., 2015). In *Arabidopsis Tween (twn)* mutants, secondary embryo proper is produced from the suspensor accompanied by impaired development of the primary embryo leading to formation of multiple seedlings with slow growth (reviewed in Bozhkov et al., 2005a). Some *Arabidopsis* embryo suspensor mutants e.g., *vcll* and *raspberry* show abnormal division pattern and increased proliferation of suspensor cells culminating in embryo lethality (reviewed in Bozhkov et al., 2005a).

Contrasting fates of the embryonic and suspensor cells provide opportunity to use them as a model system to study molecular regulation of pro-life and pro-death signalling. Our understanding of molecular mechanisms regulating embryogenesis, especially the balance between cell proliferation and death has, in large part, been gained from two model species: angiosperm *Arabidopsis thaliana* (Thale cress) and gymnosperm *Picea abies* (Norway spruce).

### 1.1.1 Development of *Arabidopsis* embryo: an angiosperm model

#### 1.1.1.1 Developmental stages

Angiosperm embryogenesis begins with double fertilization during which one sperm nucleus fuses with the egg cell to produce the zygote while the second sperm nucleus fuses with the central cell to form the endosperm (Russell, 1992). The latter functions as nutrient reservoir required for germination. Zygotic embryogenesis in angiosperms e.g., *Arabidopsis* can be divided into three main phases: postfertilization-proembryogeny, globular-heart transition and organ expansion and maturation (Goldberg et al., 1994) (Figure 1A).

Postfertilization-proembryogenesis in *Arabidopsis* includes zygote to octant stages of the developing embryo. During proembryogenesis, the zygote

elongates and divides asymmetrically, perpendicular to the future apical-basal axis to form small apical daughter cell and a large basal daughter cell (ten Hove et al., 2015). Two longitudinal divisions of the apical daughter cell forms tetrad and a transverse division of the tetrad cells creates octant stage of the embryo proper (ten Hove et al., 2015).

Dermatogen embryo proper is formed by tangential division of the octant cells, giving rise to the epidermis precursor, the protoderm, and the ground and vascular tissue precursor, the inner tissues. Anticlinal division of the protoderm cells and longitudinal division of the inner cells leads to the early globular stage embryo proper (ten Hove et al., 2015). During the late globular stage, hypophysis is formed from the uppermost suspensor cell, which upon asymmetric division generates a small upper lens-shaped cell, the origin of future root meristem quiescent center, and a large basal cell, the origin of columella stem cell of root meristem (De Smet et al., 2010, ten Hove et al., 2015). Continued cell division at different division planes shifts the morphological symmetry from radial to bilateral during the transition from late globular to heart stage of embryo development. During the heart stage, cotyledons start to grow out along with the initiation of shoot- (SAM) and root apical meristem (RAM).

During the torpedo stage, the cotyledons are fully grown and by the bent cotyledon stage, the embryo is mature and ready to germinate into a new plant.

#### 1.1.1.2 Molecular regulation

After fertilization, the *Arabidopsis* zygote is elongated through *YODA* (*YDA*) signaling pathway (Lukowitz et al., 2004). *YDA* encodes a mitogen-activated protein kinase kinase (MAPKK), which is activated by a paternally delivered receptor like kinase SHORT SUSPENSOR (SSP) (Bayer et al., 2009). A zinc finger transcription factor encoded by *WRKY2* gene repolarizes the nucleus from mid to apical zone of the elongated zygote. *WRKY2* increases the expression level of *WUSCHEL-RELATED HOMEODOMAIN* genes *WOX8/9* in the basal part of the elongated zygote (Ueda et al., 2011), which in turn increases the expression of *WOX2* in the apical zone. Together with RKD4 protein encoded by *GROUNDING* (*GRD*), *WOX8/9* redundantly regulate the first asymmetric division of the zygote (Wendrich and Weijers, 2013). *WOX2* has been implicated in *Arabidopsis* embryo protoderm development (Breuninger et al., 2008).

During embryo development at 2/4 cell and octant stage, the suspensor identity is maintained by several AUXIN RESPONSIVE FACTORS (ARFs) (Guilfoyle and Hagen, 2007). The basal boundary between embryo proper and suspensor during octant stage is maintained by GATA transcription repressor encoded by *HANABA TARANU* (*HAN*) gene (Nawy et al., 2010).

During early globular stage, specification of the uppermost suspensor cell as

hypophysis is regulated by expression of *MONOPTEROS* (*MP*) or *ARF5* gene and by movement of TARGET OF MONOPTEROS 7 (*TMO7*) transcription factor from the basal inner cell of proembryo to the upper suspensor cells (Schlereth et al., 2010). *CLASS THREE HOMEODOMAIN-LEUCINE ZIPPER* genes (*HD\_ZIP III*) regulate the shoot apical identity, whereas genes *PLT1* and *PLT2* encoding PLETHORA (*PLT*) transcription factors regulate the root meristem specification of the early globular embryo (Galinha et al., 2007). *HD\_ZIP III* and *PLT* repress one another to maintain the specificity of the apical meristems in the early globular proembryo (Wendrich and Weijers, 2013). *SQUAMOSA PROMOTER BINDING PROTEIN-LIKE 10* (*SPL10*) and *11* (*SPL11*) are involved in the transition from early globular to late globular stage (Wendrich and Weijers, 2013).

Auxin signalling is crucial for embryo patterning (Wendrich and Weijers, 2013). In *Arabidopsis*, auxin binding protein 1 (*ABP1*) has been shown to be involved in cell elongation and thus, transition from globular to bilateral symmetrical heart stage embryo. A T-DNA insertion mutant of *ABP1* showed developmental arrest at early globular stage, with aberrant cell division pattern in both embryo proper and suspensor leading to embryo lethality (Chen et al., 2001). *PIN FORMED* (*PIN*) proteins play crucial role in polar auxin transport and thus embryo development. After the first asymmetric division, auxin is locally produced in the basal cell and *PIN7* mediates auxin flow towards the proembryo during early globular embryo development (ten Hove et al., 2015). *PIN1* mediates auxin flow from the early globular embryo to the hypophysis region of globular embryo and specifies the future RAM formation (ten Hove et al., 2015)

*Arabidopsis* embryo-suspensor is composed of a file of 6-9 cells containing large vacuoles. The furthest suspensor cell starts to die during the heart stage and the cell death progresses towards the upper suspensor cells during the following developmental stages (De Smet et al., 2010). According to GENEVESTIGATOR (Hruz et al., 2008), three metacaspase genes, *AtMC1*, *AtMC4* and *AtMC5* are highly expressed in the suspensor cells suggesting that they may control suspensor cell death individually or redundantly.

### 1.1.2 Development of Norway spruce (*Picea abies*) embryo: a gymnosperm model

#### 1.1.2.1 Developmental stages

Unlike zygotic embryogenesis of angiosperms, gymnosperms e.g., Norway spruce (*Picea abies*) embryogenesis starts with a single fertilization of the ovule. The developing zygote is surrounded by a haploid female gametophyte which has a nutritive function, analogous to that of endosperm. Conifer embryogenesis is divided in three main phases: proembryogeny, early embryogeny and late

embryogeny (Singh, 1978) (Figure 1B).

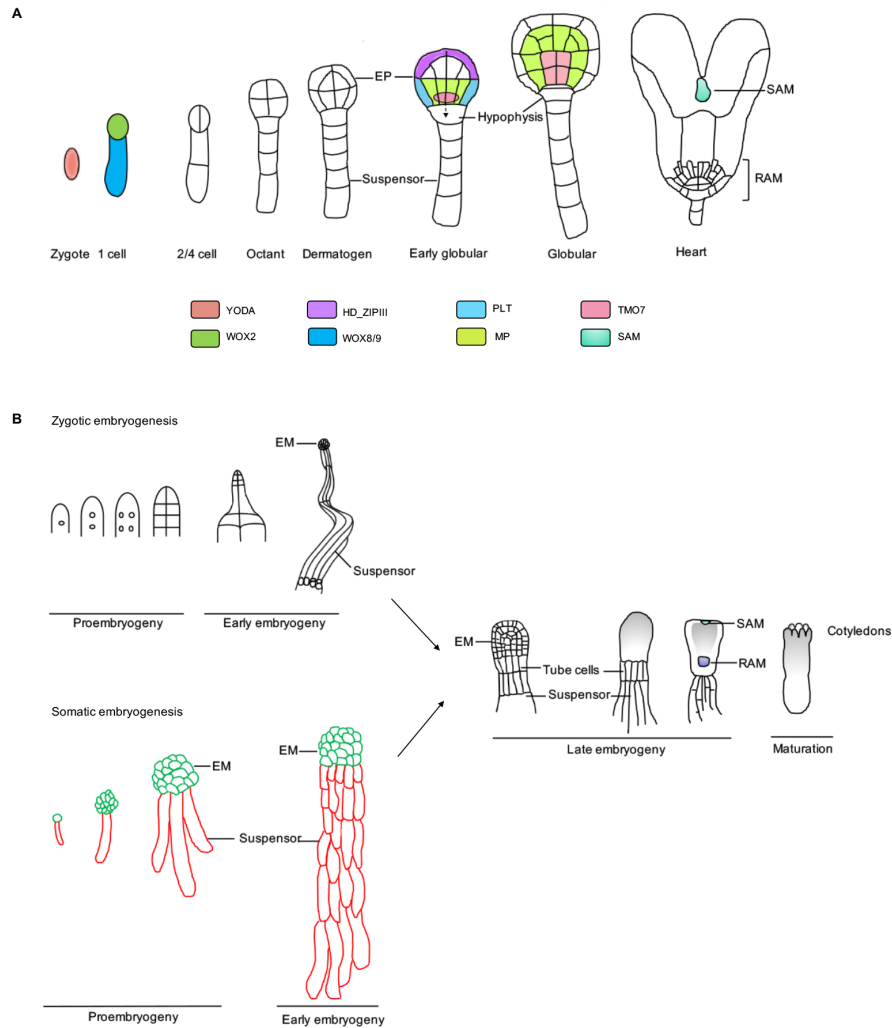


**Figure 1.** Embryogenesis in angiosperms and gymnosperms. (A) Schematic overview of *Arabidopsis thaliana* embryogenesis (modified from Wendrich and Weijers, 2013). Asymmetric division of zygote generates a small apical cell and a large basal cell giving rise to embryo proper (EP) and suspensor, respectively (Smertenko and Bozhkov, 2014). The embryo proper develops to plant, while the suspensor is eliminated by the heart stage through PCD. Expression domains of key regulatory genes are denoted by different colors. SAM, shoot apical meristem; RAM, root apical meristem. (B) Schematic overview of Norway spruce (*Picea abies*) zygotic and somatic embryogenesis (modified from Smertenko and Bozhkov, 2014). Spruce zygote undergoes a few rounds of free nuclear divisions before cellularization and formation of several tiers of cells. The upper tiers form embryonal mass (EM), while the lower tiers establish suspensor. In somatic embryogenesis pathway, specification of EM and suspensor during proembryogeny does not involve free-nuclear stage. Subsequent growth of suspensor during early and beginning of late embryogeny is brought about by the formation of new cell layers originating through asymmetric cell divisions within the proximal region of the EM. The first cell layer within the suspensor

adjacent to the EM is made of embryonal tube cells. Suspensor is eliminated by PCD during late embryogeny. Morphology of zygotic and somatic embryos is similar beginning from early embryogeny onwards. The embryo structures are not drawn to scale.

During the proembryogeny, the zygote undergoes several rounds of karyokinesis without cytokinesis leading to the formation of free-nuclear proembryo. The proembryo then undergoes cellularization and forms eight cells arranged in two tiers. Further cell divisions in these two tiers result in four tiers of cells of which first two tiers form the EM and the last two tiers form suspensor (Cairney and Pullman, 2007).

Early embryogeny starts with the elongation of the suspensor. The suspensor contains several files of elongated cells which are derived through cell divisions in the EM. The EM and suspensor are separated by a layer of cells called tube cells. Anticlinal and periclinal divisions of the outer layer of embryonal mass cells form a functional protoderm showing the first signs of histogenesis (Zhu et al., 2016a).

Both histogenesis and organogenesis occur during late embryogeny when SAM and RAM are specified followed by cotyledon formation (Zhu et al., 2016a). In the beginning of late embryogeny the suspensor cells undergo vacuolar PCD and are ultimately eliminated (Filonova et al., 2000).

Somatic embryogenesis of conifers differs from zygotic embryogenesis mainly during proembryogeny. In somatic embryos, polar structure is formed containing proliferating cells and large vacuolated non-proliferating cells at two opposite poles. Suspensor is formed from the vacuolated cells and ultimately dies during embryo maturation, whereas the cotyledonary embryo is produced from the EM through stereotyped sequence of events similar to zygotic embryogenesis (Smertenko and Bozhkov, 2014).

Large size of Norway spruce embryos and especially several millimeter-long suspensors (as compared to e.g. *Arabidopsis* where suspensor is composed of a single file of 6-9 small cells), availability of unlimited number of somatic embryos at specific developmental stage with identical genetic background make somatic embryos of Norway spruce a powerful model system for studying regulation of cell division and death.

#### 1.1.2.2 Molecular regulation

Our knowledge about molecular regulation of gymnosperm embryo development and pattern formation is limited (Cairney and Pullman, 2007) in comparison to angiosperm embryogenesis and has slowly started to enrich with recent discoveries.

Polar auxin transport from suspensor to EM is crucial for maintaining the suspensor cell fate and apical-basal pattern formation of spruce embryos (Larsson et al., 2008a). In particular, polar auxin transport mediates expression of two KNOTTED1-like homeobox (KNOX) genes, *PaHBK2* and *PaHBK4*, involved in SAM formation during early embryogeny (Larsson et al., 2012a) and spruce homologue of *Arabidopsis* CUC (*CUP-SHAPED COTYLEDON*) gene, *PaNAC01* suggested to be involved in the differentiation of cotyledons (Larsson et al., 2012b).

During differentiation, the suspensor cells in Norway spruce embryos elongate and anisotropically expand with simultaneous growth of lytic vacuoles and become committed to PCD. In loblolly pine, it has been suggested that suspensor specific expression of an aquaglyceroporin encoding gene *PtNIP1:1* may help to elongate and expand the cells upon increasing solute transportation during early embryogeny (Ciavatta et al., 2001, Ciavatta et al., 2002). In Norway spruce, a type II metacaspase *mclI-Pa* (Suarez et al., 2004, Bozhkov et al., 2005b) and autophagy-related genes (Minina et al., 2013) are required for developmental PCD of the embryo-suspensor and deficiency of either the metacaspase or autophagy blocks embryo development (Minina et al., 2013).

Protoderm formation is the earliest event during radial patterning of conifer embryos and several genes play role in this differentiation process, some of which start functioning during early embryogeny. In Norway spruce, high level of *PaWOX2* expression has been observed in the EM and upper part of the suspensor at the early embryogeny and at the beginning of late embryogeny (Zhu et al., 2016a). RNA interference (RNAi) lines of *PaWOX2* do not form distinct border between EM and suspensor and exhibit aberrant protoderm layer as well as suppressed elongation of suspensor cells at early embryogeny (Zhu et al., 2016a). Down-regulation of *PaWOX8/9* changes the cell division plane from transverse to periclinal or inclined during early stages of spruce somatic embryo development leading to abnormal pattern formation during embryo maturation (Zhu et al., 2016b). *Picea abies* HOMEBOX 1 (*PaHB1*) has been shown to regulate differentiation of outer cell layer in the EM during spruce somatic embryo protoderm development (Ingouff et al., 2001). During late embryogeny, *Picea abies* HOMEBOX 2 (*PaHB2*) expression is restricted to cortical cell layers (Ingouff et al., 2003). Expression of lipid transfer proteins (LTPs) coding genes must be restricted to the protodermal cells for normal spruce embryo development (Sabala et al., 2000). During white spruce (*Picea glauca*) embryo development, an Argonaut family member gene *PgAGO* is required for proper shoot and root meristem differentiation (Tahir et al., 2006).

## 1.2 Regulation of cell division

Life cycle of actively dividing eukaryotic cells is divided into G1, S, G2 and M phases. G1 and G2 are the two gap phases between the DNA synthesis S phase

and division M phase, when cell divides its nucleus and cytoplasm between two daughter cells. The immediate stage after cell division is G1 phase during which the cell is metabolically active and prepares itself for DNA replication in S phase. After completion of DNA replication, the cell passes through comparatively short G2 phase during which the cell prepares for division and corrects any possible error of DNA that happened during replication. G1, S and G2 phases are collectively called interphase (O'Connor, 2008).

The cell division phase (M) is of two types: mitosis and meiosis. During each mitotic division, the cell divides once to produce diploid (containing two copies of each chromosome) daughter cells which are genetically identical to mother cell. While mitosis produces somatic cells for growth, meiosis takes place during formation of germ (male or female gamete) cells in reproductive organs. During meiosis, the cells divide twice to form four haploid (containing one copy of each chromosome) daughter cells which are genetically different from parent cell and each other and containing half of the number of parental cell chromosomes (O'Connor, 2008).

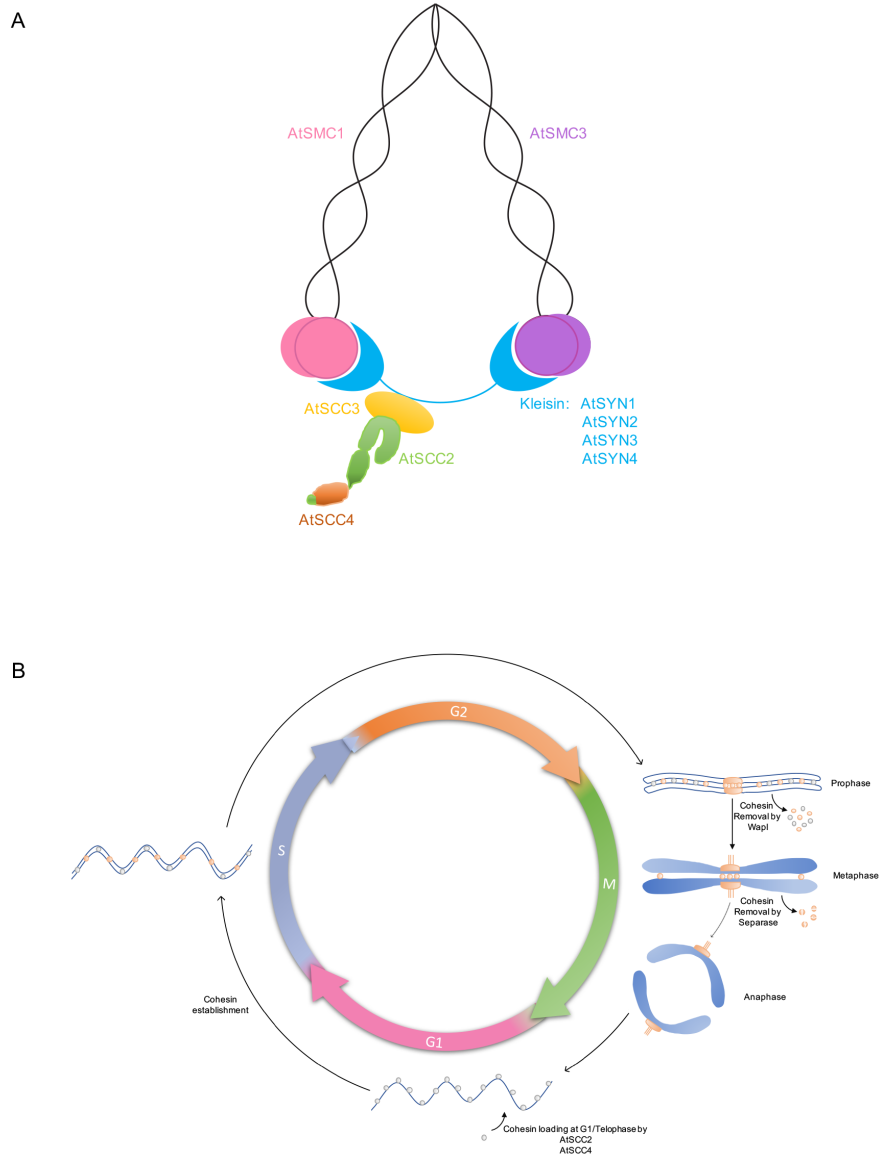
### 1.2.1 Cohesin

Proper replication of DNA, sister chromatid cohesion and their controlled separation to the next generation during cell division is crucial to maintain the genetic homeostasis of any organism, and a multiprotein complex cohesin plays vital role in these processes. Cohesin forms a large ring-like structure to encircle DNA and consists of four subunits: two structural maintenance of chromosome protein 1 (SMC1) and 3 (SMC3), sister chromatid cohesion 3 (SCC3) and a kleisin subunit (Figure 2A). SMC proteins are long helical polypeptides that form antiparallel coiled-coil structure upon folding back on themselves. SMC1 and SMC3 form a V shaped structure through heterodimerization. Both the N- and C-terminal domains of SMC proteins together form nucleotide binding domains (NBD) that can bind the kleisin subunit to close the V shape and form a ring (Gligoris and Lowe, 2016). Cohesin binds the sister chromatids in the chromosome arms and in the centromere.

### 1.2.2 Loading of cohesin

Although cohesin is loaded on the chromosome throughout the entire cell cycle, most of this event happens during the telophase/G1 phase and cohesin-chromatin binding is dynamic prior to S phase (De et al., 2014). In non-plant species e.g., *Homo sapiens*, *Xenopus*, *Drosophila melanogaster* and *Saccharomyces cerevisiae*, it has been shown that cohesin is loaded on chromosome through SCC2/SCC4 complex (Figure 2A). This complex is composed of three domains: a globular head domain, a central body and a hook-like tail domain. The N-terminus of SCC2 is entrapped into a SCC4 superhelix core to make the globular head domain. The C-terminus of SCC2 forms the body and hook like-structure

domains. The head domain is believed to bind chromatin receptors, whereas the hook captures the hinge and head spanning cohesin ring upon extended to compact conformational changes, and ATP binding to NBD may open the cohesin ring and entraps the DNA. The SCC2/SCC4 complex is released upon NBD-dependent hydrolysis of ATP (Chao et al., 2015).



Defective cohesin loading has been found to result in developmental abnormalities in various organisms (Barbero, 2013). Mutation in the Arabidopsis *Scc2* gene (*AtSCC2*) caused early embryo lethality and giant endosperm formation. Embryos of the 25% seeds in the siliques of heterozygous *AtSCC2* mutant showed suspensor abnormality with enlarged cell size or multiple nuclei in one cell, abnormal cell division plane and sometimes double files of cells. Thus, the balance of cell division and death was disturbed which led to embryonal growth arrest at pre- or early globular stages (Sebastian et al., 2009). Human and yeast SCC4 and its *Caenorhabditis elegans* ortholog MAU-2 are required for association of cohesin with chromatin and sister chromatid cohesion. HeLa cells depleted of human SCC4 lost sister chromatid cohesion precociously and arrested at prometaphase with misaligned chromosomes (Watrín et al., 2006). The function of SCC4 in plants remained unknown and was addressed in Paper I.

### 1.2.3 Removal of cohesin

Cohesin is released from the sister chromatid arms by a protein complex composed of WAPL (wings apart-like protein), PDS5 (Precocious dissociation of sisters 5) and SCC3. In *Arabidopsis*, *WAPL* mutant showed chromosome bridges and uneven segregation in meiotic cells leading to male and female sterility (De et al., 2014). Altered plane of suspensor cell division and suspensor cell number at the preglobular and early globular stages coupled with uncontrolled division of the hypophysis cell observed in *Arabidopsis wapl1-wapl2* embryos resulted in developmental delay or embryonal arrest (De et al., 2014).

During anaphase, the centromeric cohesion is released by the enzyme separase (or Extra Spindle Pole, ESP) (Figure 2B). Mitotic kinase keeps the separase inactive upon phosphorylation. Inactivation of mitotic kinase and degradation of separase inhibitor securin leads to activation of separase during the metaphase-anaphase transition (Rankin, 2015). Active separase cleaves the kleisin subunit and opens the cohesin ring to release the sister chromatids (De et al., 2014). Due to obligatory role of separase in anaphase, its absence leads to abnormalities in different organisms. In *Arabidopsis*, a T-DNA insertion mutant of separase showed embryo lethality and a RNAi line showed defective SYN1 removal (one of the four kleisin subunits in *Arabidopsis*) during meiosis (Liu and Makaroff, 2006). At restrictive temperature (~30°C), a temperature-dependent separase mutant *RADIALLY SWOLLEN 4 (rsw4)* showed chromosome non-disjunction phenotype with disruption of radial microtubule in the male meiocytes (Yang et al., 2011) and accumulation of mitosis-specific Cyclin B1;1 and disorganized microtubules in the roots (Wu et al., 2010). Recently, the role for *Arabidopsis* separase in the establishment of cell polarity has also been established (Moschou et al., 2016, Moschou et al., 2013). We wondered whether dual function of separase is conserved between angiosperms

and gymnosperms, and used Norway spruce embryos to address this question (Paper II).

### 1.3 Regulation of programmed cell death

Apoptosis (Kerr et al., 1972) and other types of PCD are processes of removing unwanted or abnormal cells from multicellular organism in controlled manner for physiological and cytoprotective purposes. During apoptosis, various extrinsic and intrinsic factors trigger cascade of energy-dependent molecular events to activate the initiator caspase enzymes (caspase-8, caspase-9 and caspase-10). The initiator caspases, in turn, activate the executioner caspases 3, 6 and 7 (Elmore, 2007, Taylor et al., 2008). The executioner caspases in turn activate cytoplasmic endonucleases and proteases to degrade chromosomal DNA and nuclear and cytoskeletal proteins, respectively, resulting in chromatin and cytoplasmic condensation, nuclear fragmentation, cytoskeletal reorganization and formation of apoptotic bodies (Elmore, 2007; Taylor et al., 2008). The apoptotic bodies are engulfed by phagocytic cells upon binding of the phagocytic cells receptors to apoptotic body expressed ligands (Elmore, 2007, Taylor et al., 2008).

The molecular regulation, physiological roles and morphology of plant PCD differs markedly from animal PCD. Plant cells are immobile and plant genomes do not contain genes encoding key components of the animal apoptotic machinery, including caspases and Bcl-2 family proteins (Ishikawa et al., 2011). The morphologies of plant cell disassembly during PCD differ from that of animal apoptosis and are classified into two broad classes: vacuolar cell death and necrosis (van Doorn et al., 2011). During vacuolar cell death, the cell contents are gradually removed by a combination of autophagy and vacuolar collapse (van Doorn et al., 2011). Necrosis is characterized by mitochondrial dysfunction, early rupture of plasma membrane, shrinkage of the protoplast and incomplete removal of cell contents (van Doorn et al., 2011). Vacuolar cell death is common during tissue and organ patterning, whereas necrosis is typically found under abiotic stress. Hypersensitive response (HR)-related cell death in response to biotrophic pathogens expresses features of both necrosis and vacuolar cell death (van Doorn et al., 2011). According to this classification, most examples of developmental PCD in plants belong to a class of vacuolar cell death.

#### 1.3.1 Regulation of developmental PCD

PCD has been implicated in different processes of reproductive and vegetative development of plants (Daneva et al., 2016). The molecular regulation of plant PCD may be described in four main phases: preparation, initiation, execution and post mortem cell clearance (Huysmans et al., 2017, Van Durme and Nowack, 2016).

Upon hormonal signalling e.g., jasmonic acid, ethylene, auxin and strigolactones, the plants prepare transcriptionally for PCD through expression of specific transcription factors (TFs) (Huysmans et al., 2017, Van Durme and Nowack, 2016). In *Arabidopsis*, a NAC domain containing TF ANAC075 binds to VND7 promoter and regulates xylem differentiation and PCD (Endo et al., 2015). Another NAC TF SMB promotes *Arabidopsis* root cap differentiation and PCD (Fendrych et al., 2014).

During initiation of PCD, ethylene, reactive oxygen species (ROS) and calcium flux may work as PCD trigger in cells of different plant tissues (Van Durme and Nowack, 2016). Ethylene signaling has been implicated in PCD responsible for leaf perforation of lace plant, elimination of synergid cells and pollen tube rupture in *Arabidopsis* and xylem differentiation and death in *Zinnia elegans* (reviewed in Huysmans et al., 2017, Van Durme and Nowack, 2016). Calcium signalling has been implicated in self-incompatible *Papaver* pollen tube PCD (Bosch and Franklin-Tong, 2008), *FERONIA (FER)* signaling-dependent death of pollen tube and one synergid cell of *Arabidopsis* (Ngo et al., 2014) and secondary cell wall synthesis in *Zinnia* culture (reviewed in Van Durme and Nowack, 2016). Reactive oxygen species (ROS) induce membrane leakage and thus PCD and has been implicated in pollen tube degradation in self-incompatible *Papaver* (Bosch and Franklin-Tong, 2008) and pollen tube burst in *Arabidopsis* (Duan et al., 2014).

Several hydrolytic enzymes including proteases and nucleases are involved in the execution and post mortem cell clearance during developmental PCD. In *Arabidopsis*, a type II metacaspase AtMC9, XYLEM CYSTEINE PEPTIDASE 1 (XCP1) and 2 (XCP2) are involved in post mortem clearance of root xylem cell contents (Bollhoner et al., 2013). Cathepsin H-like protease NtCP14 has been shown to be involved in *Nicotiana tabacum* embryo-suspensor death (Zhao et al., 2013). CYSTEINE ENDOPEPTIDASE 1 (CEP1) is involved in tapetal PCD in *Arabidopsis* (Zhang et al., 2014). Beside cysteine proteases, PLANT ASPARTIC PROTEASE A3 (PASPA3) expression level rises during *Arabidopsis* lateral root cap death (Fendrych et al., 2014). At the final stage of PCD execution, nuclear membrane is dismantled and DNA is fragmented. In *Arabidopsis*, a S1-P1 type nuclease BIFUNCTIONAL NUCLEASE 1 (BFN1) is involved in DNA degradation during lateral root cap cell death (Fendrych et al., 2014). A S1-type nuclease *Zinnia* endonuclease 1 (ZEN1) is involved in degradation of DNA during PCD associated with tracheary element formation (Ito and Fukuda, 2002).

### 1.3.2 Norway spruce embryogenesis: a model system for developmental PCD

The terminal differentiation and elimination of the embryo-suspensor is the earliest manifestation of PCD in plant life. In Norway spruce, the embryo-suspensor is composed of several layers of terminally differentiated cells, originating from asymmetric cell divisions in the EM. Suspensor cells do not divide but instead become committed to PCD as soon as they are produced. While the cells in the upper layer of the suspensor (i.e. adjacent to the embryonal mass) are in the commitment phase of PCD, the cells in the lower layers exhibit a gradient of successive stages of vacuolar cell death towards the basal end of the suspensor where hollow walled cell corpses are located (Figure 3). Thus, successive cell-death processes can be observed simultaneously in a single embryo. Moreover, the position of the cell within the embryo can be used as a marker of stage of vacuolar cell death (Bozhkov PV, 2005a). This PCD process is characterized by the reorganization of actin cytoskeleton, breakdown of microtubules, growth of lytic vacuoles, tonoplast rupture and DNA fragmentation (Smertenko et al., 2003). Type II metacaspase mcII-Pa and autophagy are essential for suspensor cell degradation in Norway spruce (Bozhkov et al., 2005b), and their downregulation leads to switch from vacuolar cell death to necrosis and defective embryo patterning. Apart from the sequence of cell disassembly events and the role of mcII-Pa and autophagy, molecular regulation of Norway spruce embryo-suspensor PCD remains largely unknown and has been addressed in Paper III.

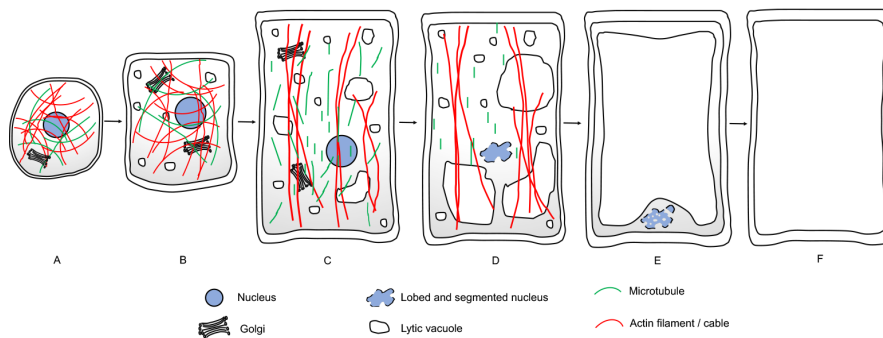


*Figure 3.* Schematic model of a gradient of successive stages of suspensor PCD in Norway spruce embryos. A living EM cell (stage A) divides to form two daughter cells: one cell remains within EM (not shown), whereas its sister cell becomes terminally-differentiated embryonal tube cell (stage B) incorporated to the first layer of the suspensor. The embryonal tube cell commits to vacuolar PCD and undergoes a series of stereotypical morphological alterations (stages C-E), leading to complete clearance of all cellular content by stage F. Successive stages of vacuolar PCD can thus be observed simultaneously along the apical-basal axis of the early embryo, with each cell layer of the suspensor featuring one stage of PCD (modified after Bozhkov et al., 2005a).



## 2 Aims of this study

Plant embryos contain two structurally and functionally distinct domains: the living apical embryo proper (in angiosperms) or embryonal mass (EM, in gymnosperms) and the dying basal suspensor. Alteration of the balance between the cell division and death fates of two embryonic domains leads to embryo pattern abnormalities and sometimes lethality. The overall goal of this thesis was to establish molecular regulators of cell division and cell death operating in two distinct domains of plant embryos and to elucidate their functional roles during embryogenesis, using *Arabidopsis* and Norway spruce embryos as model systems.

The following specific aims were addressed:

- Identify plant homologue of *Scd4/MAU2* and examine its function in cell division and embryo development.
- Investigate requirement of gymnosperm separase in cell division and embryo development.
- Compare transcriptomes of Norway spruce embryo-suspensor *versus* embryonal mass and identify new potential regulators of developmental cell death.
- Investigate whether *BI-1* is required for developmental cell death and embryo development.



## 3 Results and Discussion

### 3.1 AtSCC4 is required for cohesin loading and embryo development (Paper I)

BLASTP search for the presence of human Scc4 (HsMau2) homologue(s) in *Arabidopsis* genome revealed a single gene (At5g51340) showing 78% and 24% query coverage and identity, respectively. The *Arabidopsis Scc4* (*AtSCC4*) encodes a putative protein of 726 amino acids containing two typical tetratricopeptide repeats (TPR) arranged in tandem order between amino acids 525 and 600, within a predicted structural motif TPR 12 (pfam 13424, (Marchler-Bauer et al., 2015). Phylogenetic analysis revealed a separate clade for plant Scc4 orthologues with high divergence. However, significant similarity of secondary structure and conservation of tertiary structure among plant Scc4 orthologues suggests trans-kingdom conservation of their role in cohesin loading onto chromatin. In this study, we have characterized AtSCC4 subunit of plant cohesin loading complex and demonstrated its function in cell fate and pattern determination during plant embryo development.

#### 3.1.1 Localization of AtSCC4

Using GUS ( $\beta$ -glucuronidase) staining, we have observed *AtSCC4* expression in both meristematic and non-meristematic cells of *Arabidopsis* plant. Using AtSCC4-GFP fusion protein under the control of *AtSCC4* native promoter, we have observed the localization of AtSCC4 in the cytoplasm during prometaphase, metaphase, anaphase and telophase stages of cell division. The AtSCC4-GFP signal disappears from nuclei during prometaphase and returns during late telophase. We used split-nuclei iFRAP (inverse fluorescence recovery after photobleaching) to demonstrate that AtSCC4 stably localizes in the nucleus during interphase, most probably by forming a cohesin-loading complex that recruits AtSCC4 to immobilize on chromatin (Lopez-Serra et al., 2014).

### 3.1.2 AtSCC4 is essential for embryonic cell fate determination

We did not observe any obvious growth phenotype in plants heterozygous for two separate T-DNA insertion alleles *Atsc4-1* and *Atsc4-2* and the level of *AtSCC4* mRNA was similar to that of wild type. However, we have found that ca. 25% seeds of the *Atsc4-1/AtSCC4* and *Atsc4-2/AtSCC4* plants were aborted, leading to 1:2:0 (wild-type: heterozygous: homozygous) segregation pattern for the *Atsc4* T-DNA insertion, suggesting that *AtSCC4* disruption leads to embryo lethality. Using DIC microscopy of the *Atsc4/Atsc4* embryos from the *Atsc4/AtSCC4* plants, we have observed that the embryo proper of the mutant embryos displayed unsynchronized cell division at octant stage, loss of bilateral symmetry and signs of deterioration at heart stage. The division pattern of the suspensor cells of the *Atsc4/Atsc4* embryos was also changed, leading to formation of supernumerary cells and sometimes raspberry-like phenotype (Yadegari et al., 1994). Introduction of auxin response maxima reporter Dr5rev::3xVENUS-N7 (Heisler et al., 2005) in the *Atsc4/AtSCC4* lines has revealed that the ectopic cell division pattern in the suspensor of *Atsc4/Atsc4* embryos coincided with the shift of localization of auxin response maxima towards basal part of the suspensor.

### 3.1.3 AtSCC4 and AtSCC2 act in same pathway

In animal and yeast cells, Scc2 and Scc4 form a complex where the N terminus of Scc2 is entrapped into a Scc4 superhelix core (Chao et al., 2015). Using yeast two-hybrid assay and co-immunoprecipitation, we have shown that AtSCC4 interacts with the N-terminus of AtSCC2 in yeast and plant, respectively. Split-nuclei iFRAP assay of WT and AtSCC2-depleted embryos expressing AtSCC4-GFP has demonstrated that the physical interaction between AtSCC4 and AtSCC2 is not required for immobilization of AtSCC4 in the nuclei.

Interestingly, while the phenotype of *Atsc4* embryos recapitulated that of *Atsc2* embryos, we did not observe any gross phenotype, including formation of giant nuclei in the *Atsc4* endosperm, which is however typical for *Atsc2* endosperm (Sebastian et al., 2009). This observation points to different roles that individual components of AtSCC2-AtSCC4 complex might play in endosperm development. In contrast to the situation in the endosperm, similarities of the embryo phenotype suggest that AtSCC2 and AtSCC4 act in the same pathway during embryonic pattern formation. This notion was further supported by 9:7 segregation pattern of the number of viable seeds vs number of aborted seeds observed in double heterozygous *Atsc2/AtSCC2;Atsc4/AtSCC4* plants and that the double mutation does not exert any additive effect on the embryo phenotype.

### 3.1.4 AtSCC4 is required for nuclear immobilization of cohesin

We have established an *in vivo* live cell imaging assay of cohesin loading onto chromatin using TagRFP fused SYN4 (one of the four *Arabidopsis* kleisin subunits) driven under a weak embryo-specific promoter *ABI3* (ABA insensitive 3) (Devic et al., 1996). We observed that TagRFP-SYN4 colocalized with plant chromatin during interphase, was removed by metaphase during cell division and colocalized again with chromatin at late telophase. Using split-nuclei iFRAP assay of WT and *Atscc4/AtSCC4* plants expressing *pABI3::TagRFP-SYN4*, we have found that AtSCC4 is required for chromatin immobilization of SYN4 and thus cohesin loading onto interphase nuclei in octant to globular stage embryos.

### 3.1.5 The role of AtSCC4 in post-embryonic development

Using GUS staining, we have observed that *AtSCC4* promoter is active in all tissues examined, indicating the possible function of *AtSCC4* throughout the whole plant. Using T-DNA insertion lines we have revealed that AtSCC4 is essential for embryonic cell fate determination and embryo pattern formation. As *Atscc4/Atscc4* embryos are not viable, we could not study the role of *AtSCC4* in post-embryonic development. To overcome this problem, we have used constitutive and  $\beta$ -estradiol inducible *AtSCC4*-RNAi lines. The RNAi lines showed up to 50% decrease of *AtASCC4* mRNA level, but no apparent phenotype during reproductive development and vegetative growth, indicating that 50% expression level of *AtSCC4* is sufficient for normal plant development. We have also attempted to silence the *AtSCC4* by Tobacco Rattle Virus (TRV)-based VIGS (virus induced gene silencing). VIGS is a rapid method of gene silencing by-passing development of stable transformants which might otherwise show lethal phenotype (Burch-Smith et al., 2004). However, VIGS-mediated silencing of *AtASCC4*, again, failed to furnish any consistent phenotype and the positive control line tempted to lose gene silencing effect after a while. Since  $\beta$ -estradiol inducible promoter can be leaky thus rendering the induced and uninduced lines incomparable, we have recently produced dexamethasone inducible *AtASCC4*-RNAi lines using pOpOFF vector and the plants remain to be analyzed and phenotyped.

Taken together, findings from this study show that AtSCC4 is an evolutionary conserved subunit of cohesin loading machinery and AtSCC4 forms a complex with AtSCC2. We have established split-nuclei iFRAP assay for plant cohesin visualization *in vivo* and shown that AtSCC4 immobilizes on nuclei independently of AtSCC2 and is required for cohesin immobilization on nuclei, most probably by attaching it onto chromatin. Furthermore, AtSCC4 contributes to auxin-mediated cell fate determination during plant embryo development.

## 3.2 *PaESP* controls cell expansion during Norway spruce embryo development (Paper II)

*PaESP* mRNA and protein are highly abundant in actively proliferating tissues, such as proembryogenic masses (PEMs) and EMs of early spruce somatic embryos. By contrast, tissues and organs largely composed of non-dividing, terminally-differentiated cells e.g., embryo-suspensors, needles, cotyledons, hypocotyls and roots contain five times less *PaESP* mRNA and no detectable amount of PaESP protein, indicating developmental regulation of *PaESP*. In this study, we used a combination of reverse genetics and microscopy to explore the role of PaESP in spruce embryo development.

### 3.2.1 *PaESP* is required for cytoskeleton organization and cell division

Using immunofluorescence microscopy, we have found that PaESP localizes to cortical microtubules of EM cells during interphase. In dividing EM cells, PaESP localizes to perinuclear basket of microtubules, kinetochore microtubules and spindle midzone during prophase, metaphase and anaphase, respectively. During early cytokinesis (telophase), PaESP localizes in the phragmoplast midzone and on the microtubules at the leading edge of the phragmoplast. During late cytokinesis, PaESP remains on the cell plate after phragmoplast microtubule depolymerization. PaESP is absent in anisotropically expanded tube cells, which elongate to form suspensor cells, consistent with the low level of *PaESP* mRNA in the suspensor.

In the EM cells from *PaESP* RNAi lines we have observed no significant alteration in cortical microtubule array. In contrast, the cortical microtubules of tube cells and hypocotyl cells showed reduced density and length with predominance of oblique and longitudinal orientation rather than transverse orientation. This indicates that the low level of *PaESP* expression in the differentiated cells is essential for microtubule network organization (Moschou et al., 2016).

Transient silencing of *PaESP* using RNAi revealed chromosome non-disjunction phenotype in spruce EM cells. Furthermore, ectopically expressed *PaESP* could rescue chromosome non-disjunction phenotype of root cells from *AtESP*-deficient *rsw4* line of *Arabidopsis* (Moschou et al., 2013). Collectively, these data demonstrate that the major role of *ESP* in daughter chromatid separation is conserved between gymnosperms and angiosperms.

### 3.2.2 *PaESP* is required for correct embryo patterning

*PaESP* RNAi lines showed inhibition of early embryo development from PEMs. Instead of forming compact EMs attached to several files of anisotropically expanded suspensor cells, *PaESP* RNAi lines generated irregularly-shaped EMs

connected to suspensor-like structures, as detected by double staining with fluorescein diacetate (FDA) and Evans blue. These suspensor-like structures were composed of supernumerary cells that failed to expand anisotropically leading to the inhibition of suspensor elongation. A similar phenotype of spruce embryos was observed upon treatment with auxin transport inhibitor 1-N-naphthylphthalamic acid (Larsson et al., 2008b), suggesting the possible causative link between PaESP deficiency and disturbed auxin signalling. Thus, depletion of PaESP changes the balance of life and death events in the two embryonic domains and impairs embryo patterning. Although *PaESP* could rescue the chromosome non-disjunction phenotype of *Arabidopsis AtESP* mutant *rsw4* (Moschou et al., 2013), it failed to rescue the root-swelling phenotype of *rsw4*. Therefore, we propose that angiosperms and gymnosperms have evolved different effector mechanism downstream of ESP to regulate anisotropic cell expansion.

### 3.3 RNA-seq analysis of embryonic domains in Norway spruce reveals new potential regulators of developmental cell death (Paper III)

Elimination of the embryo-suspensor is the earliest manifestation of developmental PCD in the plant life cycle. To explore regulators of this PCD, we have carried out transcriptomic analysis of the Norway spruce EM vs embryo-suspensor using RNA sequencing. A total of 451 genes showed differential expression between the EM and the suspensor, of which 53 and 398 were up-regulated in the two respective domains.

#### 3.3.1 Genes encoding flavonoid pathway enzymes are up-regulated in the EM

Several genes encoding flavonoid biosynthesis enzymes (e.g. chalcone synthase (*TT4*), flavanone 3-hydroxylase (*TT6*) and chalcone flavanone isomerase (*CHI*)) and transcription factors regulating expression of these enzymes (e.g. MYB12) were up-regulated in the EM. This indicates that flavonoids might play a vital role in the maintaining growth of the EM through regulation of auxin transport (Peer and Murphy, 2007) and ROS scavenging (Peer et al., 2013).

#### 3.3.2 Genes related to cell differentiation and death are up-regulated in the suspensor

The elongation of the terminally-differentiated suspensor cells in Norway spruce is accompanied by the growth of lytic vacuoles, which degrade cellular content delivered by autophagy (Smertenko and Bozhkov, 2014, Filonova et al., 2000). Among genes up-regulated in the suspensor, we have found a subset of genes that might be directly responsible for the elongation of the suspensor cells. These

included genes encoding aquaporins, which are known to facilitate cell expansion upon water uptake (Tyerman et al., 2002), and choline kinase involved in the biosynthesis of phosphatidylcholine (Tasseva et al., 2004), the major component of plasma membrane and tonoplast (Yoshida and Uemura, 1986). We have also observed up-regulation of genes encoding cell wall modifying enzymes, such as xyloglucan endotransglucosylase/hydrolase, galactosidases and pectinesterase.

Genes for TFs that mediate expression of PCD triggers and executioners were likewise up-regulated in the suspensor. Survey of plant TF database PlantTFDB 4.0 have revealed enhanced expression of nine TFs belonging to six protein families, including bHLH, C2H2, ERF, LBD, MYB and NAC. Among these TFs, two were homologues to *Arabidopsis* XYLEM NAC DOMAIN 1 (*XND1*) and *ANAC075*, known to be involved in other examples of developmental PCD (Tadashi Kunieda, 2008, Hitoshi Endo, 2015).

Stress-responsive genes, such as those encoding cytochrome p450, alcohol oxidase, heat shock proteins (HSPs), a spruce homologue of *Bax inhibitor-1* (*PaBI-1*) and *Bcl2-associated anthanogene 1* (*BAG1*), along with triggers of H<sub>2</sub>O<sub>2</sub> production (*L-ascorbate oxidase* and *germin*) formed another large group of suspensor-specific differentially expressed genes. Their enhanced expression indicates their direct involvement in either initiating PCD or preventing rapid demise of suspensor cells through necrosis.

Finally, transcriptome of the suspensor was enriched with catabolic enzymes required for processing of nucleic acids and proteins during execution of PCD. We have observed transcriptional up-regulation of several spruce homologues of *Arabidopsis* cysteine peptidases (e.g., papain-like protease *CEP1*, metacaspase *AtMC9* and cathepsin B-like protease), as well as of nuclease *RNS3* (*RIBONUCLEASE 3*). All these enzymes have been previously shown to execute diverse types of PCD in *Arabidopsis* (Bollhoner et al., 2013, Bariola et al., 1994, Gilroy et al., 2007, McLellan et al., 2009, Zhang et al., 2014, Ge et al., 2016).

### 3.3.3 Cell-death components are largely conserved between angiosperms and gymnosperms

It has been suggested by Olvera-Carrillo and colleagues (Olvera-Carrillo et al., 2015) that the core developmental PCD genes, such as *RNS3*, *BFN1*, *PASPA3*, *AtMc9*, *SCPL48* are evolutionary conserved in green plants, including higher and lower angiosperms, lower land plants and algae, with the exception for *BFN1* in algae. Finding some of these genes, as well as PCD-related TFs *XND1* and *ANAC075* in the transcriptome of the spruce embryo-suspensor provides further evidence for the conservation of developmental PCD genes between angiosperms and gymnosperms.

### 3.3.4 *PaBI-1* is involved in developmental PCD and embryo development

One of the genes up-regulated in the suspensor was a spruce homologue of Bax inhibitor-1 (*PaBI-1*, for *Picea abies BI-1*). BI-1 localizes to ER membrane and in animals, it acts as a suppressor of Bax (a cell-death effector)-induced apoptosis (Watanabe and Lam, 2008). Although plant genomes lack *Bax*, they still encode for *BI-1* (Bozhkov and Lam, 2011). In *Arabidopsis*, *BI-1* has been reported to suppress chemically induced ER stress-mediated and necrotrophic fungi- and heat stress-induced cell death (Watanabe and Lam, 2006, Watanabe and Lam, 2008, Businge et al., 2013). The relevance of *BI-1* to plant development and associated PCD remains unknown.

Using RNAi, we have suppressed the expression of *PaBI-1* in the embryonic cell line. Instead of vacuolar cell death, suspensor cells in the resulting *PaBI-1* RNAi lines exhibited necrosis characterized by shrunken and largely undigested protoplast. This change of the mode of cell death in the *PaBI-1* RNAi lines led to the suppression of anisotropic expansion of the suspensor cells, impaired apical-basal polarity of the developing embryo and ultimately decreased number of cotyledonary embryos.

Vacuolar cell death is a slow process featuring gradual cell dismantling (van Doorn et al., 2011) and demands high metabolic activity until vacuolar collapse. In *Arabidopsis*, ER stress-induced unfolded protein response (UPR) results in transcriptional up-regulation of *AtBI-1* to keep the cell alive until the ER homeostasis is re-established by the activity of ER chaperons such as Bip2 (Watanabe and Lam, 2008). In *Nicotiana benthamiana*, BI-1 interacts with autophagy-related protein ATG6 and silencing of *BI-1* reduces autophagic flux (Xu et al., 2017). In spruce, ATG6 is required for vacuolar cell death and protection of suspensor cells against necrosis (Minina et al., 2013). We propose that *PaBI-1* might act to suppress rapid necrotic cell death by either maintaining ER homeostasis or interacting with autophagy pathway or a combination of both to allow gradual cell dismantling characteristic for vacuolar PCD.

### 3.4 *Arabidopsis* metacaspases (unpublished experimental data not included in manuscripts)

Metacaspases are cysteine-dependent proteases that are distantly related to metazoan caspases. Genome of *Arabidopsis* encodes three type I (*AtMC1-AtMC3*) and six type II (*AtMC4-AtMC9*) metacaspases. There is a growing evidence that metacaspases can regulate plant developmental PCD, one example being the involvement type II metacaspase *mclI-Pa* in terminal differentiation and PCD of the Norway spruce embryo suspensor (Suarez et al., 2004). Thus far, the only *Arabidopsis* metacaspase reported to play a role in developmental PCD process is type II metacaspase *AtMC9* shown to participate in *post mortem*

autolysis of xylem vessel elements after vacuolar rupture (Bollhoner et al., 2013).

Spruce metacaspase *mcII-Pa* cleaves evolutionary conserved regulator of gene expression Tudor staphylococcal nuclease (TSN) (Sundstrom et al., 2009), whereas *Arabidopsis* metacaspases *AtMC9* cleaves PEPCK1 (phosphoenolpyruvate carboxykinase), a key enzyme of gluconeogenesis that regulates hypocotyl growth of germinating seedling (Tsiatsiani et al., 2013), as well as GRIM REAPER, an extracellular protein required for signal transduction of oxidative stress and thus cell death in *Arabidopsis* (Wrzaczek et al., 2009, Wrzaczek et al., 2015). Other potential targets of *AtMC9* identified by COFRADIC (COmbined FRActional DIagonal Chromatography) (Tsiatsiani et al., 2013) are to be individually validated *in vivo*. Substrates as well as interactors of other eight *Arabidopsis* metacaspases remain elusive.

We have attempted to investigate the role of metacaspases in *Arabidopsis* embryo development and suspensor PCD using genetics and microscopy. In another project, we have isolated potential interactors of *AtMC4* and *AtMC5* using tandem affinity purification (TAP).

#### 3.4.1 Expression and localization analysis of *Arabidopsis* metacaspases

qRT-PCR analysis of RNA samples prepared from whole seeds containing embryos at early developmental stages (globular to early heart) showed expression of all nine metacaspases at different levels. However, GENEVESTIGATOR microarray database points to a possibility that *AtMC1*, *AtMC4* and *AtMC5* may represent orthologues of *mcII-Pa*, as *AtMC1* and *AtMC4* are highly and *AtMC5* is moderately expressed in the *Arabidopsis* embryo-suspensor (Hruz et al., 2008). Furthermore, *AtMC5* appears to be suspensor-specific gene, since its expression is barely detected in other organs and tissues. Expression of *AtMC4*-GFP and *AtMC5*-GFP under both native and constitutive (35S) promoters revealed perinuclear and cytoplasmic localization of the metacaspases in the root epidermal cells.

#### 3.4.2 Single metacaspase knockout mutants exhibit low-frequency embryonic defects

DIC microscopy of cleared seeds at different developmental stages (early globular to torpedo) from *atmc1*, *atmc4* and *atmc5* T-DNA insertion mutants exhibited embryonic defects, with a level of penetrance ranging from 0.81 to 5.44% for different lines. The defects included periclinal cell divisions in the suspensor, sometimes leading to the formation of raspberry-like phenotype (Yadegari et al., 1994), irregular cell divisions in the embryo proper, defective embryo proper patterning and developmental arrest of the embryo. The embryo proper defects were more prominent in the globular stage embryos, whereas the

suspensor abnormality was higher in the heart stage embryos. Furthermore, *atmc1* and *atmc5* plants displayed significant increase in the frequency of unfertilized ovules in comparison to wild type Col 0 plants. Alexander staining revealed that 40% of pollen produced by *atmc1* plants were dead. *atmc1* plants also revealed increased incidents of embryo abortion.

### 3.4.3 *Arabidopsis* metacaspases may function redundantly in embryo development

The low penetrance of embryonic defects in single mutants can be explained by potential redundancy of metacaspases. To obtain stronger genetic tools, we generated double *atmc1atmc4* and *atmc1atmc5* T-DNA insertion mutants, whereas simultaneous knockout of *AtMC4* and *AtMC5* and thus generation of triple *atmc1atmc4atmc5* T-DNA insertion mutant is unfeasible owing to tandem distribution of *AtMC4* and *AtMC5* on the first chromosome. Since DIC microscopy analysis of *atmc1atmc4* and *atmc1atmc5* plants did not reveal any further increase in the frequencies of abnormal embryos, as compared to single mutants, we have checked the compensatory effect of *AtMC4* or *AtMC5* in seeds of double knockout plants *atmc1atmc5* and *atmc1atmc4*, respectively, by absolute qRT-PCR. Indeed, we have observed up-regulation of *AtMC4* in *atmc1atmc5*, whereas expression level of *AtMC5* in *atmc1atmc4* was similar to that of WT. Next, we have generated *AtMC4* RNAi construct driven under promoter of *AtMC5*, which is active in the embryo, as revealed by GUS ( $\beta$ -glucuronidase) staining, and transformed to *atmc1atmc5* double mutant. Plants depleted for three metacaspases (*atmc1atmc5* expressing *AtMC4* RNAi) did not show further increase in the frequency of developmental aberrations as compared to single lines. Results of these experiments point to potential redundant function of *Arabidopsis* metacaspases in embryogenesis, the hypothesis that requires further investigations.

### 3.4.4 Isolation of AtMC4 and AtMC5 interactors

The mass spectrometry analysis of purified fractions bound to C-terminally TAP-tagged WT and catalytically inactive mutant (C139A) AtMC4 and AtMC5, as well as TAP-GFP (control) expressed in *Arabidopsis* plants revealed only one common interactor of WT AtMC4 and AtMC5 (Table 1). The number of interactors bound to WT metacaspases was significantly higher than that of catalytically inactive mutants, indicating that catalytic cysteine residues are required for binding interactors. The absence of a few interactors of mutant metacaspases among interactors of WT metacaspases can be due to their transient binding and rapid release upon proteolytic cleavage. Several interactors have been further confirmed *in vivo* using co-immunoprecipitation (CoIP) of TAP-tagged metacaspases expressed in *Nicotiana benthamiana*.

Table 1. *Interactors of wild-type AtMC4 and AtMC5 and their catalytically inactive mutants detected by mass spectroscopy*

Gene Name	Full name	TAIR Ac	MC4_W	MC4_M	MC5_W	MC5_M
EF1a	Elongation factor 1-alpha	At1g07930			2, +	+
CRU3	Cruciferin 3	AT4G28520		9		
Unknown	Cysteine proteinases superfamily protein	At1g02305	1			
ndpk3	Nucleoside diphosphate kinase III	At4g11010	11			
TPR	Pentatricopeptide repeat-containing protein	At2g27800			1	
PGM	Phosphoglycerate mutase-like protein	AT5G64460	1, +	+	1	
PyDe	Pyruvate dehydrogenase	At1g24180			3	
ATS6A.2	Regulatory Particle 5a of AAA-ATPases	At3g05530			7, +	
EHD1	Eps15 homology domain proteins involved in endocytosis	At3g20290			1	
Subtil	Senescence-associated subtilisin protease	At3g14067			1	
SEUSS	Transcription regulator SEUSS	AT1G43850	4			
PEPC1	Phosphoenolpyruvate carboxylase 1	At1g53310	1			
RHM2	Rhamnose biosynthesis 2	AT1G53500	9, +	+		
GLN1.3	Glutamine synthetase 1.3	At3g17820			2	
NadhUbOxR	NADH-ubiquinone oxidoreductase-related	At5g52840			2	
FTSZ2-1	Tubulin-like protein	At2g36250			3	
CHR5	Chromatin remodeling 5	At2g13370	2			
Unknown	Actin-like ATPase superfamily protein	At4g22720	2, +			
26sN9	26S Proteasome component (PCI) domain protein	AT5G45620			1	
KNAT4	Knotted1-like homeobox gene 4	At5g11060			2	
LECRK1.9	Lectin receptor kinase	At5g60300				1
REV1	Myb-like transcription factor	AT5G17300				2
TCP1	TCP-1/cpn60 chaperonin family protein	At1g24510			2, +	+
2OGD	2-oxoglutarate dehydrogenase	At5g65750			3	
SOBIR1	Suppressor of bir1 1	AT2G31880			1	
Unknown	Unknown	At3g08030	4			
VfATPase	Vesicle fusing atpase	At4g04910	3			

MC, Metacaspase, W, Wild type; M, Catalytic mutant. Numbers in the last four columns indicate number of peptides detected by mass spectroscopy. +, interaction was confirmed by CoIP.

## 4 Conclusions

The key findings of this thesis are:

AtSCC4 is an evolutionary conserved subunit of cohesin loading machinery and contributes to auxin-mediated cell fate determination during *Arabidopsis* embryo development. AtSCC4 physically interacts with AtSCC2. However, this interaction is not required for immobilization of AtSCC4 in the nuclei. AtSCC2 and AtSCC4 act in the same pathway during embryonic pattern formation.

PaESP is essential for cytoskeleton organization and cell division during embryo pattern formation in Norway spruce. The functions of ESP in sister chromatid separation and cell expansion are conserved in angiosperms and gymnosperms. However, these lineages have evolved different mechanism of ESP-mediated regulation of cell expansion.

RNAseq analysis of Norway spruce embryonic domains revealed a large number of potential regulators of suspensor PCD, including transcription factors, cell-wall modifying enzymes and hydrolytic enzymes. PaBI-1 is essential for progression of vacuolar cell death in spruce embryo-suspensor and for embryo pattern formation.



## 5 Future perspectives

In this thesis, I have presented functional study of a small subset of molecular regulators of life and death events occurring during plant embryo development. The findings of this study ignite an interest in further deciphering molecular regulation of plant embryo development. Below, I have summed up some of the most interesting directions of future research.

Analysis and phenotyping of dexamethasone inducible *AtASCC4*-RNAi lines transformed with pOpOFF vector may reveal the role of AtSCC4 in post-embryonic development. A cellular role of cytoplasmic fraction of AtSCC4 and its interacting proteins remains unknown. Furthermore, study of genetic interaction of *AtSCC4* and *WAPL* (Wings Apart-Like), physical and genetic interaction of *AtSCC4* and *CTF7* (Chromosome Transmission Fidelity 7) and their role in mitotic and meiotic cell division during vegetative growth and reproductive development, respectively, should give an important insight into regulation of plant cell division.

Further study to identify separase (ESP) substrate(s) will reveal the signalling pathways and effector mechanisms downstream of ESP that regulate anisotropic cell expansion in angiosperms and gymnosperms, which is interesting from evolutionary perspective.

Although direct homologue of *Bax* gene is absent in plant, we have observed that *PaBI-1* is present and functioning in spruce embryo development. It would be interesting to study the interactor of *PaBI-1* to reveal the mechanism of *PaBI-1* mediated regulation of developmental PCD and embryo development. Furthermore, functional study of the other genes differentially expressed in the EM and embryo-suspensor will increase our understanding of the molecular regulation of life and death events in plant embryo development.



## References

- Barbero, J. L. 2013. Genetic basis of cohesinopathies. *Appl Clin Genet*, 6, 15-23.
- Bariola, P. A., Howard, C. J., Taylor, C. B., Verburg, M. T., Jaglan, V. D. & Green, P. J. 1994. The Arabidopsis ribonuclease gene RNS1 is tightly controlled in response to phosphate limitation. *Plant J*, 6, 673-85.
- Bayer, M., Nawy, T., Giglione, C., Galli, M., Meinel, T. & Lukowitz, W. 2009. Paternal control of embryonic patterning in Arabidopsis thaliana. *Science*, 323, 1485-8.
- Bollhoner, B., Zhang, B., Stael, S., Denance, N., Overmyer, K., Goffner, D., Van Breusegem, F. & Tuominen, H. 2013. Post mortem function of AtMC9 in xylem vessel elements. *New Phytol*, 200, 498-510.
- Bosch, M. & Franklin-Tong, V. E. 2008. Self-incompatibility in Papaver: signalling to trigger PCD in incompatible pollen. *J Exp Bot*, 59, 481-90.
- Bozhkov, P. V. & Lam, E. 2011. Green death: revealing programmed cell death in plants. *Cell Death Differ*, 18, 1239-40.
- Bozhkov, P. V., Filonova, L. H. & Suarez, M. F. 2005a. Programmed cell death in plant embryogenesis. *Curr Top Dev Biol*, 67, 135-79.
- Bozhkov, P. V., Suarez, M. F., Filonova, L. H., Daniel, G., Zamyatnin, A. A., Jr., Rodriguez-Nieto, S., Zhivotovsky, B. & Smertenko, A. 2005b. Cysteine protease mcII-Pa executes programmed cell death during plant embryogenesis. *Proc Natl Acad Sci U S A*, 102, 14463-8.
- Breuninger, H., Rikirsch, E., Hermann, M., Ueda, M. & Laux, T. 2008. Differential expression of WOX genes mediates apical-basal axis formation in the Arabidopsis embryo. *Dev Cell*, 14, 867-76.
- Burch-Smith, T. M., Anderson, J. C., Martin, G. B. & Dinesh-Kumar, S. P. 2004. Applications and advantages of virus-induced gene silencing for gene function studies in plants. *Plant J*, 39, 734-46.
- Businge, E., Bygdell, J., Wingsle, G., Moritz, T. & Egertsdotter, U. 2013. The effect of carbohydrates and osmoticum on storage reserve accumulation and germination of Norway spruce somatic embryos. *Physiol Plant*, 149, 273-85.
- Cairney, J. & Pullman, G. S. 2007. The cellular and molecular biology of conifer embryogenesis. *New Phytol*, 176, 511-36.
- Chao, W. C., Murayama, Y., Munoz, S., Costa, A., Uhlmann, F. & Singleton, M. R. 2015. Structural Studies Reveal the Functional Modularity of the Scc2-Scc4 Cohesin Loader. *Cell Rep*, 12, 719-25.
- Chen, J. G., Ullah, H., Young, J. C., Sussman, M. R. & Jones, A. M. 2001. ABP1 is required for organized cell elongation and division in Arabidopsis embryogenesis. *Genes Dev*, 15, 902-11.
- Ciavatta, V. T., Egertsdotter, U., Clapham, D., Von Arnold, S. & Cairney, J. 2002. A promoter from the loblolly pine PtNIP1;1 gene directs expression in an early-embryogenesis and suspensor-specific fashion. *Planta*, 215, 694-8.

- Ciavatta, V. T., Morillon, R., Pullman, G. S., Chrispeels, M. J. & Cairney, J. 2001. An aquaglyceroporin is abundantly expressed early in the development of the suspensor and the embryo proper of loblolly pine. *Plant Physiol*, 127, 1556-67.
- Daneva, A., Gao, Z., Van Durme, M. & Nowack, M. K. 2016. Functions and Regulation of Programmed Cell Death in Plant Development. *Annu Rev Cell Dev Biol*, 32, 441-468.
- De Smet, I., Lau, S., Mayer, U. & Jurgens, G. 2010. Embryogenesis - the humble beginnings of plant life. *Plant J*, 61, 959-70.
- De, K., Sterle, L., Krueger, L., Yang, X. & Makaroff, C. A. 2014. Arabidopsis thaliana WAPL is essential for the prophase removal of cohesin during meiosis. *PLoS Genet*, 10, e1004497.
- Devic, M., Albert, S. & Delseny, M. 1996. Induction and expression of seed-specific promoters in Arabidopsis embryo-defective mutants. *Plant J*, 9, 205-15.
- Duan, Q., Kita, D., Johnson, E. A., Aggarwal, M., Gates, L., Wu, H. M. & Cheung, A. Y. 2014. Reactive oxygen species mediate pollen tube rupture to release sperm for fertilization in Arabidopsis. *Nat Commun*, 5, 3129.
- Elmore, S. 2007. Apoptosis: a review of programmed cell death. *Toxicol Pathol*, 35, 495-516.
- Endo, H., Yamaguchi, M., Tamura, T., Nakano, Y., Nishikubo, N., Yoneda, A., Kato, K., Kubo, M., Kajita, S., Katayama, Y., Ohtani, M. & Demura, T. 2015. Multiple classes of transcription factors regulate the expression of VASCULAR-RELATED NAC-DOMAIN7, a master switch of xylem vessel differentiation. *Plant Cell Physiol*, 56, 242-54.
- Fendrych, M., Van Hautegeem, T., Van Durme, M., Olvera-Carrillo, Y., Huysmans, M., Karimi, M., Lippens, S., Guerin, C. J., Krebs, M., Schumacher, K. & Nowack, M. K. 2014. Programmed cell death controlled by ANAC033/SOMBRERO determines root cap organ size in Arabidopsis. *Curr Biol*, 24, 931-40.
- Filonova, L. H., Bozhkov, P. V., Brukhin, V. B., Daniel, G., Zhivotovsky, B. & Von Arnold, S. 2000. Two waves of programmed cell death occur during formation and development of somatic embryos in the gymnosperm, Norway spruce. *J Cell Sci*, 113 Pt 24, 4399-411.
- Galinha, C., Hofhuis, H., Luijten, M., Willemsen, V., Blilou, I., Heidstra, R. & Scheres, B. 2007. PLETHORA proteins as dose-dependent master regulators of Arabidopsis root development. *Nature*, 449, 1053-7.
- Ge, Y., Cai, Y. M., Bonneau, L., Rotari, V., Danon, A., McKenzie, E. A., McLellan, H., Mach, L. & Gallois, P. 2016. Inhibition of cathepsin B by caspase-3 inhibitors blocks programmed cell death in Arabidopsis. *Cell Death Differ*, 23, 1493-501.
- Gilroy, E. M., Hein, I., Van Der Hoorn, R., Boevink, P. C., Venter, E., McLellan, H., Kaffarnik, F., Hrubikova, K., Shaw, J., Holeva, M., Lopez, E. C., Borrás-Hidalgo, O., Pritchard, L., Loake, G. J., Lacomme, C. & Birch, P. R. 2007. Involvement of cathepsin B in the plant disease resistance hypersensitive response. *Plant J*, 52, 1-13.
- Gligoris, T. & Lowe, J. 2016. Structural Insights into Ring Formation of Cohesin and Related Smc Complexes. *Trends Cell Biol*, 26, 680-93.
- Goldberg, R. B., De Paiva, G. & Yadegari, R. 1994. Plant embryogenesis: zygote to seed. *Science*, 266, 605-14.
- Guilfoyle, T. J. & Hagen, G. 2007. Auxin response factors. *Curr Opin Plant Biol*, 10, 453-60.
- Heisler, M. G., Ohno, C., Das, P., Sieber, P., Reddy, G. V., Long, J. A. & Meyerowitz, E. M. 2005. Patterns of auxin transport and gene expression during primordium development revealed by live imaging of the Arabidopsis inflorescence meristem. *Curr Biol*, 15, 1899-911.
- Hitoshi Endo, M. Y., Taizo Tamura, Yoshimi Nakano, Nobuyuki Nishikubo, Arata Yoneda, Ko Kato, Minoru Kubo, Shinya Kajita, Yoshihiro Katayama, Misato Ohtani, Taku Demura. 2015. Multiple Classes of Transcription Factors Regulate the Expression of VASCULAR-RELATED NAC-DOMAIN7, a Master Switch of Xylem Vessel Differentiation. *Plant Cell and Physiology*, 56, 242-254.
- Hruz, T., Laule, O., Szabo, G., Wessendorp, F., Bleuler, S., Oertle, L., Widmayer, P., Gruissem, W. & Zimmermann, P. 2008. Genevestigator v3: a reference expression database for the meta-analysis of transcriptomes. *Adv Bioinformatics*, 2008, 420747.
- Huysmans, M., Lema, A. S., Coll, N. S. & Nowack, M. K. 2017. Dying two deaths - programmed cell death regulation in development and disease. *Curr Opin Plant Biol*, 35, 37-44.

- Ingouff, M., Farbos, I., Lagercrantz, U. & Von Arnold, S. 2001. PaHB1 is an evolutionary conserved HD-GL2 homeobox gene expressed in the protoderm during Norway spruce embryo development. *Genesis*, 30, 220-30.
- Ingouff, M., Farbos, I., Wiweger, M. & Von Arnold, S. 2003. The molecular characterization of PaHB2, a homeobox gene of the HD-GL2 family expressed during embryo development in Norway spruce. *J Exp Bot*, 54, 1343-50.
- Ishikawa, T., Watanabe, N., Nagano, M., Kawai-Yamada, M. & Lam, E. 2011. Bax inhibitor-1: a highly conserved endoplasmic reticulum-resident cell death suppressor. *Cell Death Differ*, 18, 1271-8.
- Ito, J. & Fukuda, H. 2002. ZEN1 is a key enzyme in the degradation of nuclear DNA during programmed cell death of tracheary elements. *Plant Cell*, 14, 3201-11.
- Kerr, J. F., Wyllie, A. H. & Currie, A. R. 1972. Apoptosis: a basic biological phenomenon with wide-ranging implications in tissue kinetics. *Br J Cancer*, 26, 239-57.
- Larsson, E., Sitbon, F. & Von Arnold, S. 2008a. Polar auxin transport controls suspensor fate. *Plant Signal Behav*, 3, 469-70.
- Larsson, E., Sitbon, F. & Von Arnold, S. 2012a. Differential regulation of Knotted1-like genes during establishment of the shoot apical meristem in Norway spruce (*Picea abies*). *Plant Cell Rep*, 31, 1053-60.
- Larsson, E., Sitbon, F., Ljung, K. & Von Arnold, S. 2008b. Inhibited polar auxin transport results in aberrant embryo development in Norway spruce. *New Phytol*, 177, 356-66.
- Larsson, E., Sundstrom, J. F., Sitbon, F. & Von Arnold, S. 2012b. Expression of PaNAC01, a *Picea abies* CUP-SHAPED COTYLEDON orthologue, is regulated by polar auxin transport and associated with differentiation of the shoot apical meristem and formation of separated cotyledons. *Ann Bot*, 110, 923-34.
- Liu, Y., Li, X., Zhao, J., Tang, X., Tian, S., Chen, J., Shi, C., Wang, W., Zhang, L., Feng, X. & Sun, M. X. 2015. Direct evidence that suspensor cells have embryogenic potential that is suppressed by the embryo proper during normal embryogenesis. *Proc Natl Acad Sci U S A*, 112, 12432-7.
- Liu, Z. & Makaroff, C. A. 2006. Arabidopsis separase AESP is essential for embryo development and the release of cohesin during meiosis. *Plant Cell*, 18, 1213-25.
- Lopez-Serra, L., Kelly, G., Patel, H., Stewart, A. & Uhlmann, F. 2014. The Scc2-Scc4 complex acts in sister chromatid cohesion and transcriptional regulation by maintaining nucleosome-free regions. *Nat Genet*, 46, 1147-51.
- Lukowitz, W., Roeder, A., Parmenter, D. & Somerville, C. 2004. A MAPKK kinase gene regulates extra-embryonic cell fate in Arabidopsis. *Cell*, 116, 109-19.
- Marchler-Bauer, A., Derbyshire, M. K., Gonzales, N. R., Lu, S., Chitsaz, F., Geer, L. Y., Geer, R. C., He, J., Gwadz, M., Hurwitz, D. I., Lanczycki, C. J., Lu, F., Marchler, G. H., Song, J. S., Thanki, N., Wang, Z., Yamashita, R. A., Zhang, D., Zheng, C. & Bryant, S. H. 2015. CDD: NCBI's conserved domain database. *Nucleic Acids Res*, 43, D222-6.
- Mclellan, H., Gilroy, E. M., Yun, B. W., Birch, P. R. & Loake, G. J. 2009. Functional redundancy in the Arabidopsis Cathepsin B gene family contributes to basal defence, the hypersensitive response and senescence. *New Phytol*, 183, 408-18.
- Minina, E. A., Filonova, L. H., Fukada, K., Savenkov, E. I., Gogvadze, V., Clapham, D., Sanchez-Vera, V., Suarez, M. F., Zhivotovsky, B., Daniel, G., Smertenko, A. & Bozhkov, P. V. 2013. Autophagy and metacaspase determine the mode of cell death in plants. *J Cell Biol*, 203, 917-27.
- Moschou, P. N., Gutierrez-Beltran, E., Bozhkov, P. V. & Smertenko, A. 2016. Separase Promotes Microtubule Polymerization by Activating CENP-E-Related Kinesin Kin7. *Dev Cell*, 37, 350-61.
- Moschou, P. N., Smertenko, A. P., Minina, E. A., Fukada, K., Savenkov, E. I., Robert, S., Hussey, P. J. & Bozhkov, P. V. 2013. The caspase-related protease separase (extra spindle poles) regulates cell polarity and cytokinesis in Arabidopsis. *Plant Cell*, 25, 2171-86.
- Nawy, T., Bayer, M., Mravec, J., Friml, J., Birnbaum, K. D. & Lukowitz, W. 2010. The GATA factor HANABA TARANU is required to position the proembryo boundary in the early Arabidopsis embryo. *Dev Cell*, 19, 103-13.

- Ngo, Q. A., Vogler, H., Lituiev, D. S., Nestorova, A. & Grossniklaus, U. 2014. A calcium dialog mediated by the FERONIA signal transduction pathway controls plant sperm delivery. *Dev Cell*, 29, 491-500.
- O'Connor, C. (2008) Cell Division: Stages of Mitosis. *Nature Education* 1(1):188
- Olvera-Carrillo, Y., Van Bel, M., Van Hautegeem, T., Fendrych, M. & Huysmans, M. 2015. A Conserved Core of Programmed Cell Death Indicator Genes Discriminates Developmentally and Environmentally Induced Programmed Cell Death in Plants. 169, 2684-99.
- Peer, W. A. & Murphy, A. S. 2007. Flavonoids and auxin transport: modulators or regulators? *Trends Plant Sci*, 12, 556-63.
- Peer, W. A., Cheng, Y. & Murphy, A. S. 2013. Evidence of oxidative attenuation of auxin signalling. *J Exp Bot*, 64, 2629-39.
- Rankin, S. 2015. Complex elaboration: making sense of meiotic cohesin dynamics. *Febs j*, 282, 2426-43.
- Russell, S. D. 1992. Double Fertilization. *International Review of Cytology*, 140, 357-388.
- Sabala, I., Elfstrand, M., Farbos, I., Clapham, D. & Von Arnold, S. 2000. Tissue-specific expression of Pa18, a putative lipid transfer protein gene, during embryo development in Norway spruce (*Picea abies*). *Plant Mol Biol*, 42, 461-78.
- Schlereth, A., Moller, B., Liu, W., Kientz, M., Flipse, J., Rademacher, E. H., Schmid, M., Jurgens, G. & Weijers, D. 2010. MONOPTEROS controls embryonic root initiation by regulating a mobile transcription factor. *Nature*, 464, 913-6.
- Sebastian, J., Ravi, M., Andreuzza, S., Panoli, A. P., Marimuthu, M. P. & Siddiqi, I. 2009. The plant adherin AtSCC2 is required for embryogenesis and sister-chromatid cohesion during meiosis in Arabidopsis. *Plant J*, 59, 1-13.
- Singh, H. (1978). Embryology of gymnosperms. In: Zimmerman, W., Carlquist, Z., Ozenda, P. & Wulff, H. (ed). *Handbuch der pflanzenanatomie*. Gebrüder Borntraeger, Berlin, Stuttgart. 187-241.
- Smertenko, A. & Bozhkov, P. V. 2014. Somatic embryogenesis: life and death processes during apical-basal patterning. *J Exp Bot*, 65, 1343-60.
- Smertenko, A. P., Bozhkov, P. V., Filonova, L. H., Von Arnold, S. & Hussey, P. J. 2003. Re-organisation of the cytoskeleton during developmental programmed cell death in *Picea abies* embryos. *Plant J*, 33, 813-24.
- Suarez, M. F., Filonova, L. H., Smertenko, A., Savenkov, E. I., Clapham, D. H., Von Arnold, S., Zhivotovsky, B. & Bozhkov, P. V. 2004. Metacaspase-dependent programmed cell death is essential for plant embryogenesis. *Curr Biol*, 14, R339-40.
- Sundstrom, J. F., Vaculova, A., Smertenko, A. P., Savenkov, E. I., Golovko, A., Minina, E., Tiwari, B. S., Rodriguez-Nieto, S., Zamyatin, A. A., Jr., Valineva, T., Saarikettu, J., Frilander, M. J., Suarez, M. F., Zavialov, A., Stahl, U., Hussey, P. J., Silvennoinen, O., Sundberg, E., Zhivotovsky, B. & Bozhkov, P. V. 2009. Tudor staphylococcal nuclease is an evolutionarily conserved component of the programmed cell death degradome. *Nat Cell Biol*, 11, 1347-54.
- Tadashi Kunieda, N. M., Masaru Ohme-Takagi, Seiji Takeda, Mitsuhiro Aida, Masao Tasaka, Maki Kondo, Mikio Nishimura, Ikuko Hara-Nishimura. 2008. NAC Family Proteins NARS1/NAC2 and NARS2/NAM in the Outer Integument Regulate Embryogenesis in Arabidopsis. *The Plant Cell*, 20, 1631-2642.
- Tahir, M., Law, D. A. & Stasolla, C. 2006. Molecular characterization of PgAGO, a novel conifer gene of the Argonaute family expressed in apical cells and required for somatic embryo development in spruce. *Tree Physiol*, 26, 1257-70.
- Tasseva, G., Richard, L. & Zachowski, A. 2004. Regulation of phosphatidylcholine biosynthesis under salt stress involves choline kinases in Arabidopsis thaliana. *FEBS Lett*, 566, 115-20.
- Taylor, R. C., Cullen, S. P. & Martin, S. J. 2008. Apoptosis: controlled demolition at the cellular level. *Nat Rev Mol Cell Biol*, 9, 231-41.
- Ten Hove, C. A., Lu, K. J. & Weijers, D. 2015. Building a plant: cell fate specification in the early Arabidopsis embryo. *Development*, 142, 420-30.

- Tsiatsiani, L., Timmerman, E., De Bock, P. J., Vercammen, D., Stael, S., Van De Cotte, B., Staes, A., Goethals, M., Beunens, T., Van Damme, P., Gevaert, K. & Van Breusegem, F. 2013. The Arabidopsis metacaspase9 degradome. *Plant Cell*, 25, 2831-47.
- Tyerman, S. D., Niemietz, C. M. & Bramley, H. 2002. Plant aquaporins: multifunctional water and solute channels with expanding roles. *Plant Cell Environ*, 25, 173-194.
- Ueda, M., Zhang, Z. & Laux, T. 2011. Transcriptional activation of Arabidopsis axis patterning genes WOX8/9 links zygote polarity to embryo development. *Dev Cell*, 20, 264-70.
- Van Doorn, W. G., Beers, E. P., Dangl, J. L., Franklin-Tong, V. E., Gallois, P., Hara-Nishimura, I., Jones, A. M., Kawai-Yamada, M., Lam, E., Mundy, J., Mur, L. A., Petersen, M., Smertenko, A., Taliany, M., Van Breusegem, F., Wolpert, T., Woltering, E., Zhivotovsky, B. & Bozhkov, P. V. 2011. Morphological classification of plant cell deaths. *Cell Death Differ*, 18, 1241-6.
- Van Durme, M. & Nowack, M. K. 2016. Mechanisms of developmentally controlled cell death in plants. *Curr Opin Plant Biol*, 29, 29-37.
- Watanabe, N. & Lam, E. 2006. Arabidopsis Bax inhibitor-1 functions as an attenuator of biotic and abiotic types of cell death. *Plant J*, 45, 884-94.
- Watanabe, N. & Lam, E. 2008. BAX inhibitor-1 modulates endoplasmic reticulum stress-mediated programmed cell death in Arabidopsis. *J Biol Chem*, 283, 3200-10.
- Watrin, E., Schleiffer, A., Tanaka, K., Eisenhaber, F., Nasmyth, K. & Peters, J. M. 2006. Human Sec4 is required for cohesin binding to chromatin, sister-chromatid cohesion, and mitotic progression. *Curr Biol*, 16, 863-74.
- Weijers, D., Sauer, M., Meurette, O., Friml, J., Ljung, K., Sandberg, G., Hooykaas, P. & Offringa, R. 2005. Maintenance of embryonic auxin distribution for apical-basal patterning by PIN-FORMED-dependent auxin transport in Arabidopsis. *Plant Cell*, 17, 2517-26.
- Wendrich, J. R. & Weijers, D. 2013. The Arabidopsis embryo as a miniature morphogenesis model. *New Phytol*, 199, 14-25.
- Williams, E. G. & Maheswaran, G. 1986. Somatic Embryogenesis: Factors Influencing Coordinated Behaviour of Cells as an Embryogenic Group. *Annals of Botany*, 57, 443-462.
- Wrzaczek, M., Brosche, M., Kollist, H. & Kangasjarvi, J. 2009. Arabidopsis GRI is involved in the regulation of cell death induced by extracellular ROS. *Proc Natl Acad Sci U S A*, 106, 5412-7.
- Wrzaczek, M., Vainonen, J. P., Stael, S., Tsiatsiani, L., Help-Rinta-Rahko, H., Gauthier, A., Kaufholdt, D., Bollhoner, B., Lamminmaki, A., Staes, A., Gevaert, K., Tuominen, H., Van Breusegem, F., Helariutta, Y. & Kangasjarvi, J. 2015. GRIM REAPER peptide binds to receptor kinase PRK5 to trigger cell death in Arabidopsis. *Embo j*, 34, 55-66.
- Wu, S., Scheible, W. R., Schindelasch, D., Van Den Daele, H., De Veylder, L. & Baskin, T. I. 2010. A conditional mutation in Arabidopsis thaliana separase induces chromosome non-disjunction, aberrant morphogenesis and cyclin B1;1 stability. *Development*, 137, 953-61.
- Xu, G., Wang, S., Han, S., Xie, K., Wang, Y., Li, J. & Liu, Y. 2017. Plant Bax Inhibitor-1 interacts with ATG6 to regulate autophagy and programmed cell death. *Autophagy*, 13, 1161-1175.
- Yadegari, R., Paiva, G., Laux, T., Koltunow, A. M., Apuya, N., Zimmerman, J. L., Fischer, R. L., Harada, J. J. & Goldberg, R. B. 1994. Cell Differentiation and Morphogenesis Are Uncoupled in Arabidopsis raspberry Embryos. *Plant Cell*, 6, 1713-1729.
- Yang, X., Boateng, K. A., Yuan, L., Wu, S., Baskin, T. I. & Makaroff, C. A. 2011. The radially swollen 4 separase mutation of Arabidopsis thaliana blocks chromosome disjunction and disrupts the radial microtubule system in meiocytes. *PLoS One*, 6, e19459.
- Yoshida, S. & Uemura, M. 1986. Lipid Composition of Plasma Membranes and Tonoplasts Isolated from Etiolated Seedlings of Mung Bean (*Vigna radiata* L.). *Plant Physiol*, 82, 807-12.
- Zhang, D., Liu, D., Lv, X., Wang, Y., Xun, Z., Liu, Z., Li, F. & Lu, H. 2014. The cysteine protease CEP1, a key executor involved in tapetal programmed cell death, regulates pollen development in Arabidopsis. *Plant Cell*, 26, 2939-61.

- Zhao, P., Zhou, X. M., Zhang, L. Y., Wang, W., Ma, L. G., Yang, L. B., Peng, X. B., Bozhkov, P. V. & Sun, M. X. 2013. A bipartite molecular module controls cell death activation in the Basal cell lineage of plant embryos. *PLoS Biol*, 11, e1001655.
- Zhu, T., Moschou, P. N., Alvarez, J. M., Sohlberg, J. J. & Von Arnold, S. 2016a. WUSCHEL-RELATED HOMEODOMAIN 2 is important for protoderm and suspensor development in the gymnosperm Norway spruce. *BMC Plant Biol*, 16, 19.
- Zhu, T., Moschou, P. N., Alvarez, J. M., Sohlberg, J. J. & Von Arnold, S. 2016b. Wuschel-related homeobox 8/9 is important for proper embryo patterning in the gymnosperm Norway spruce. *J Exp Bot*, 65, 6543-52.

## Acknowledgements

Doing a PhD requires continuous support from parents, family members, supervisors, colleagues and friends. I am feeling lucky to have such a bunch of great people around me who continuously supported me throughout my life, especially during my PhD period and still doing so.

At first, I would pay my gratitude to my supervisor Prof. Peter Bozhkov for accepting me to do PhD research in his group and for his continuous guidance and support during my PhD study. Next, I would thank my cosupervisor Dr. Elena A. Minina for her constructive discussion and continuous support in the lab and teaching me how to do experiments properly. Many thanks to Dr. Hannele Tuominen for cosupervising me online and sharing some plant materials for experiments. I would thank Prof. Daniel Hofius, Dr. Mattias Thelander and Dr. Jens Sundström for evaluating my PhD progress and their suggestions during the evaluation meeting. I would specially thank Prof. Sara Von Arnold for arranging our Tuesday scientific meeting and her suggestions about my presentations and research. Thanks to our PhD director Prof. Christina Dixelius for taking care of my thesis writing.

I would pay my especial gratitude to Dr. Panagiotis Nikolaou Moschou for inviting me to join his projects and always trying to find some time for me when I needed to discuss any scientific matter or help with experiments. Panos, you are a real teacher. I would thank Dr. Emilio Gutiérrez Beltrán for guiding me throughout the PhD period for different experiments, especially during metacaspase interactor study. I appreciate the help of Dr. Kerstin Dalman and Pernilla Helena Elander from Department of Molecular science for translating my thesis abstract from English to Swedish. I would also thank rest of our group members whom I have worked with at different time points, especially Catarina, Prashanth and Ana, for their support and making good environment in the lab.

I appreciate the help of Dr. Nicolas Delhomme and Dr. Nathaniel R. Street from Umeå Plant Science Centre for arranging the RNA-seq of spruce embryo domains, doing the initial bioinformatics analysis, and always willing to discuss

issues when needed. I would also thank Dr. Simon Stael from VIB, Ghent and Dr. Nuria Sanchez Coll from CRAG, Barcelona for sharing some plant material for experiments. Special thanks go to Dr. Eugene Savenkov and Dr. Bijoy Sarosh as well for sharing some plasmids and plant material.

Many thanks go to Ramesh, Anders, Ooi-kock, Qinsong, Kai, Malin, Daniel, Joel, Tian, Irene and Jose for making good scientific and social environment in the lab. I would especially thank Tian, Daniel, Irene and Jose for sharing some plant material and their suggestions about the spruce genomics project. Kai, you helped me a lot by running my qPCR plates in my absence. Anders and Ooi-kock, you made the lab environment enjoyable with your funs and laughter and of course, your scientific instructions helped me a lot. I would also thank my office buddies Ramesh, Eric, Jennifer, Kai and Kerstin for making nice and social office environment.

I appreciate the help of Kanita for taking care of my spruce cali and would thank her for sharing some materials and obviously, I will remember her for being such a nice social person. I would thank Cecilia and Marie for their technical supports in the lab. Special thanks to Urban and Per for taking care of our green environment in the phytotron and greenhouse. Thank you Dr. Björn Nicander and Dr. Nils Mikkelsen (from Department of Molecular science) for taking care of my computer. I would thank Lotta, Qing, Monica, Mona and Anneli for their continuous administrative support throughout the PhD period.

I have also enjoyed my teaching period and so would like to thank Daniel Uddenberg, Izabela, Selcuk, Andrea, Sashi, Qinsong, Tian, Sultana, Rita, Shirin and Pruthvi. I have learned a lot from all you as well.

In a single sentence, I would thank all past and present colleagues at VBSG for creating such an enjoyable and friendly scientific environment.

I would thank my friends in Uppsala and Stockholm for making an enjoyable social life during my PhD period. I would especially thank Masud, Jamal, Russel, Shatu, Shipu, Shama, Foteh Ali, Fatima, Munna, Surovi, Azazul, Shoaib, Shabbir, Kabir and Manzur (my driving teacher) for being such a good friend who made my life enjoyable and easier in many aspects.

Last but not the least, I would thank all my teachers at different study levels and my family members for their continuous support. I am grateful to my parents-my first teachers, for teaching me to dream and their continuous support throughout my life to chase the dream. No word would be enough to express my gratitude to my wife Tania for her continuous support and sacrifice during my PhD period. You have done a great job by taking care of our son Tahsin almost alone, which is, in my opinion, more than a PhD degree. I would thank my parents-in-law as well for their continuous inspiration.

I

## RESEARCH ARTICLE

# The *Arabidopsis* homolog of Scc4/MAU2 is essential for embryogenesis

Elena A. Minina<sup>1,§,\*</sup>, Salim Hossain Reza<sup>1,2,\*</sup>, Emilio Gutierrez-Beltran<sup>1</sup>, Pernilla H. Elander<sup>1</sup>, Peter V. Bozhkov<sup>1,§</sup> and Panagiotis N. Moschou<sup>2,§</sup>

## ABSTRACT

Factors regulating dynamics of chromatin structure have direct impact on expression of genetic information. Cohesin is a multi-subunit protein complex that is crucial for pairing sister chromatids during cell division, DNA repair and regulation of gene transcription and silencing. In non-plant species, cohesin is loaded on chromatin by the Scc2–Scc4 complex (also known as the NIBPL–MAU2 complex). Here, we identify the *Arabidopsis* homolog of Scc4, which we denote *Arabidopsis thaliana* (At)SCC4, and show that it forms a functional complex with AtSCC2, the homolog of Scc2. We demonstrate that AtSCC2 and AtSCC4 act in the same pathway, and that both proteins are indispensable for cell fate determination during early stages of embryo development. Mutant embryos lacking either of these proteins develop only up to the globular stage, and show the suspensor overproliferation phenotype preceded by ectopic auxin maxima distribution. We further establish a new assay to reveal the AtSCC4-dependent dynamics of cohesin loading on chromatin *in vivo*. Our findings define the Scc2–Scc4 complex as an evolutionary conserved machinery controlling cohesin loading and chromatin structure maintenance, and provide new insight into the plant-specific role of this complex in controlling cell fate during embryogenesis.

**KEY WORDS:** *Arabidopsis*, Auxin, Cohesin-loading complex, Embryogenesis, MAU2, Scc4, NIBPL, Scc2

## INTRODUCTION

The establishment of sister chromatid cohesion and its controlled release is necessary for the proper segregation of chromosomes at mitosis and meiosis (Moschou and Bozhkov, 2012). Sister chromatids are bound and held together by multi-protein subunit complexes called cohesins (Nasmyth, 2001). Mutations in genes encoding cohesin subunits and their regulatory proteins are found in different types of cancer and in cohesinopathies, developmental disorders such as Cornelia de Lange syndrome, Roberts syndrome and the age-related increased occurrence of trisomy 21 (Barbero, 2013).

The cohesin complex belongs to the class of structural maintenance of chromosome (SMC) complexes (Cobbe and

Heck, 2004) and comprises four highly conserved core subunits: an SMC1 subunit, an SMC3 subunit, a stromalin subunit (e.g. Scc3; also known as STAG2) and a kleisin subunit [e.g. Scc1 (also known as Rad21) and Rec8] (Fig. 1A). Components of the cohesin complex are often represented by several homologs, and the function of cohesin complex is at least partially defined by the combination of the different subunit homologs it comprises. Most of the studied organisms have at least two kleisin subunit orthologs, functionally separated into those predominantly involved in mitosis or meiosis (Schleiffer et al., 2003). The *Arabidopsis* genome encodes four kleisin subunits (Fig. 1A): the meiosis-specific SYN1 (Cai et al., 2003) and SYN3, involved in gene expression of meiotic genes, but also expressed in somatic cells (Yuan et al., 2012; Jiang et al., 2007), and SYN2 and SYN4, which have been suggested to participate in mitotic cell division (da Costa-Nunes et al., 2006).

In non-plant species, e.g. *Saccharomyces cerevisiae*, *Saccharomyces pombe*, *Homo sapiens*, *Xenopus*, *Drosophila melanogaster* and *Coprinopsis cinerea*, the cohesin ring is loaded on chromatin and locked around DNA by the Scc2–Scc4 protein complex (Scc2 is also known as the NIBPL, and Scc4 as MAU2) in an ATP-dependent manner (Ciosk et al., 2000; Dorsett, 2004; Watrin et al., 2006; Arumugam et al., 2003). The cohesin-loading complex defines both the timing and initial location of cohesin rings on chromatin (Ciosk et al., 2000). Scc2 physically interacts with cohesin and its C-terminus is sufficient to entrap DNA in a cohesin ring *in vitro* (Chao et al., 2015).

The Scc4 subunit of the cohesin-loading complex contains multiple tetratricopeptide repeats (TPRs) forming a barrel-like superhelix essential for interaction with the N-terminus of Scc2 (Chao et al., 2015; Hinshaw et al., 2015). While Scc2 is required for closing the cohesin ring around DNA, Scc4 is necessary for delivering the complex to DNA *in vivo* (Chao et al., 2015; Hinshaw et al., 2015). A highly conserved region on the surface of Scc4 is required for targeting the Scc2–Scc4 complex to centromeric regions of chromosomes (Hinshaw et al., 2015).

Studies in yeast and animal systems have established cohesin as an essential actor in virtually all aspects of chromosome biology, including chromosome segregation, maintenance of genome stability, regulation of gene expression via defining chromatin structure, 3D genome organization (Watrin et al., 2016) and binding of enhancer RNAs (eRNAs) (Li et al., 2013). Loss-of-function mutants of *Arabidopsis thaliana* (At)SCC2 show phenotypes similar to mutants of the cohesin complex subunits, e.g. *Atsmc1* and *Atsmc3* (also known as *titan8* and *titan7*, respectively) (Tzafir et al., 2002; Liu et al., 2002). All these mutations cause embryonic lethality and formation of giant endosperm nuclei, indicating that these genes are indispensable for plant growth and development (Sebastian et al., 2009; Liu et al., 2002). In addition, transient induction of AtSCC2 silencing causes aberrations in meiosis, culminating in pollen abortion (Sebastian et al., 2009).

<sup>1</sup>Department of Molecular Sciences, Uppsala BioCenter, Swedish University of Agricultural Sciences and Linnean Center for Plant Biology, PO Box 7015, Uppsala SE-75007, Sweden. <sup>2</sup>Department of Plant Biology, Uppsala BioCenter, Swedish University of Agricultural Sciences and Linnean Center for Plant Biology, PO Box 7080, Uppsala SE-75007, Sweden.

\*These authors contributed equally to this work

§Authors for correspondence (alena.minina@slu.se; peter.bozhkov@slu.se; panagiotis.moschou@slu.se)

© E.A.M., 0000-0002-2619-1859; P.V.B., 0000-0002-8819-3884; P.N.M., 0000-0001-7212-0595

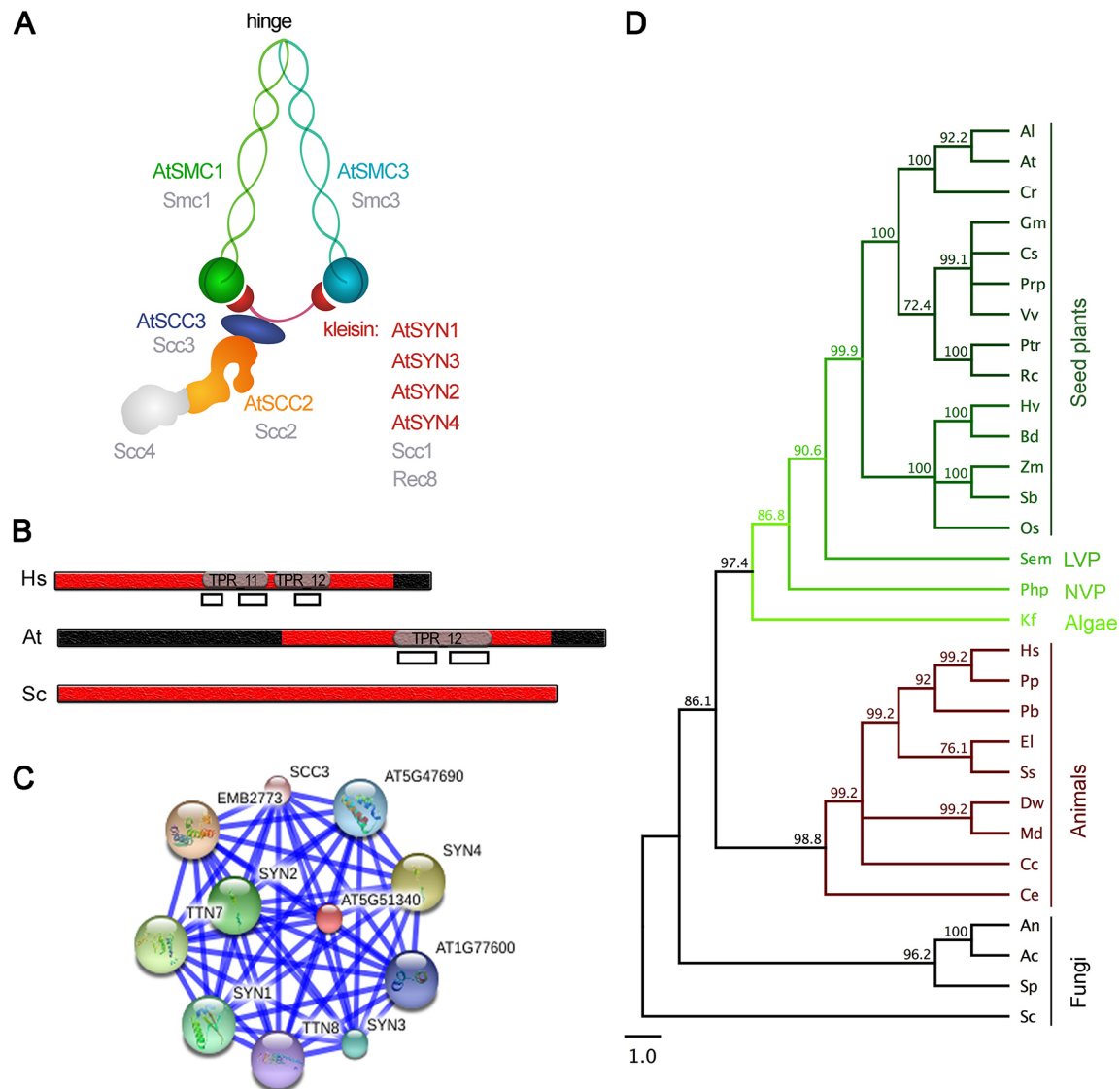


**Fig. 1. Analysis of Scc4 sequences.** (A) Schematic representation of cohesin and cohesin-loading complexes structures. Colored text indicates known orthologs in *Arabidopsis*; gray text denotes the yeast orthologs. SMC subunits self-fold through intramolecular antiparallel coiled-coil interactions, creating a rod-shaped molecule with an ATP-binding 'head' at one end and a 'hinge' domain at the other. Cohesin forms a tripartite ring in which SMC1 and SMC3 subunits associate with each other via their hinge domains, producing a V-shaped heterodimer (Melby et al., 1998; Anderson et al., 2002). The V-like structure is closed by the simultaneous binding of the N- and C-terminal regions of the kleisin (Scc2, Rec8) to the head domains of SMC3 and SMC1, respectively (Gruber et al., 2003; Nasmyth and Haering, 2005). The stromalin (Scc3) subunit of the cohesin complex binds the kleisin subunit to facilitate interaction between cohesin ring and its regulating complexes (Orgil et al., 2015). The NIBPL (Scc2) subunit of the cohesin-loading complex interacts directly with Scc3 and is sufficient for loading of cohesin rings on DNA *in vitro*. The MAU2 (Scc4) subunit is required for bringing the cohesin ring towards its loading location on the chromatin *in vivo*. (B) Domain organization of selected Scc4 orthologs. The predicted cohesin-loading motif is marked with red, empty rectangles indicate positions of the TPR within predicted structural motifs (TRP11 and TRP12; pfam IDs are PF13414 and PF13424, respectively). (C) Interactome of AtSCC4 predicted by the STRING database. AtSCC4 (AT5G51340) forms a network with known plant cohesin subunits, including stromalin (SCC3), kleisins SYN1, SYN2, SYN3 and SYN4, AtSMC1 (TTN8), AtSMC3 (TTN7), as well as with cohesin-loading (AtSCC2; EMBL2773), cohesin-unloading (PDS5a; AT5G47690) and PDS5b (AT1G77600) proteins. (D) Phylogenetic tree of Scc4 protein orthologs. *Saccharomyces cerevisiae* protein sequence was used as an out-group. The bootstrap values are indicated at the branching points. Accession numbers are provided in the Table S1. LVP, lower vascular plants; NVP, non-vascular land plants, Al, *Arabidopsis lyrata*; At, *Arabidopsis thaliana*; Cr, *Capsella rubella*; Gm, *Glycine max*; Cs, *Cucumis sativus*; Prp, *Prunus persica*; Vv, *Vitis vinifera*; Ptr, *Populus trichocarpa*; Rc, *Ricinus communis*; Hv, *Hordeum vulgare*; Bd, *Brachypodium distachyon*; Zm, *Zea mays*; Sb, *Sorghum bicolor*; Os, *Oryza sativa*; Sem, *Selaginella moellendorffii*; Php, *Physcomitrella patens*; Kf, *Klebsormidium flaccidum*; Hs, *Homo sapiens*; Pp, *Pan paniscus*; Pb, *Python bivittatus*; El, *Esox lucius*; Ss, *Salmo salar*; Dw, *Drosophila willistoni*; Md, *Musca domestica*; Cc, *Cyphomyrmex costatus*; Ce, *Caenorhabditis elegans*; An, *Aspergillus niger*; Ac, *Aspergillus calidoustus*; Sp, *Schizosaccharomyces pombe*; Sc, *Saccharomyces cerevisiae*.

Here, we identify and characterize AtSCC4, the *Arabidopsis* ortholog of Scc4. We show that it physically interacts with the N-terminal domain of AtSCC2 and is immobilized within interphase nuclei in an AtSCC2-independent manner. We demonstrate that each subunit of AtSCC2–AtSCC4 complex is indispensable for

plant embryogenesis and for controlling cell fate at the early stages of embryogenesis, but differ in their impact on seed endosperm development. Finally, we establish a novel *in vivo* assay for tracking cohesin-loading dynamics in *Arabidopsis* embryos, which allowed us to reveal that mitotic cohesin re-colocalizes to

chromatin during late telophase and that AtSCC4 is required for this process.

## RESULTS

### Identification and analysis of an *Arabidopsis* Scc4 homolog

A BLASTP search for Scc4 homologs in *Arabidopsis* using the *Homo sapiens* Scc4 (HsMau2) as a query revealed a single gene, At5g51340 ( $E$ -value= $7 \times 10^{-10}$ ). The At5g51340 encodes a putative protein of 726 amino acids with 78% and 24% of HsMau2 query coverage and identity, respectively. Protein sequence analysis revealed that the two typical tetratricopeptide repeats (TPR) that are present in Scc4 orthologs are arranged in tandem between amino acids 525 and 600, within a predicted structural motif TPR 12 (pfam13424, Marchler-Bauer et al., 2015) (Fig. 1B).

Searches for potential proteins that interact with At5g51340 using the STRING database (Szklarczyk et al., 2015) (Fig. 1C) predicted that it might form complexes with plant cohesin subunits and the cohesin-regulating proteins, thus supporting the hypothesis that At5g51340 (hereafter referred to as AtSCC4) is involved in sister chromatid cohesion.

A phylogenetic analysis of Scc4 orthologs revealed that plant Scc4 orthologs form a separate clade (Fig. 1D; Fig. S5). Scc4 orthologs demonstrated a high evolutionary divergence of their primary structure (Fig. S5) and significant similarity of their secondary structures. Conservation of tertiary structure might explain how highly different Scc4 orthologs play similar roles in loading of cohesin onto chromatin.

Despite having a conserved function in cell division, Scc4 family members show quite high divergence even within the same kingdom (Fig. 1D), suggesting that Scc4 might have also acquired specific functions in each lineage.

### Expression and localization analysis of AtSCC4

Analysis of the GENEVESTIGATOR microarray database revealed that AtSCC4 mRNA levels do not correlate with the mRNA levels of AtSCC2 and those of some of the kleisins (Fig. S1A). To further gain insight into the tissue-specific expression pattern of AtSCC4, we generated transgenic *Arabidopsis* lines expressing  $\beta$ -glucuronidase (GUS) under control of the AtSCC4 promoter (a 2 kb region upstream of the AtSCC4 start codon). Interestingly, we could detect GUS expression in all tissues examined, both in meristematic and non-meristematic cells (Fig. S1B).

We established transgenic *Arabidopsis* lines expressing an AtSCC4–GFP fusion protein under the control of the AtSCC4 native promoter to assess the turnover rate of AtSCC4 and further verify the presence of the AtSCC4 in different cell types (Fig. 2A). Expression of the full-length fusion protein in transgenic lines was confirmed by immunodetecting GFP (Fig. S1C). AtSCC4 was consistently observed in the nuclei and cytoplasm of differentiated and meristematic cells (Fig. 2A), indicating that, similarly to other Scc4 orthologs, AtSCC4 protein might act not only during cell division but also in the interphase (Peters et al., 2008; Ball et al., 2014).

In cells at the interphase and preprophase stages, most of the AtSCC4–GFP localized in the nucleus, but not in the nucleolus, and a weak signal was also detected in the cytoplasm (Fig. 2A,B), consistent with observations made in non-plant organisms, e.g. *Homo sapiens*, *Drosophila melanogaster* and *Caenorhabditis elegans* (Seitan et al., 2006; Benard et al., 2004). During prometaphase, metaphase, anaphase and telophase, the GFP signal was cytoplasmic (Fig. 2B) indicating that AtSCC4 does not decorate chromatin during cell division, when it would be expected

that cohesin would be removed from chromatids by the wings-apart-like (WAPL) and separase pathways (Buheitel and Stemmann, 2013; Gerlich et al., 2006; Moschou and Bozhkov, 2012). Shortly after completion of cell division, AtSCC4–GFP regained its nuclear localization (Fig. 2B). Split-nuclei inverse fluorescence recovery after photobleaching (iFRAP) (Fig. 2C,D) analyses showed that a significant portion of AtSCC4 is immobilized in the interphase nuclei, most probably by its association with chromatin (Fig. 2D,E). This result suggests the possible involvement of the plant cohesin-loading complex in sculpting chromatin of interphase nuclei (Lopez-Serra et al., 2014).

### Characterization and genetic analysis of *Atsc4* T-DNA mutants

We obtained two *Atsc4* transfer (T)-DNA insertional alleles from the SAIL and SALK mutant collections (Alonso, 2003). The corresponding alleles were designated *Atsc4-1* and *Atsc4-2*; the lines were shown to carry palindrome insertions in the 7th and 8th exons, respectively (Fig. S2A,B). Plants heterozygous for *Atsc4-1* and *Atsc4-2* showed no obvious growth phenotypes and had a similar AtSCC4 mRNA level to that in wild-type (Fig. S2C).

We were unable to identify homozygous mutants among the progeny of the heterozygous plants. The *Arabidopsis* genome is diploid and the 1:2:0 (wild-type:heterozygous:homozygous) segregation pattern for the *Atsc4* T-DNA insertions suggested that disruption of AtSCC4 could lead to embryo lethality (Fig. S2D). We examined siliques from *Atsc4-1/AtSCC4* and *Atsc4-2/AtSCC4* plants, and found that ~25% of the seeds were aborted in both mutant backgrounds (Fig. 3; Fig. S3A). Interestingly, we did not detect abnormalities in the transmission of T-DNA when pollen or ovules of mutants were used for crossing with ovules or pollen of wild-type (Fig. S2D). Lack of the phenotype in *Atsc4* gametes might be a consequence of carryover of AtSCC4 protein or mRNA from the parental tissues.

We analyzed seed abortion rate in the complemented *Atsc4-1/AtSCC4* and *Atsc4-2/AtSCC4* lines expressing AtSCC4–GFP under the control of the AtSCC4 native promoter (*Atsc4-1/AtSCC4 pAtSCC4::AtSCC4* and *Atsc4-2/AtSCC4 pAtSCC4::AtSCC4*, respectively) and determined that in the T1 generation of the complemented lines seed abortion decreased to the expected 6.25% (Fig. 3; Fig. S3A). Furthermore, in the T3 generation we were able to detect four viable homozygous-knockout *Atsc4-2 pAtSCC4::AtSCC4* plants in three independent complemented lines (Fig. S3B). Collectively, our results demonstrate that the observed seed abortion phenotype was caused by disruption of *AtSCC4*.

### AtSCC4 disruption impairs embryo development

To further investigate the cause of the seed abortion phenotype in *Atsc4/AtSCC4* mutants, we tracked phenotypes of *Atsc4/Atsc4*, *Atsc4/AtSCC4* and wild-type embryos throughout successive stages of embryogenesis. Zygotes of all backgrounds were normal, and the first cell division produced small apical and elongated basal cells (Fig. 4Aa,i). At the octant stage of embryo development, we observed the first aberrations in mutant embryos when cell division in the embryo proper became unsynchronized resulting in the disruption of the typical bilateral symmetry (Fig. 4Al). From the dermatogen stage onwards, ~25% of the embryos in siliques from *Atsc4-1/AtSCC4* and *Atsc4-2/AtSCC4* exhibited cell division defects in the embryo proper (Fig. 4Am–o), and at the heart stage, knockout embryos began to deteriorate (Fig. 4Ap). Following the octant stage, cell division defects were also observed in the suspensor of mutant embryos, wherein

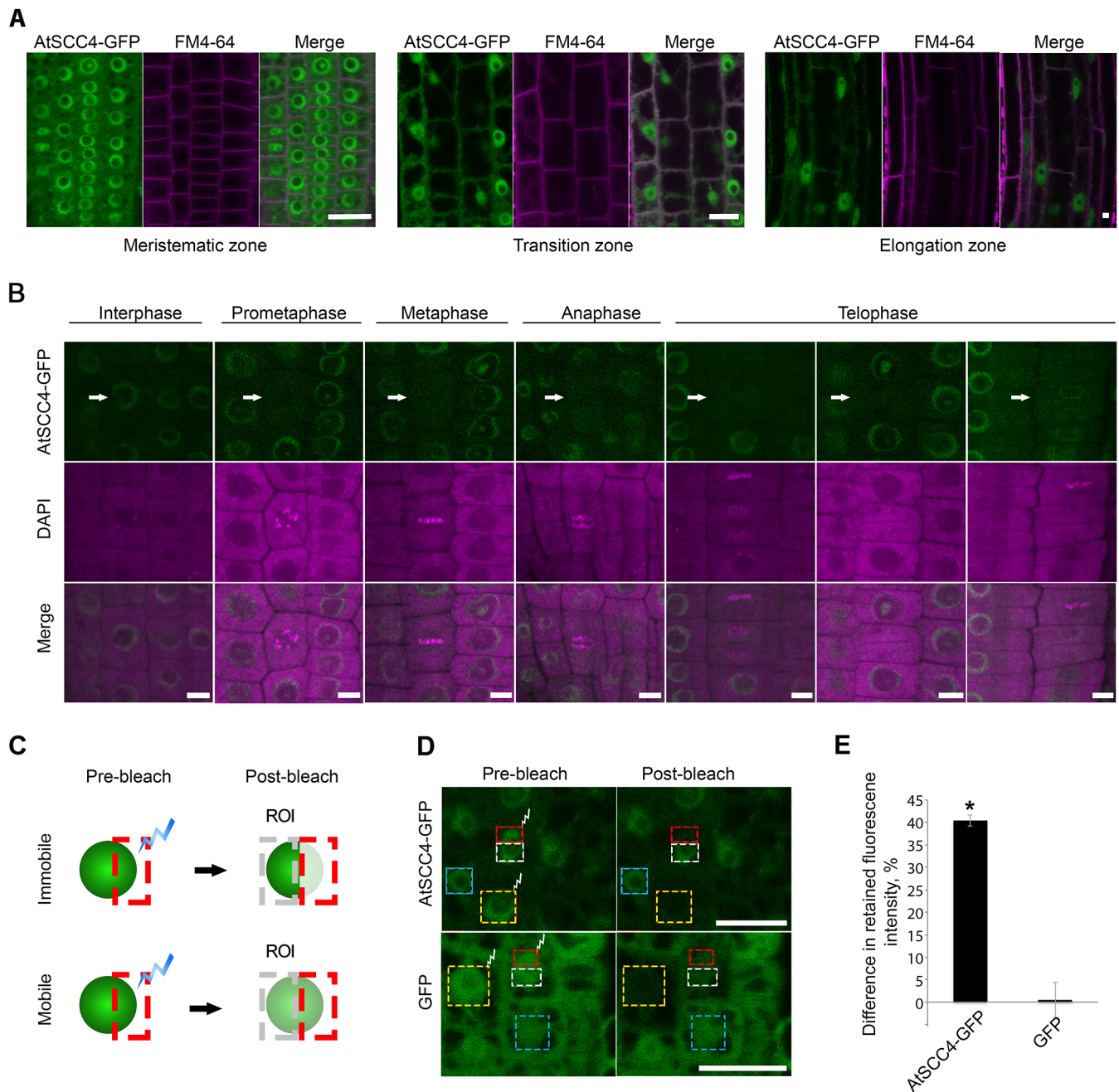


**Fig. 2. Localization of AtSCC4-GFP protein in root cells of *Arabidopsis*.** (A) Presence of AtSCC4 in root cells was assessed in plants expressing the AtSCC4-GFP fusion protein under the control of the *AtSCC4* promoter (*pAtSCC4::AtSCC4-GFP*). 35 individual lines were analyzed; images represent typical expression and localization patterns of the AtSCC4. AtSCC4 was detected in the meristematic, and transition and elongation zones of the roots. Regardless of the root zone, most of the AtSCC4 localized in nuclei and was excluded from nucleoli. A small fraction of the protein was present in the cytoplasm of the cells. 5  $\mu$ M FM4-64 was added to the medium to visualize cell membranes. Scale bars: 20  $\mu$ m. (B) Changes in AtSCC4 localization during cell division: AtSCC4 was excluded from chromatin at prometaphase and decorated it again in late telophase. AtSCC4 localization was assessed in root cells of fixed wild-type seedlings expressing *pAtSCC4::AtSCC4-GFP* stained with DAPI. Three individual lines were used in the experiment; images represent the typical localization of AtSCC4. Arrows indicate dividing cells. Scale bars: 5  $\mu$ m. (C) Schematic representation of a split nuclei iFRAP experiment. In the scenario shown on the top, a fluorescent protein of interest is immobilized. Bleaching of the selected region in a nucleus (red rectangle) only slightly affects the fluorescence signal in the region of interest (ROI, gray rectangle). In the scenario shown in the bottom, the fluorescent protein of interest is mobile, thus bleaching of the selected region causes a significant reduction of the signal in the ROI. (D) Split nuclei iFRAP assay of AtSCC4 reveals that a significant portion of nuclear AtSCC4 is immobilized, most probably by being associated with chromatin. Regions denoted by red rectangles were photobleached; ROIs are denoted by white rectangles. Nuclei within yellow or blue rectangles were fully bleached or unbleached, respectively. Scale bars: 20  $\mu$ m. (E) Quantification of iFRAP efficacy. Difference in retained fluorescence intensity between bleached and non-bleached area of a nucleus is proportional to the size of immobile fraction of the protein. Regions exposed to a high-intensity laser (red rectangles in D) were used to quantify the bleaching efficacy for each nucleus. Regions not exposed to a high-intensity laser (white rectangles in D) were used to assess retardation of fluorescent protein. Fully bleached nuclei (yellow rectangles in D) were used to estimate possible delivery of newly synthesized fluorescent protein from the cytoplasm. Unbleached nuclei (blue rectangles in D) were used to assess photobleaching caused by scanning. Data represent mean  $\pm$  s.e.m.,  $n=15$ . \* $P<0.0001$  (Dunnett's test versus GFP). Roots of *Arabidopsis* plants were mounted in 0.5 $\times$  MS medium.

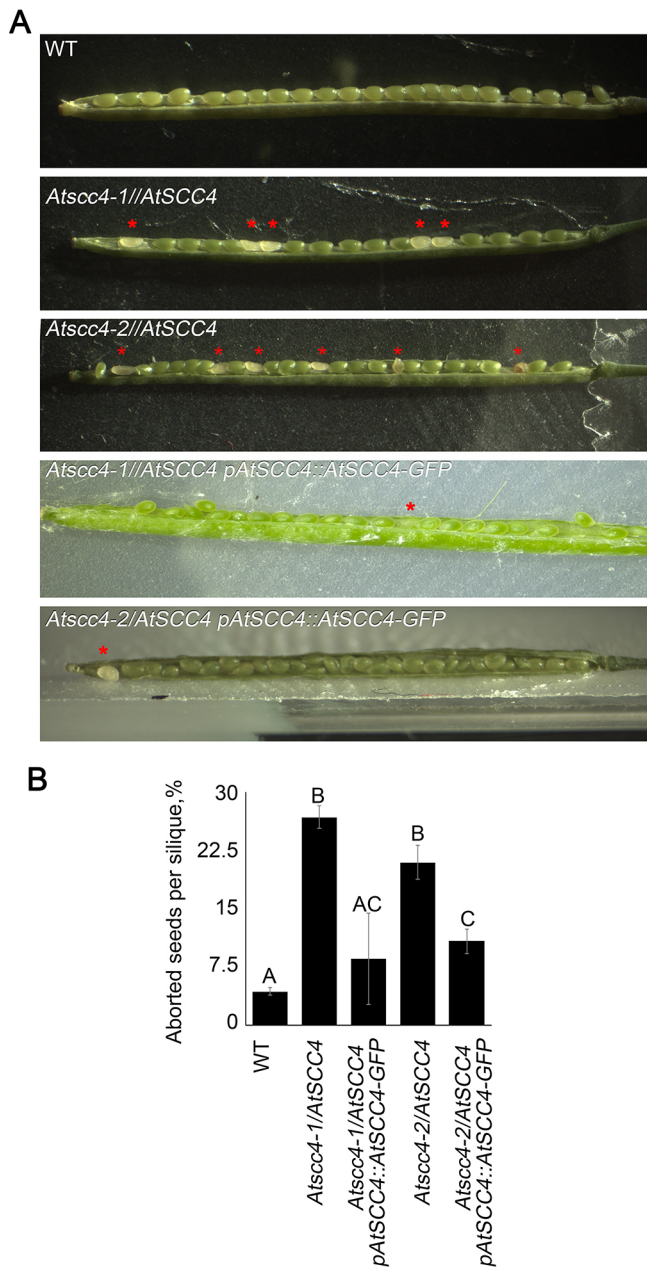


**Fig. 3. Depletion of AtSCC4 leads to seed abortion.** (A) Open siliques of Col-0 wild-type plants (WT), *Atsc4* heterozygous T-DNA insertion lines (*Atsc4-1/AtSCC4* and *Atsc4-2/AtSCC4*) and corresponding complemented lines (*Atsc4-1/AtSCC4 pAtSCC4::AtSCC4-GFP* and *Atsc4-2/AtSCC4 pAtSCC4::AtSCC4-GFP*). Aborted seeds are marked with a red asterisk. (B) Decrease of seed abortion frequency in the T1 generation of complemented lines confirms that the seed abortion phenotype was caused by the AtSCC4 deficiency. Data represent mean $\pm$ s.e.m.,  $n=10$ . Pairwise comparison of the means was performed using Student's *t*-test. Mean values showing statistically significant difference are annotated with different letters.

supernumerary cells were formed (Fig. 4Am–o), sometimes leading to a raspberry-like phenotype (Yadegari et al., 1994). These phenotypes were very similar to the embryo development aberrations associated with depletion of another subunit of the cohesin complex, AtSCC2 (Sebastian et al., 2009). Interestingly, in contrast to *AtSMC1*, *AtSMC3* or *AtSCC2* loss-of-function mutants, AtSCC4 deficiency did not cause severe developmental aberrations in the endosperm (Fig. 4B) (Tzafrir et al., 2002; Liu et al., 2002).

This indicates that the AtSCC2–AtSCC4 complex might play different roles in embryo and endosperm development, and that there might be additional cell division-related functions specific for each subunit.

### Disruption of the embryo proper in the cohesin-loading complex mutants compromises suspensor cell fate

The suspensor is a temporary structure of the plant embryo that serves as a conduit of nutrients and hormones to sustain the embryo proper (Yeung and Meinke, 1993; Friml et al., 2003). Although suspensor cells in *Arabidopsis* have embryogenic potential, they are destined to die during embryo maturation (Bozhkov et al., 2005). It has been suggested that the embryogenic potential of the suspensor cells is suppressed by the embryo proper and that the plant hormone auxin plays an important role in this process. Indeed, redistribution of auxin in the suspensor cells of *Arabidopsis* after laser ablation of the embryo proper precedes re-initiation of cell proliferation (Liu et al., 2015; Gooh et al., 2015).

To examine whether the increased embryogenic potential of suspensor cells in cohesin-loading complex mutants is associated with the redistribution of auxin response maxima, we introduced the auxin-response maxima reporter *DR5rev::3xVENUS-N7* (Heisler et al., 2005) into *Atsc4-1/AtSCC4* and *Atsc4-2/AtSCC2* backgrounds. While in the wild-type-like embryos the reporter was mostly observed in the upper part of the suspensor, *Atsc4-1* embryos displayed irregular distribution of the reporter (Fig. 5). Before the globular stage, the reporter was detectable in all cells of mutant embryos, with an atypically high intensity in the embryo proper. This abnormal pattern of auxin-response maxima coincided with the loss of cell division synchrony in the embryo proper and subsequently with the loss of bilateral symmetry and retardation of cell proliferation (Figs 4A and 5). From the globular stage onward, when cells of the *Atsc4-1* embryo proper showed signs of degradation, the auxin-response reporter was mostly visible in the suspensor cells, with the highest intensity observed in the basal cells (Fig. 5). This inverse distribution of auxin response maxima in the mutant embryos preceded the onset of ectopic cell division in the suspensors (Figs 4A and 5). Our observations strengthen the notion that the embryo proper of *Arabidopsis* produces an inhibitory signal blocking the embryogenic potential of the suspensor. Since similar patterns in the spatial distribution of auxin response maxima were observed in the *Atsc2-2* embryos (Fig. 5), we assumed that AtSCC2 and AtSCC4 might act in the same pathway during embryonic pattern formation.

### AtSCC4 directly interacts with AtSCC2

In yeast and animals, Scc2 physically interacts with Scc4 (Lopez-Serra et al., 2014). To investigate whether a similar complex is formed in plants, we first employed a yeast two-hybrid assay. We found that AtSCC4 associates with the N-terminus of AtSCC2 (Fig. 6A). To confirm this interaction in plants, we co-immunoprecipitated Myc-tagged AtSCC4 using a CFP-tagged AtSCC2 as a bait. For this experiment, both proteins were transiently co-expressed under the constitutive 35S CaMV (Cauliflower mosaic virus) promoter in *Nicotiana benthamiana* (Fig. 6B).

Next, we examined the genetic interaction between AtSCC2 and AtSCC4 by crossing heterozygous plants carrying an *Atsc4-1* or *Atsc4-2* mutant allele with heterozygous plants carrying an *Atsc2-2* or *Atsc2-3* mutant allele (Sebastian et al., 2009). We estimated the seed abortion rate in 200 siliques from 20 individual plants of the F1 generation. Seed abortion in siliques from *Atsc2/AtSCC2*;

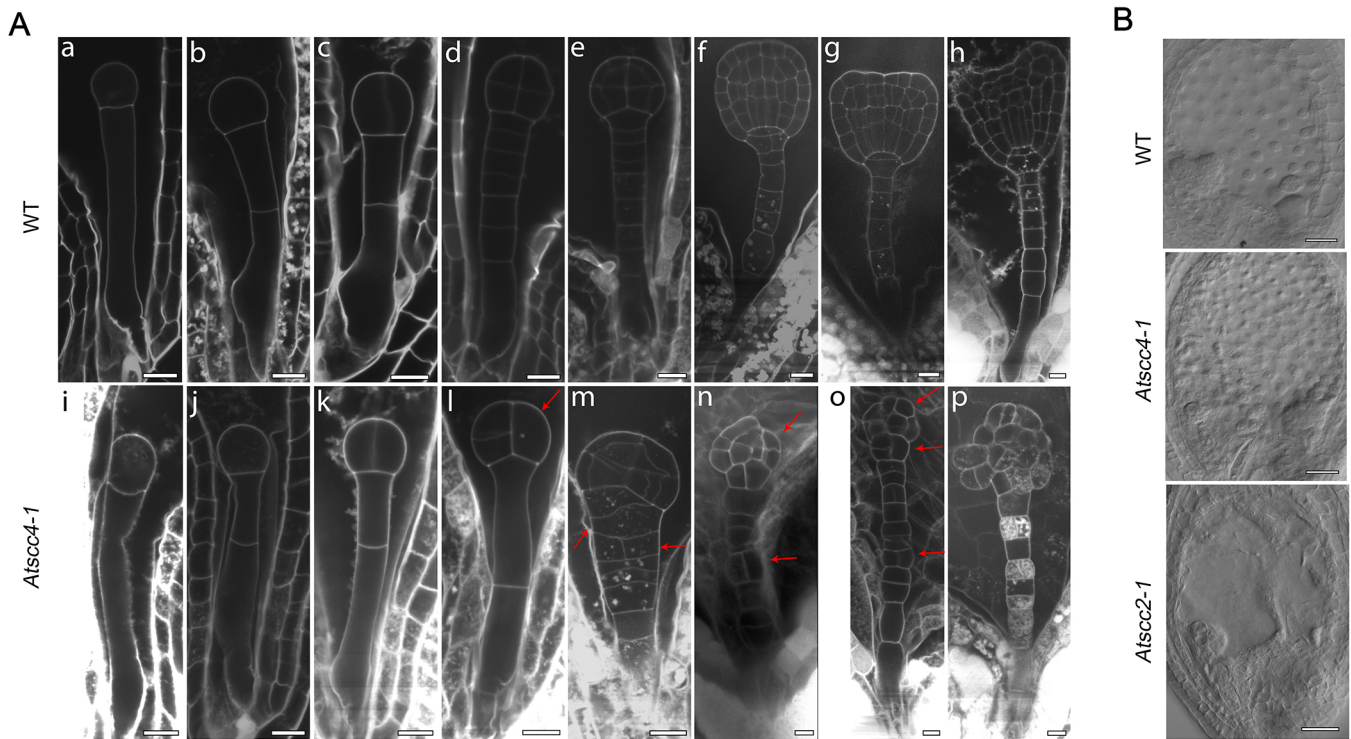


**Fig. 4. Loss-of-function mutants of AtSCC4 show an abnormal embryo phenotype but normal endosperm development.** (A) Propidium iodide staining of *AtScC4-1* and wild-type (WT) embryos. The earliest aberrations in the *AtScC4-1* embryos were visible at the octant stage. (a–h) WT; (i–p) *AtScC4-1* embryos. Embryos were imaged at the following stages; first cell division (a,i); second division (b,j); four cells (c,k); octant (d,l); dermatogen (e,m); globular (f,n); transition (g,o); heart (h,p). Images represent typical phenotype observed at the corresponding stage. The experiment was repeated three times with similar results. The developmental stage of mutant homozygous embryos was extrapolated from developmental stage of wild-type and heterozygous embryos from the same siliques. Red arrows, cells undergoing abnormal cell divisions. Scale bars: 10 µm. (B) Deficiency in AtSCC4 does not cause abnormalities in endosperm development, while lack of AtSCC2 causes a severe phenotype. DIC microscopy images of WT, *AtscC4-1* and *AtscC2-1* endosperm. Scale bars: 100 µm.

*AtscC4/AtSCC4* followed the predicted 9:7 segregation (number of viable seeds:number of aborted seeds). (The segregation rate was predicted based on the following assumptions: only one copy of the complementation insert was present in the diploid genome of the T1 generation of the complemented lines; the complementation insert was inherited independently from the corresponding *AtscC4* T-DNA insertion; only seeds containing embryos homozygous for the *AtscC4* T-DNA insertion would be aborted; and the presence of the complementation insert would restore viability of the embryos homozygous for the *AtscC4* T-DNA insertion) (Fig. S2E). We next assessed embryo development in the double *AtscC2/AtSCC2*; *AtscC4/AtSCC4* mutants by examining ~600 embryos. We did not observe an additive effect of the double mutation on the phenotype of early embryos when compared to the single *AtscC2/AtSCC2* or *AtscC4/AtSCC4* mutants. Collectively, these results confirm that AtSCC2 and AtSCC4 act in the same pathway during plant embryogenesis.

#### Immobilization of AtSCC4 in the nuclei does not depend on AtSCC2

Yeast Scc2 interacts with the cohesin ring and facilitates its loading on DNA *in vitro* in the absence of Scc4 (Chao et al., 2015), while Scc4 is required for loading cohesin rings at specific sites on chromosomes (Hinshaw et al., 2015). Immobilization of AtSCC4 in the nuclei is most likely a result of its association with chromatin and is indicative that AtSCC4 might serve as an adapter between the AtSCC2–cohesin complex and the sites of cohesin loading on chromatin. We investigated whether the immobilization of AtSCC4 was dependent on AtSCC2 by performing the split nuclei iFRAP

assay with AtSCC4–GFP expressed under *AtSCC4* promoter in *AtscC2-2* embryos (Fig. 7). The results revealed no statistically significant difference in the proportion of AtSCC4 immobilized on chromatin in wild-type or AtSCC2-deficient backgrounds, indicating that chromatin-mediated immobilization of AtSCC4 in the nuclei is independent of AtSCC2.

#### *In vivo* imaging of cohesin loading

In non-plant model organisms, e.g. *Saccharomyces cerevisiae*, *Saccharomyces pombe*, *Homo sapiens*, *Xenopus*, *Drosophila melanogaster* and *Coprinopsis cinerea*, the cohesin ring is loaded on chromatin by the Scc2–Scc4 complex (Fernius et al., 2013; Dorsett, 2004). *Arabidopsis* cohesin loading complex subunit AtSCC2 has been reported to control localization of cohesin during meiotic cell division, which was demonstrated using immunostaining of fixed plant material (Sebastian et al., 2009).

To examine the role of AtSCC4 in loading cohesin *in vivo*, we established a dedicated live-cell imaging assay. Constitutive expression of cohesin subunits using 35S promoter was shown to perturb *Arabidopsis* development (Yuan et al., 2014). To avoid this effect, we used the *ABA INSENSITIVE 3* (*ABI3*) promoter, which is relatively weak and, in seeds, mostly embryo specific (Devic et al., 1996; Ng et al., 2004), to drive expression of TagRFP fusions of the four known *Arabidopsis* kleisin subunits, RAD21.1/SYN2, RAD21.1.2/SYN3, RAD21.3/SYN4 and Rec8/SYN1 (da Costa-Nunes et al., 2006; Dong et al., 2001). The obtained constructs were introduced into wild-type and *AtscC4-1/AtSCC4* backgrounds. Notably, the T1 generation of all but the SYN4-expressing plants were highly susceptible to even mild environmental changes, and displayed decreased fertility phenotypes,

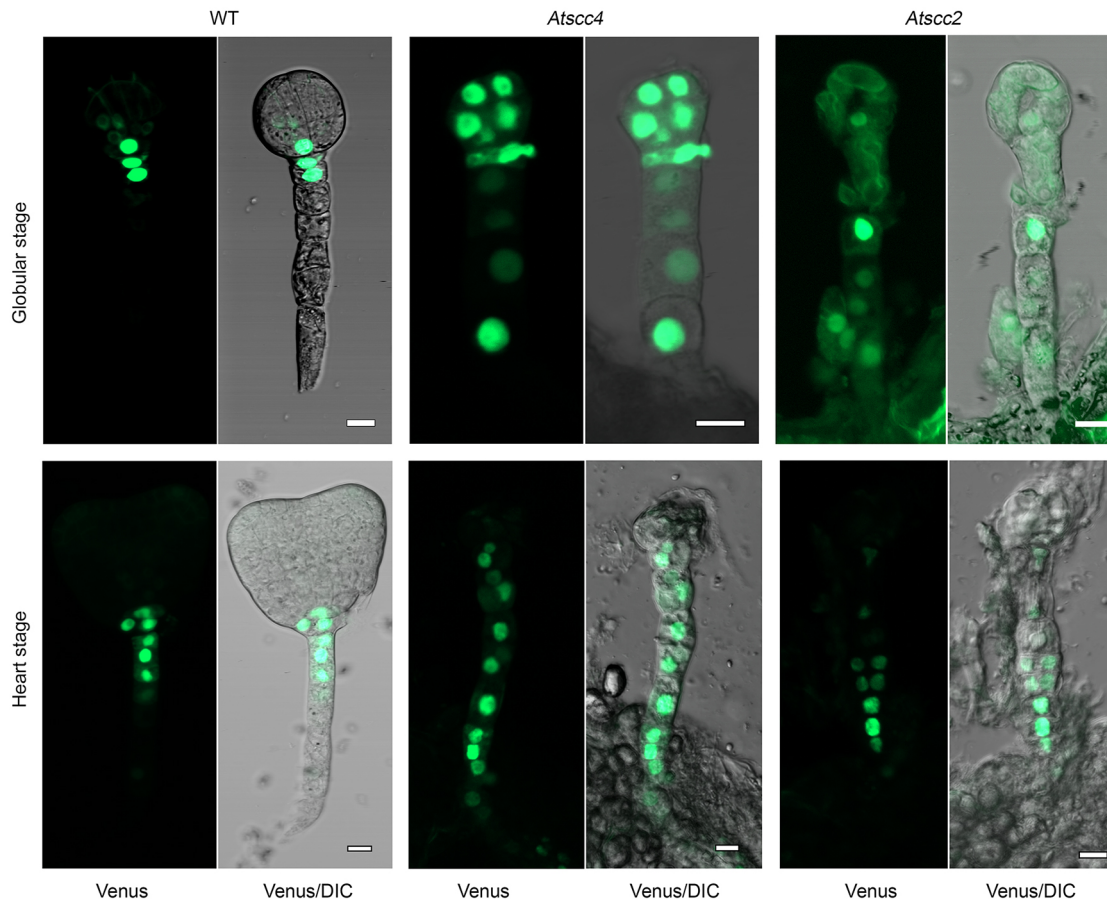


**Fig. 5. Lack of AtSCC4 or AtSCC2 causes a shift of auxin response maxima preceding proliferation of the suspensor.** Auxin response maxima in the wild-type (WT), *Atsc4* and *Atsc2* backgrounds were visualized using the reporter construct *DR5rev::3xVENUS-N7*, which encodes nuclei-targeted Venus fluorescent protein under the control of the auxin-responsive DR5rev promoter. An aberrant pattern of auxin response maxima in the mutants was detected at the early stages of development, prior to the onset of ectopic cell proliferation in suspensor (see globular stage). At later stages of development, mutant embryos exhibited inverse pattern of auxin response maxima, as compared to WT, with the peak response in the basal cells of the suspensors (see heart stage). Scale bars: 10  $\mu$ m.

e.g. development of short siliques with few seeds (Fig. S4). Interestingly, the aberrant phenotypes seemed to be dependent on the condition, probably following induction of *ABI3* promoter in response to short-term drought caused by strong ventilation in one of our growth chambers. SYN4–TagRFP-expressing plants did not display any noticeable phenotype in T1 and T2 generations and were used for further experiments. *Arabidopsis* plants of corresponding backgrounds expressing free TagRFP under the control of the *ABI3* promoter were used as a control.

TagRFP–SYN4 localized predominantly in the nuclei of embryonic cells, while free TagRFP was detected in both nuclei and cytoplasm (Fig. 8A). In accordance to the predicted activity of the *ABI3* promoter (Ng et al., 2004; supported also by the eFP browser and GENEVESTIGATOR), we observed a progressive increase of TagRFP–SYN4 or free TagRFP expression during embryogenesis, starting from the octant stage (Fig. 8B). In dividing cells, TagRFP–SYN4 was excluded from chromatin during metaphase and anaphase and colocalized with it again at late telophase (Fig. 8C). Surprisingly, we could detect a pool of TagRFP–SYN4 residing between separating chromosomes during anaphase (Fig. 8C). Under our experimental conditions, we failed to find embryonic cells in prometaphase to verify whether localization of SYN4 also correlates with the distribution of AtSCC4 at this stage. Collectively, our results suggest that, in plants, cohesin is

loaded on chromatin during the G1 phase and is already removed from chromatin by metaphase.

#### The AtSCC4 is required for cohesin immobilization in nuclei

Previous experiments performed on normal rat kidney (NRK) cells indicated that cohesin diffuses throughout the nucleus and cytosol and binds to unreplicated DNA with a residence time in the range of minutes (Gerlich et al., 2006). This ‘dynamic binding mode’ is thought to be the result of continuous loading of cohesin onto chromatin and subsequent release by WAPL (Buheitel and Stemann, 2013).

To analyze the mobility of plant cohesin, we performed iFRAP in interphase nuclei. The method was verified using wild-type plants expressing free TagRFP or TagRFP–SYN4 under the control of the *ABI3* promoter (Fig. 8D). We demonstrated that, in the wild-type background, TagRFP showed high motility while TagRFP–SYN4 was immobilized in the nuclei (Fig. 8D), thus confirming that iFRAP is an efficient method to study SYN4 motility.

Next, we assessed the efficacy of cohesin immobilization in nuclei of *AtSCC4* knockouts. We performed iFRAP analyses at the octant to globular stages of embryogenesis, when *Atsc4/Atsc4* embryos are still viable. In the wild-type background only a small fraction (~10%) of TagRFP–SYN4 signal was lost in the region of interest (ROI), suggesting strong immobilization of TagRFP–SYN4

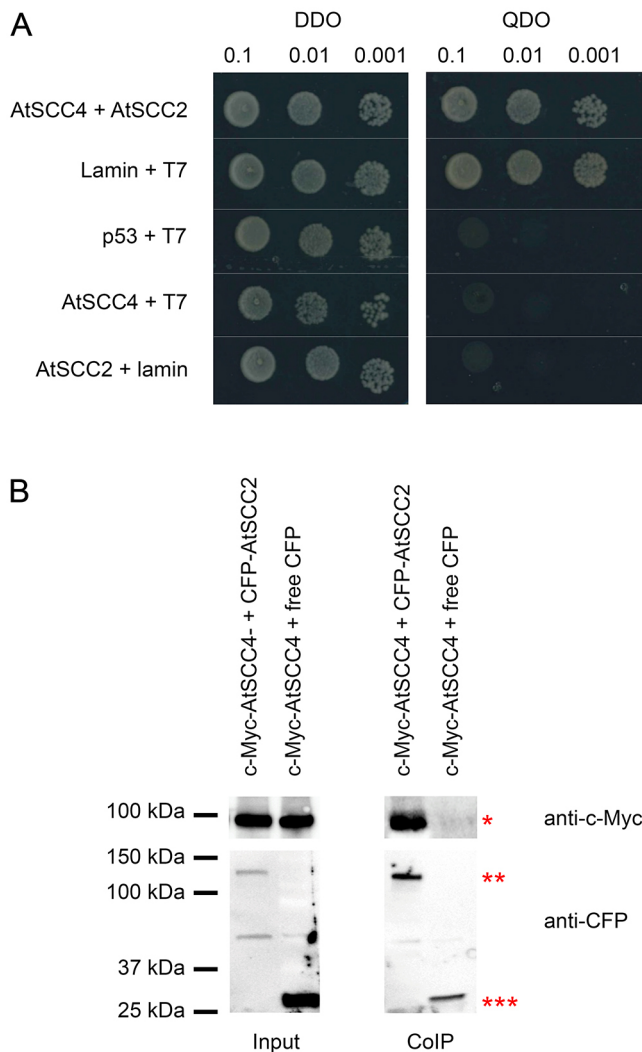


**Fig. 6. AtSCC4 interacts with the N-terminal domain of AtSCC2.** (A) Yeast two-hybrid assay shows strong interaction between full-length AtSCC4 and the N-terminus of AtSCC2. Transgenic yeast cells expressing AD- (GAL4 activation domain) and BD- (DNA-binding domain) fusion proteins were preselected on double drop-out medium (DDO) by plating 30  $\mu$ l of culture with an optical density at 600 nm ( $OD_{600}$ ) of 0.1, 0.01 or 0.001. Protein interaction was verified using quadruple dropout medium (QDO) and the same plating method. Lamin+T7, positive control; p53+T7, negative control; AtSCC4+T7 and AtSCC2+lamin, controls for autoactivation of the GAL promoter. (B) AtSCC4 interacts with N-terminal domain of AtSCC2 in plants. An co-IP assay was performed using protein extracts of *N. benthamiana* leaves transiently expressing Myc-tagged AtSCC4 together with CFP-tagged AtSCC2 or with free CFP. Nuclear protein fractions were purified using anti-YFP columns and blotted with anti-CFP and anti-Myc. \*, predicted molecular mass of Myc-AtSCC4; \*\*, predicted molecular mass of CFP-tagged N-terminal domain of AtSCC2; \*\*\*, predicted molecular mass of free CFP.

(Fig. 8E,F). By contrast, in *Atsc4/Atsc4* embryos, TagRFP-SYN4 was mostly mobile (Fig. 8E,F). These results strongly indicate the requirement of AtSCC4 protein for immobilizing plant cohesin in nuclei, most probably by anchoring it onto chromatin.

## DISCUSSION

### AtSCC4 is a nuclear protein required for embryonic cell fate determination

We demonstrate that, as with some other Scc4 orthologs (Seitan et al., 2006), most of the AtSCC4 localizes in the nucleus and is

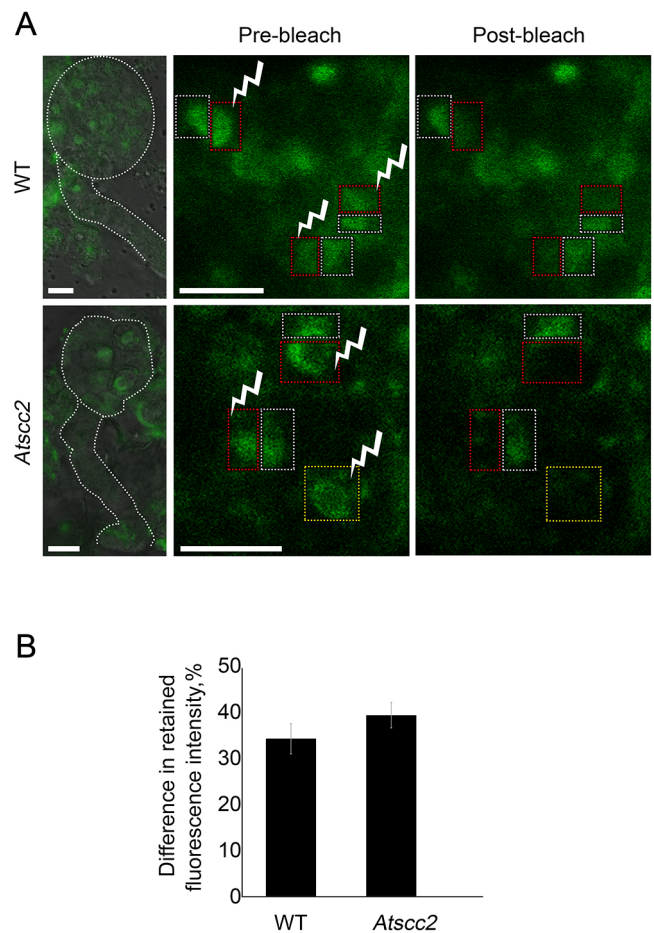


**Fig. 7. AtSCC2 is not required for immobilization of AtSCC4-GFP in nuclei.** (A) A split nuclei iFRAP assay of AtSCC4 in wild-type (WT) and AtSCC2-depleted (*Atsc2-2*) backgrounds reveals that AtSCC2 is not required for immobilization of AtSCC4 in nuclei. Red rectangles, photobleached regions; white rectangles, ROI; yellow rectangles, fully bleached nuclei. Dotted line designates shape of the embryo. Scale bars: 10  $\mu$ m. (B) Quantification of iFRAP efficacy. The difference in retained fluorescence intensity between the photobleached area of a nucleus and ROI is proportional to size of the immobile fraction of the protein. Photobleached area (red rectangles in A) were used to quantify bleaching efficacy for each nucleus. ROIs (white rectangles in A) were used to assess retardation of fluorescent protein. Fully bleached nuclei (yellow rectangles in A) were used to estimate possible delivery of newly synthesized fluorescent protein from the cytoplasm. Unbleached nuclei were used to assess photobleaching caused by scanning. Data represent mean  $\pm$  s.e.m.,  $n=10$ . The experiment was repeated twice. Student's two-tailed *t*-test revealed no statistically significant difference between iFRAP results for WT and *Atsc2-2* backgrounds.

excluded from the nucleolus, while a small amount of the protein can be detected in the cytoplasm (Fig. 2A,B). Furthermore, a large fraction of the AtSCC4 in interphase nuclei is immobile, most probably due to its association with chromatin.

Our genetic experiments confirm that AtSCC2 and AtSCC4 act in the same pathway, suggesting that plant Scc2-Scc4 is a functional complex. Similar to with loss-of-function mutations of some other cohesin-regulating proteins [e.g. AtSCC2 (Sebastian et al., 2009), separase AtESP (Liu and Makaroff, 2006) and either cohesin subunits, AtSMC1 and AtSMC3 (Tzafirir et al., 2002; Liu et al., 2002)], knockout of *AtSCC4* is embryonic lethal (Fig. 3; Figs S2D,E and S3A), thus confirming the crucial role of AtSCC4 in regulating cohesin. Loss-of-function mutants depleted of either cohesin or of cohesin-regulating proteins exhibit distinct phenotypes. Embryos of

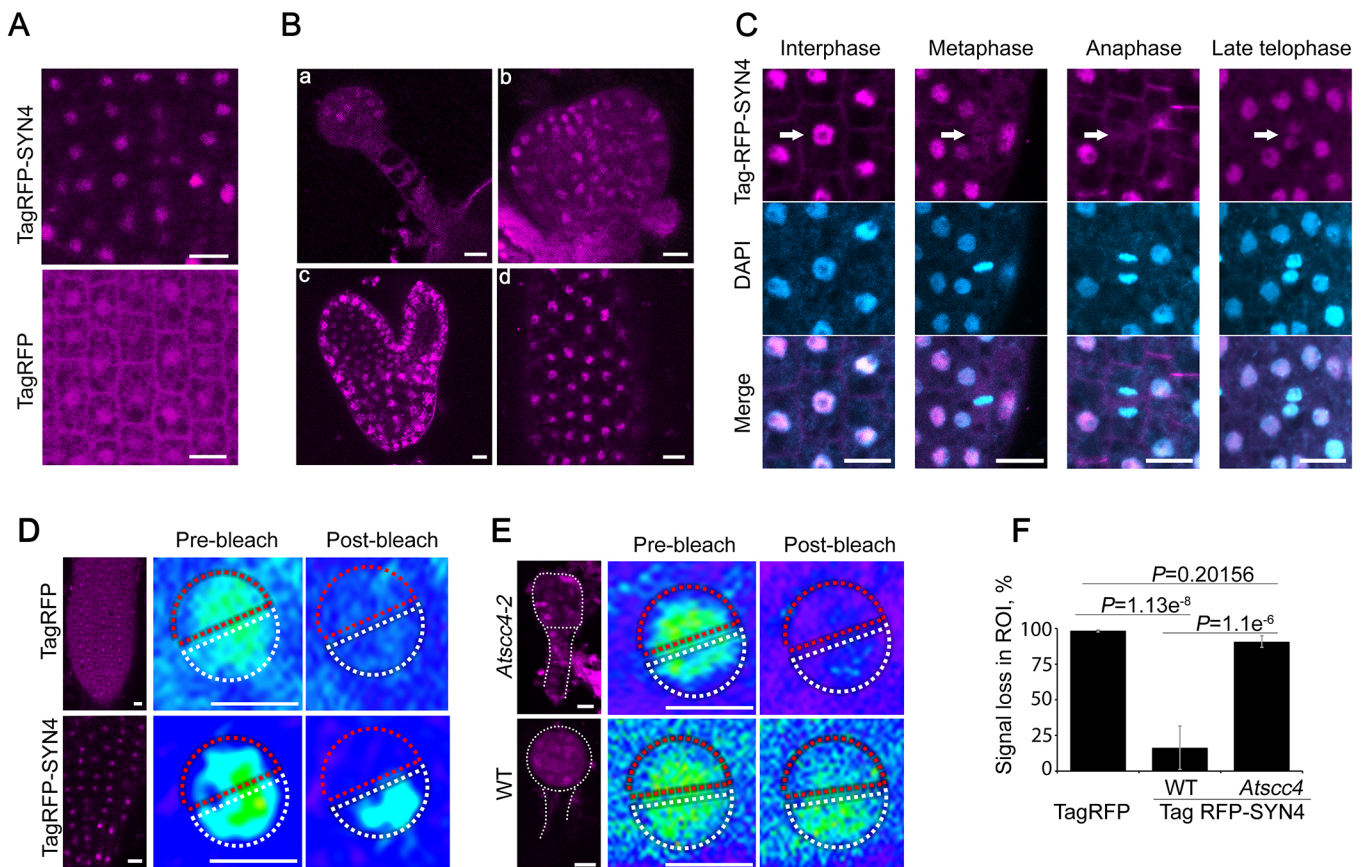


**Fig. 8. Cohesin re-colocalizes with chromatin in the G1 phase in an AtSCC4-dependent manner.** (A) Nuclear localization of SYN4 in the embryo hypocotyl cells expressing *pABI3::TagRFP-SYN4* (top) or *pABI3::TagRFP* (bottom). (B) *pABI3::TagRFP-SYN4* expression in the embryos at (a) globular, (b) transition, (c) heart and (d) bent cotyledons stages. (C) Localization dynamics of SYN4 during cell division: SYN4 is excluded from chromatin during metaphase and anaphase and colocalizes again with it at late telophase. SYN4 localization was assessed in fixed cells and stained with DAPI from wild-type embryos expressing *ABI3::TagRFP-SYN4*. Arrows indicate dividing cells. (D) In wild-type plants, SYN4 is tightly associated with chromatin. The *in vivo* cohesin-loading assay is based on split-nuclei iFRAP of *pABI3::TagRFP* (top) or *pABI3::TagRFP-SYN4* (bottom). Intensities in the nuclei are shown in a color-coded mode. Photobleached regions and regions of interest (ROI) are denoted with red and white dotted lines, respectively. Lower magnification images of embryo hypocotyl cells used in the experiment are shown on the left. Images are representative of an experiment repeated multiple times (>50 nuclei in three biological replicates). (E) AtSCC4 is indispensable for immobilization of SYN4 in nuclei. Split-nuclei iFRAP of *Atsc4-2* (top) and wild type (WT; bottom) globular stage embryos expressing *pABI3::TagRFP-SYN4*. Embryos are shown on the left, with the contours denoted by white dotted lines. Images are representative of an experiment repeated three times (ten nuclei in each experiment). (F) Quantification of the iFRAP efficacy. AtSCC4 deficiency leads to a dramatic increase in the motility of TagRFP-SYN4. Data represent mean  $\pm$  s.e.m.,  $n=3$ . The experiment was repeated three times. *P*-values determined by a one-way ANOVA test are indicated. Scale bars: 10  $\mu$ m.

*AtSMC1* or *AtSMC3* mutants (*ttn* mutants) arrest their development at very early stages, before the number of cells in the embryo exceeds five and cells start to enlarge (Liu et al., 2002). By contrast, embryos deficient in *AtSCC2*, *AtSCC4* or *AtESP*, can undergo multiple cell divisions prior to arrest (Liu and Makaroff, 2006; Yang et al., 2009). Efficient regulation of plant DNA packaging might require many more cohesin molecules, as compared to cohesin-regulating proteins. In such case, cohesin-regulating proteins carried over from heterozygous diploid precursors of gametes might be sufficient to sustain viability of a corresponding knockout embryo through multiple rounds of cell division. Alternatively, the stronger phenotype of SMC depletion might be due to additional important functions executed by SMC proteins, e.g. establishment of the microtubule arrays in the spindle and phragmoplast (Tzafir et al., 2002). Interestingly, in contrast to *AtSCC2*, *AtSMC1* and *AtSMC3* loss-of-function mutants, seeds of an *AtSCC4*-deficient background did not show severe abnormalities of endosperm development (Fig. 4B). This indicates that the two subunits of the *AtSCC2/4* complex might play different roles in endosperm and development of the embryo proper. Alternatively, milder phenotypes of the

*AtSCC4* loss-of-function mutants might be explained by the presence of *AtSCC4* protein carried over from the parental tissues through gametes.

The embryo phenotype observed in the *AtSCC4*-depleted embryos is similar to the previously reported phenotype of *AtSCC2* knockouts (Sebastian et al., 2009). With a low frequency, embryos of both mutants survived to develop into raspberry-like embryos. Raspberry-like embryos first display loss of symmetry and synchrony of cell divisions in the embryo proper, followed by developmental arrest (Yadegari et al., 1994). Instead of proliferating, cells of the embryo proper begin to expand, vacuolate and eventually die, mimicking the normal fate of suspensor cells. While suspensor cells acquire an embryo-proper-like fate and begin to divide. The mechanism underlying this shift of cell fate is still unknown. Laser ablation experiments have shown that removal of the embryo proper results in the induction of an embryo-proper-like pathway in the terminally differentiated suspensor cells, suggesting that the embryo proper produces a signal suppressing the embryogenic potential of suspensor cells (Liu et al., 2015; Gooh et al., 2015). This developmental transition

is associated with the redistribution of auxin. Here, we provide genetic evidence that auxin redistribution precludes ectopic cell proliferation in the suspensor and the degradation of the embryo proper (Fig. 5).

### AtSCC4 forms a stable complex with AtSCC2

In yeast and animal model organisms, Scc4 forms a stable complex with Scc2 (Ciosk et al., 2000; Watrin et al., 2006). The interacting interface comprises Scc4 TPR repeats, tandemly arranged short helices forming a superhelix that engulfs the unstructured N-terminus of Scc2 (Chao et al., 2015; Hinshaw et al., 2015). We demonstrate that AtSCC4 interacts with the N-terminus of AtSCC2 in yeast and in plants (Fig. 6), but this interaction is not necessary for immobilization of AtSCC4 in the nuclei (Fig. 7). This result indicates that, similar to for yeast Scc4 (Hinshaw et al., 2015), AtSCC4 might be determining sites for cohesin loading by recognizing receptor proteins on chromatin. Further work will show whether AtSCC4 forms an interacting scaffold for CHROMOSOME TRANSMISSION FIDELITY 7 (AtCtf) protein and how the Scc2–Scc4 complex is distributed along chromatin.

### AtSCC4 is essential for plant cohesin immobilization in the nuclei

We established a method for *in vivo* detection of cohesin immobilization dynamics during embryogenesis (Fig. 8). Overexpression of cohesin proteins affects meiotic cell division in *Arabidopsis* (Yuan et al., 2012). Therefore, we established lines expressing kleisin subunits under the control of the *ABI3* promoter, which has a relatively low and localized activity (Ng et al., 2004). Plants expressing TagRFP–SYN4 under control of the *ABI3* promoter did not show any aberrant phenotype and the expression level of SYN4 kleisin turned out to be optimal for microscopy. As expected, cohesin decorated plant chromatin during interphase, was removed by metaphase and colocalized with chromatin again at late telophase (Fig. 8C). The iFRAP assay confirmed immobilization of SYN4 in the nuclei, indicating its anchoring on chromatin in wild-type background and demonstrated requirement of AtSCC4 for cohesin loading *in vivo* (Fig. 8D–F). Importantly, analysis of dynamics of AtSCC4 and SYN4 colocalization with chromatin suggests that cohesin localization on chromatin upon cell division coincides with localization of AtSCC4 in the nuclei. This observation reinforces the mechanistic role of AtSCC4 in cohesin loading on chromatin.

### Conclusion

In this study, we identified and characterized the plant homolog of Scc4 and confirmed its evolutionary conserved features, such as a direct interaction with the N-terminal domain of Scc2. Our *in vivo* cohesin loading assay revealed the strict requirement of AtSCC4 for cohesin immobilization in the nuclei that most probably occurs due to loading of cohesin on chromatin. We also demonstrated the importance of the AtSCC2–AtSCC4 complex for cell fate determination. Further studies into the role of the cytoplasmic fraction of AtSCC4, as well as the interactome and possible post-translational modifications of AtSCC4, will provide clues to understanding its role in the spatiotemporal transcriptional regulation of gene expression and chromatin maintenance.

### MATERIALS AND METHODS

#### Identification of AtSCC4 and phylogenetic analysis

Scc4 homologs were identified using the default parameters of Protein Basic Local Alignment (Pblast) and Delta-BLAST tools. Obtained sequences were

aligned using the Clustal Omega tool (EMBL-EBI). Accession numbers are available in the Table S1 and alignment is available in the Fig. S5. The phylogenetic tree was built using the neighbor-joining method and software Geneious v6.1.8 (Saitou and Nei, 1987), with 2000 bootstrap test iterations (Felsenstein, 1985) and visualized with support threshold set to 70%.

The prediction of putative interactors of AtSCC4 was performed using STRING database (<http://string-db.org>; Szklarczyk et al., 2015).

#### *In silico* expression analysis

Expression of *AtSCC2*, *AtSCC4*, *SYN1*, *SYN2*, *SYN3* and *SYN4* in *Arabidopsis* tissues was estimated by using the Anatomy tool of the GENEVESTIGATOR database (<https://www.genevestigator.com>; Zimmermann et al., 2004) and the spatiotemporal expression tool of the eFP browser (<http://bar.utoronto.ca/~dev/eplant/>; Fucile et al., 2011).

#### Molecular biology

Sequences of all oligonucleotide primers used in this study can be found in Table S2.

#### Transcriptional reporters

The promoter of *AtSCC4* was amplified from the *Arabidopsis* genomic DNA using primers MAU2promFWGW/MAU2promRVGW and cloned into the pDONR/Zeo vector (Invitrogen, ThermoFisher Scientific, Waltham, USA). The obtained entry clone was recombined with pGWB3 vector (Nakagawa et al., 2007).

#### Translational reporter and complementation constructs

Full length *AtSCC4* (At5g51340) and its promoter was amplified from *Arabidopsis* genomic DNA using Fuc-Fw/MAU2RVGW primers and cloned into the pDONR/Zeo. The obtained entry clone was recombined with pGWB4 vector (Nakagawa et al., 2007).

#### Western blotting

Proteins were extracted from rosette leaves with Laemmli sample buffer (Laemmli, 1970), separated on 12% polyacrylamide gels and transferred onto a PVDF membrane. Anti-GFP (clone JL-8, Cat 632381, Lot A5033481, Clontech, Takara Bio Europe, Saint-Germain-en-Laye, France) was used at dilution 1:2000; HRP-conjugated anti-mouse-IgG (Cat NA931, Amersham, GE Healthcare, Uppsala, Sweden) was used at dilution 1:5000. The reaction was developed using an ECL Prime kit (Amersham, GE Healthcare, Uppsala, Sweden) and detected using ChemiDoc XRS+ and ImageLab software (BioRad, Solna, Sweden).

#### Constructs with the ABI3 promoter

The promoter of the *ABI3* (AT3G24650) gene was amplified from *Arabidopsis* genomic DNA using ABI3prFw/ABI3prRe primers and inserted into pGWB560 and 561 vectors using HindIII/XbaI sites. The coding sequences (CDS) of *SYN1* (At5g05490), *SYN2* (At5g40840.2), *SYN3* (At3g59550) and *SYN4* (At5g16270) were amplified using cDNA derived from 2-week-old leaves of *Arabidopsis* Col-0 plants and primers Fw\_SYN1/RV\_NS\_SYN1, Fw\_SYN2/RV\_NS\_SYN2, Fw\_SYN3/RV\_NS\_SYN3 and Fw\_SYN4/RV\_NS\_SYN4. PCR products were cloned into pDONR/Zeo. Obtained entry clones were recombined with pGWB560 ABI3 and pGWB561 ABI3 vectors.

#### Genotyping

A piece of rosette leaf was ground in 30  $\mu$ l of 0.5 M NaOH and resuspended in 370  $\mu$ l of 0.1 M Tris-HCl pH 8.0; 3  $\mu$ l of DNA solution were used per 15  $\mu$ l of PCR. Primers used for genotyping are listed in Table S1; genotyping of *AtSCC4* T-DNA insertion lines is presented in the Figs S2A,B and S3A. Genotyping of *AtSCC2* T-DNA insertion lines was previously described in Sebastian et al. (2009). For genotyping of the complementation lines, the *AtSCC4* wild-type allele was detected using primers AtSCC4 3UTR Re/Atscc4-F, the *Atscc4-2* T-DNA insertion was detected using primers Atscc4-R/LB1 SALK, and the complementation insert *pAtSCC4::AtSCC4-GFP* was detected with primers Atscc4-F/attB2.

### Co-immunoprecipitation

For the co-immunoprecipitation (co-IP) experiment, the *AtSCC4* and *AtSCC2* CDS were recombined into pGWB418 and pGWB641 (Nakagawa et al., 2007) vectors, respectively, and introduced into *Agrobacterium* strains GV3101. *N. benthamiana* leaves were co-infiltrated with cultures carrying Myc–SCC4 and CFP–SCC2, or Myc–SCC4 and free CFP. Samples were collected 2 days after infiltration, frozen and used for co-IP. Briefly, tissues were processed in nuclei isolation buffer [1 M hexyleneglycol, 20 mM PIPES-KOH pH 7.6, 10 mM MgCl<sub>2</sub>, 0.1 mM EGTA pH8, 20 mM NaCl, 60 mM KCl, 1× protease inhibitor (Cat P9599, Sigma, Stockholm, Sweden), 1% Triton X-100 and 5 mM β-mercaptoethanol] and incubated for 15 min at 4°C. Extracts were filtered through Miracloth and Partec CellTric filters (Cat 25004-0042-2316, Sysmex, Kungsbacka, Sweden) and centrifuged at 1500 g for 10 min at 4°C. The pelleted nuclei were resuspended and incubated for 1 h at 4°C in nuclei lysis buffer (50 mM Tris-HCl, pH 8, NaCl 400 mM and 0.1% NP-40) followed by sonication and centrifugation at 6000 g for 5 min at 4°C. Finally, nine volumes of nuclei buffer (50 mM Tris-HCl, pH 8, 1× protease inhibitor and 0.1% NP-40) were added to the supernatant. Co-IP was performed according to the manufacturer's instructions (μMACS GFP Isolation Kit; Cat 130-091-125, Miltenyi Biotec, Lund, Sweden). 1:1000 anti-Myc (Cat 11667149001, Roche, Stockholm, Sweden), 1:2000 anti-GFP (clone JL-8, Cat 632381, Lot A5033481, Clontech, Takara Bio Europe, Saint-Germain-en-Laye, France), 1:5000 HRP-conjugated anti-mouse-IgG (Cat NA931, Amersham, GE Healthcare, Uppsala, Sweden) and the ECL Prime kit (Amersham, GE Healthcare, Uppsala, Sweden) were used for the immunoblotting.

### qRT-PCR

RNA was extracted from 3-week-old seedlings of Col-0 wild-type, *Atsc4-1/AtSCC4* and *Atsc4-2/AtSCC4*, from three biological replicates per genotype. 400 ng RNA were used per reverse transcription reaction with a Maxima kit (Cat. K1671, ThermoFisher Scientific, Waltham, MA). qPCR was performed using CFX thermal cycler (Bio-Rad), DyNamo Flash qPCR kit (Cat F415S, ThermoFisher Scientific, Waltham, MA) and primers MAU2\_SAIL\_qPCR\_F/R, MAU2\_SALK\_qPCR\_F/R, PP2AqPCRf/R and HELqPCRf/R. Quantification of *AtSCC4* gene expression was assessed by ΔΔCt method (Livak and Schmittgen, 2001) and normalized to *PP2A* (At1g13320.1) and RNA helicase (At1g58050.1) expression (Czechowski et al., 2005).

### Plant growth and transformation

*Arabidopsis* seeds were surface sterilized using a 10% commercial bleach, rinsed with milli-Q water, and vernalized at 4°C for 24–48 h. Seeds were sown on half-strength Murashige and Skoog (MS) plates containing 0.8% (w/v) agar and 1% (w/v) sucrose. Plates were incubated under long-day conditions (16 h at 120 μE m<sup>-2</sup> s<sup>-1</sup> light intensity at 22°C, with an 8 h night at 20°C). For root microscopy assays, plates were kept vertically.

For growth in soil, vernalized seeds were sown directly on soil. Plants were grown under standard long-day conditions (16 h at 120 μE m<sup>-2</sup> s<sup>-1</sup> light intensity at 22°C, with an 8 h night at 20°C).

*Arabidopsis* Col-0 plants were transformed as described previously (Clough and Bent, 1998) using *Agrobacterium tumefaciens* strain GV3101.

### GUS assay

GUS detection was performed essentially as described previously (Fincato et al., 2012).

### Propidium iodide staining

Seeds were harvested and fixed overnight at 4°C in EtOH with acetic acid (9:1, v/v), treated with 1% SDS (w/v) and 0.2 M NaOH for 1 h at room temperature (RT), rinsed with water and incubated in 25% bleach solution for 1 min at RT. After rinsing with water, seeds were incubated in 1% (v/v) periodic acid at RT for 40 min, washed with water again and submerged in Schiff's reagent supplemented with propidium iodide (100 mM sodium metabisulfite and 0.15 N HCl; propidium iodide to a final concentration of 1 mg/ml was freshly added) until visibly stained. Excess staining was washed away with water, and seeds were mounted in chloral hydrate

solution (4 g chloral hydrate, 1 ml glycerol and 2 ml water), left for 1 h and then observed using a Zeiss CLSM780 microscope (Carl Zeiss GmbH, Jena, Germany) with excitation at 488 nm, emission at 568–735 nm and a 1 AU pinhole.

### Treatment of seeds for DIC microscopy

Seeds were taken out of the siliques, incubated on a sample glass in chloral hydrate solution (4 g chloral hydrate, 1 ml glycerol and 2 ml water) for 2 h at RT and observed using DIC optics with a AxioScope A1 microscope (Carl Zeiss GmbH, Jena, Germany) and ZEN lite software (Carl Zeiss GmbH, Jena, Germany).

### Auxin-responsive reporter

*Atsc4* and *Atsc2* T-DNA lines were crossed with plants expressing *DR5rev::3xVenus-N7* (Heisler et al., 2005). The F1 generation was genotyped to confirm the presence of the corresponding T-DNA. Siliques from selected plants were opened with a needle and fixed for 1 h in 3% (w/v) paraformaldehyde, 50 mM PIPES pH 6.8. Seeds were taken out, placed on a sample glass in Milli-Q water and gently pressed with the coverslip to release embryos. Only one silique at a time was analyzed to ensure that all embryos are at approximately the same developmental stage. Venus signal was detected using excitation at 514 nm, emission at 500–530 nm and the Zeiss CLSM 780 microscope. The experiment was repeated three times using plants grown either in the greenhouse or in the growth chamber; 28 to 42 embryos were imaged in each experiment.

### DAPI staining

Seeds or complete seedlings were fixed for 15–30 min in 3% (w/v) paraformaldehyde, 50 mM PIPES pH 6.8, rinsed with PBS three times and incubated for 15 min at RT in 4 μg/ml DAPI in PBS. Roots of seedlings were mounted and imaged using the Zeiss CLSM 780 microscope. Prior to imaging, embryos were taken out of seeds as described above.

### Yeast two-hybrid screen

Yeast two-hybrid analysis was performed using the Matchmaker Gold system (Clontech, Takara Bio Europe, Saint-Germain-en-Laye, France) using Y2HGold (*MATa/trp1-901/leu2-3/112/ura3-52/his3-200/gal4Δ/gal80Δ/LYS2::GAL1UAS-Gal1TATA-His3/GAL2UAS-Gal2TATA-Ade2/URA3::MEL1UAS-Mel1TATA-AURI-C/MEL1*) and Y187 (*MATa/ura3-52/his3-200/ade2-101/trp1-901/leu2-3, 112/gal4Δ/gal80Δ/URA3::GAL1UAS-GAL1TATA-lacZ*) strains for bait and prey constructs, respectively (Maier et al., 2008). The *AtSCC4* (At5g51340) CDS was amplified from cDNA derived from *Arabidopsis* Col-0 plants with MAU2FWGW/MAU2RVGW primers, cloned into the pDONR/Zeo and recombined with pGBKT7. The N-terminal part of *AtSCC2* (At5g15540) was amplified using the same cDNA and FwGWscc2/RVtruncation1GWscc2 primers, cloned into pDONR/Zeo and recombined into the prey vector pGADT7. Yeast transformation was performed by the LiAc/PEG method as described in Yeast Protocols Handbook (Clontech). Growth on quadruple dropout medium (QDO; –Ura, –His, –Trp, –Leu) plates indicated a positive interaction.

### FRAP assays

Zeiss CLSM 780 and ZEN Black software ZEN black (Carl Zeiss GmbH, Jena, Germany) were used for iFRAP experiments. Selected half of a nucleus was bleached using corresponding laser lines at 100% transmittance and 100 iterations. Typically, optical section size was optimized to fit the average diameter of nuclei in samples (6–9 μm). Three pre-bleach and at least 50 post-bleach images were acquired. Fluorescence intensity was measured in the not subjected to photobleaching regions of interest and in the photobleached regions. Average intensities of the three scans right before or after photobleaching were used for quantification. Loss of intensity or the retained intensity were calculated as the percentage of the corresponding pre-bleached value. A measurement made outside the bleached region was used as the background. Loss of intensity in a nucleus not subjected to photobleaching was used to assess bleaching

caused by scanning. Changes in the intensity in a fully bleached nucleus were used to assess the rate of possible import of fluorescent protein synthesized *de novo* into nuclei.

### Image and statistical analysis

ZEN black (Carl Zeiss GmbH, Jena, Germany) or ImageJ v 1.41 software (<http://rsb.info.nih.gov/ij/index.html>) were used for image analysis. Statistical analysis was performed using JMP software v11.

### Acknowledgements

We would like to thank Dr Eugene I. Savenkov for sharing material for some of the experiments and critical review of the results.

### Competing interests

The authors declare no competing or financial interests.

### Author contributions

P.N.M. and E.A.M. conceptualized the project, designed and performed most of the experiments, analyzed the data, prepared figures and wrote the manuscript. S.H.R. and P.H.E. performed some experiments, E.G.-B. performed optimization of the yeast two-hybrid assay and the co-IP assay. P.V.B. participated in experimental design, discussion of results and writing of the manuscript.

### Funding

This work was supported by grants from Vetenskapsrådet (Swedish Research Council; to P.N.M. and P.V.B.), Pehrssons Fund (to P.V.B.), Stiftelsen för Strategisk Forskning (Swedish Foundation for Strategic Research (to P.V.B.)), Stiftelsen Olle Engkvist Byggmästare (Olle Engkvist Foundation; to P.V.B.), the Knut och Alice Wallenbergs Stiftelse (Knut and Alice Wallenberg Foundation; to P.V.B.) and the Carl Tryggers Stiftelse för Vetenskaplig Forskning (Carl Tryggers Foundation; to E.A.M. and P.N.M.).

### Supplementary information

Supplementary information available online at <http://jcs.biologists.org/lookup/doi/10.1242/jcs.196865.supplemental>

### References

- Alonso, J. M. (2003). Genome-wide insertional mutagenesis of *Arabidopsis thaliana* (vol 301, pg 653, 2003). *Science* **301**, 1849-1849.
- Anderson, D. E., Losada, A., Erickson, H. P. and Hirano, T. (2002). Condensin and cohesin display different arm conformations with characteristic hinge angles. *J. Cell. Biol.* **156**, 419-424.
- Arumugam, P., Gruber, S., Tanaka, K., Haering, C. H., Mechtler, K. and Nasmyth, K. (2003). ATP hydrolysis is required for cohesin's association with chromosomes. *Curr. Biol.* **13**, 1941-1953.
- Ball, A. R., Jr, Chen, Y.-Y. and Yokomori, K. (2014). Mechanisms of cohesin-mediated gene regulation and lessons learned from cohesinopathies. *Biochim. Biophys. Acta* **1839**, 191-202.
- Barbero, J. L. (2013). Genetic basis of cohesinopathies. *Appl. Clin. Genet.* **6**, 15-23.
- Bénard, C. Y., Kébir, H., Takagi, S. and Hekimi, S. (2004). mau-2 acts cell-autonomously to guide axonal migrations in *Caenorhabditis elegans*. *Development* **131**, 5947-5958.
- Bozhkov, P. V., Filonova, L. H. and Suarez, M. F. (2005). Programmed cell death in plant embryogenesis. *Curr. Top. Dev. Biol.* **67**, 135-179.
- Buheitel, J. and Stemmann, O. (2013). Prophase pathway-dependent removal of cohesin from human chromosomes requires opening of the Smc3-Scc1 gate. *EMBO J.* **32**, 666-676.
- Cai, X., Dong, F., Edelman, R. E. and Makaroff, C. A. (2003). The *Arabidopsis* SYN1 cohesin protein is required for sister chromatid arm cohesion and homologous chromosome pairing. *J. Cell Sci.* **116**, 2999-3007.
- Chao, W. C. H., Murayama, Y., Muñoz, S., Costa, A., Uhlmann, F. and Singleton, M. R. (2015). Structural studies reveal the functional modularity of the Scc2-Scc4 cohesin loader. *Cell Rep.* **12**, 719-725.
- Ciosk, R., Shirayama, M., Shevchenko, A., Tanaka, T., Toth, A., Shevchenko, A. and Nasmyth, K. (2000). Cohesin's binding to chromosomes depends on a separate complex consisting of Scc2 and Scc4 proteins. *Mol. Cell* **5**, 243-254.
- Clough, S. J. and Bent, A. F. (1998). Floral dip: a simplified method for *Agrobacterium*-mediated transformation of *Arabidopsis thaliana*. *Plant J.* **16**, 735-743.
- Cobbe, N. and Heck, M. M. S. (2004). The evolution of SMC proteins: phylogenetic analysis and structural implications. *Mol. Biol. Evol.* **21**, 332-347.
- Czechowski, T., Stitt, M., Altmann, T., Udvardi, M. K. and Scheible, W. R. (2005). Genome-wide identification and testing of superior reference genes for transcript normalization in *Arabidopsis*. *Plant Physiology* **139**, 5-17.
- da Costa-Nunes, J. A., Bhatt, A. M., O'Shea, S., West, C. E., Bray, C. M., Grossniklaus, U. and Dickinson, H. G. (2006). Characterization of the three *Arabidopsis thaliana* RAD21 cohesins reveals differential responses to ionizing radiation. *J. Exp. Bot.* **57**, 971-983.
- Devic, M., Albert, S. and Delseny, M. (1996). Induction and expression of seed-specific promoters in *Arabidopsis* embryo-defective mutants. *Plant J.* **9**, 205-215.
- Dong, F., Cai, X. and Makaroff, C. A. (2001). Cloning and characterization of two *Arabidopsis* genes that belong to the RAD21/REC8 family of chromosome cohesin proteins. *Gene* **271**, 99-108.
- Dorsett, D. (2004). Adherin: key to the cohesin ring and cornelia de lange syndrome. *Curr. Biol.* **14**, R834-R836.
- Felsenstein, J. (1985). Confidence-limits on phylogenies: an approach using the bootstrap. *Evolution* **39**, 783-791.
- Fernius, J., Nerusheva, O. O., Galander, S., de Lima Alves, F., Rappsilber, J. and Marston, A. L. (2013). Cohesin-dependent association of Scc2/4 with the centromere initiates pericentromeric cohesion establishment. *Curr. Biol.* **23**, 599-606.
- Fincato, P., Moschou, P. N., Ahou, A., Angelini, R., Roubelakis-Angelakis, K. A., Federiki, R. and Tavladoraki, P. (2012). The members of *Arabidopsis thaliana* PAO gene family exhibit distinct tissue- and organ-specific expression pattern during seedling growth and flower development. *Amino Acids* **42**, 831-841.
- Friml, J., Vieten, A., Sauer, M., Weijers, D., Schwarz, H., Hamann, T., Offringa, R. and Jürgens, G. (2003). Efflux-dependent auxin gradients establish the apical-basal axis of *Arabidopsis*. *Nature* **426**, 147-153.
- Fucile, G., Di Biase, D., Nahal, H., La, G., Khodabandeh, S., Chen, Y. N., Easley, K., Christendat, D., Kelley, L. and Provart, N. J. (2011). ePlant and the 3D data display initiative: integrative systems biology on the world wide web. *PLoS ONE* **6**, e15237.
- Gerlich, D., Koch, B., Dupeux, F., Peters, J.-M. and Ellenberg, J. (2006). Live-cell imaging reveals a stable cohesin-chromatin interaction after but not before DNA replication. *Curr. Biol.* **16**, 1571-1578.
- Gooh, K., Ueda, M., Aruga, K., Park, J., Arata, H., Higashiyama, T. and Kurihara, D. (2015). Live-cell imaging and optical manipulation of *Arabidopsis* early embryogenesis. *Dev. Cell* **34**, 242-251.
- Gruber, S., Haering, C. H. and Nasmyth, K. (2003). Chromosomal cohesin forms a ring. *Cell* **112**, 765-777.
- Heisler, M. G., Ohno, C., Das, P., Sieber, P., Reddy, G. V., Long, J. A. and Meyerowitz, E. M. (2005). Patterns of auxin transport and gene expression during primordium development revealed by live imaging of the *Arabidopsis* inflorescence meristem. *Curr. Biol.* **15**, 1899-1911.
- Hinshaw, S. M., Makrantonis, V., Kerr, A., Marston, A. L. and Harrison, S. C. (2015). Structural evidence for Scc4-dependent localization of cohesin loading. *Elife* **4**, e06057.
- Jiang, L., Xia, M., Strittmatter, L. I. and Makaroff, C. A. (2007). The *Arabidopsis* cohesin protein SYN3 localizes to the nucleolus and is essential for gametogenesis. *Plant J.* **50**, 1020-1034.
- Laemmli, U. K. (1970). Cleavage of structural proteins during the assembly of the head of bacteriophage T4. *Nature* **227**, 680-685.
- Li, W. B., Notani, D., Ma, Q., Tanasa, B., Nunez, E., Chen, A. Y., Merkurjev, D., Zhang, J., Ohgi, K., Song, X. Y. et al. (2013). Functional roles of enhancer RNAs for oestrogen-dependent transcriptional activation. *Nature* **498**, 516-520.
- Liu, Z. and Makaroff, C. A. (2006). *Arabidopsis* separase AESP is essential for embryo development and the release of cohesin during meiosis. *Plant Cell* **18**, 1213-1225.
- Liu, C.-M., McElver, J., Tzafir, I., Joosen, R., Wittich, P., Patton, D., Van Lammeren, A. A. and Meinke, D. (2002). Condensin and cohesin knockouts in *Arabidopsis* exhibit a titan seed phenotype. *Plant J.* **29**, 405-415.
- Liu, Y., Li, X. B., Zhao, J., Tang, X. C., Tian, S. J., Chen, J. Y., Shi, C., Wang, W., Zhang, L. Y., Feng, X. Z. et al. (2015). Direct evidence that suspensor cells have embryogenic potential that is suppressed by the embryo proper during normal embryogenesis (vol 112, pg 12432, 2015). *P. Natl. Acad. Sci. USA* **112**, E6078-E6078.
- Livak, K. J. and Schmittgen, T. D. (2001). Analysis of relative gene expression data using real-time quantitative PCR and the 2<sup>(-T)</sup>(-Delta Delta C) method. *Methods* **25**, 402-408.
- Lopez-Serra, L., Kelly, G., Patel, H., Stewart, A. and Uhlmann, F. (2014). The Scc2-Scc4 complex acts in sister chromatid cohesion and transcriptional regulation by maintaining nucleosome-free regions. *Nat. Genet.* **46**, 1147-1151.
- Maier, R. H., Brandner, C. J., Hintner, H., Bauer, J. W. and Onder, K. (2008). Construction of a reading frame-independent yeast two-hybrid vector system for site-specific recombinational cloning and protein interaction screening. *Biotechniques* **45**, 235-244.
- Marchler-Bauer, A., Derbyshire, M. K., Gonzales, N. R., Lu, S., Chitsaz, F., Geer, L. Y., Geer, R. C., He, J., Gwadz, M., Hurwitz, D. I. et al. (2015). CDD: NCBI's conserved domain database. *Nucleic Acids Res.* **43**, D222-D226.
- Melby, T. E., Ciampaglio, C. N., Briscoe, G. and Erickson, H. P. (1998). The symmetrical structure of structural maintenance of chromosomes (SMC) and MukB proteins: long, antiparallel coiled coils, folded at a flexible hinge. *J. Cell. Biol.* **142**, 1595-1604.

- Moschou, P. N. and Bozhkov, P. V.** (2012). Separases: biochemistry and function. *Physiol. Plantarum* **145**, 67-76.
- Nakagawa, T., Kurose, T., Hino, T., Tanaka, K., Kawamukai, M., Niwa, Y., Toyooka, K., Matsuoka, K., Jinbo, T. and Kimura, T.** (2007). Development of series of gateway binary vectors, pGWBs, for realizing efficient construction of fusion genes for plant transformation. *J. Biosci. Bioeng.* **104**, 34-41.
- Nasmyth, K.** (2001). Disseminating the genome: joining, resolving, and separating sister chromatids during mitosis and meiosis. *Annu. Rev. Genet.* **35**, 673-745.
- Nasmyth, K. and Haering, C. H.** (2005). The structure and function of SMC and kleisin complexes. *Annu. Rev. Biochem.* **74**, 595-648.
- Ng, D. W.-K., Chandrasekharan, M. B. and Hall, T. C.** (2004). The 5' UTR negatively regulates quantitative and spatial expression from the ABI3 promoter. *Plant Mol. Biol.* **54**, 25-38.
- Orgil, O., Matityahu, A., Eng, T., Guacci, V., Koshland, D. and Onn, I.** (2015). A conserved domain in the scc3 subunit of cohesin mediates the interaction with both mcd1 and the cohesin loader complex. *PLoS Genet.* **11**, e1005036.
- Peters, J.-M., Tedeschi, A. and Schmitz, J.** (2008). The cohesin complex and its roles in chromosome biology. *Genes Dev.* **22**, 3089-3114.
- Saitou, N. and Nei, M.** (1987). The neighbor-joining method - a new method for reconstructing phylogenetic trees. *Mol. Biol. Evol.* **4**, 406-425.
- Schleiffer, A., Kaitna, S., Maurer-Stroh, S., Glotzer, M., Nasmyth, K. and Eisenhaber, F.** (2003). Kleisins: a superfamily of bacterial and eukaryotic SMC protein partners. *Mol. Cell* **11**, 571-575.
- Sebastian, J., Ravi, M., Andreuzza, S., Panoli, A. P., Marimuthu, M. P. A. and Siddiqi, I.** (2009). The plant adherin AtSCC2 is required for embryogenesis and sister-chromatid cohesion during meiosis in Arabidopsis. *Plant J.* **59**, 1-13.
- Seitan, V. C., Banks, P., Laval, S., Majid, N. A., Dorsett, D., Rana, A., Smith, J., Bateman, A., Krpic, S., Hostert, A. et al.** (2006). Metazoan Scc4 homologs link sister chromatid cohesion to cell and axon migration guidance. *PLoS Biol.* **4**, e242.
- Szklarczyk, D., Franceschini, A., Wyder, S., Forslund, K., Heller, D., Huerta-Cepas, J., Simonovic, M., Roth, A., Santos, A., Tsafou, K. P. et al.** (2015). STRING v10: protein-protein interaction networks, integrated over the tree of life. *Nucleic Acids Res.* **43**, D447-D452.
- Tzafir, I., McElver, J. A., Liu, C.-M., Yang, L. J., Wu, J. Q., Martinez, A., Patton, D. A. and Meinke, D. W.** (2002). Diversity of TITAN functions in Arabidopsis seed development. *Plant Physiol.* **128**, 38-51.
- Watrin, E., Schleiffer, A., Tanaka, K., Eisenhaber, F., Nasmyth, K. and Peters, J.-M.** (2006). Human Scc4 is required for cohesin binding to chromatin, sister-chromatid cohesion, and mitotic progression. *Curr. Biol.* **16**, 863-874.
- Watrin, E., Kaiser, F. J. and Wendt, K. S.** (2016). Gene regulation and chromatin organization: relevance of cohesin mutations to human disease. *Curr. Opin. Genet. Dev.* **37**, 59-66.
- Yadegari, R., De Paiva, G. R., Laux, T., Koltunow, A. M., Apuya, N., Zimmerman, J. L., Fischer, R. L., Harada, J. J. and Goldberg, R. B.** (1994). Cell-differentiation and morphogenesis are uncoupled in arabidopsis raspberry embryos. *Plant Cell* **6**, 1713-1729.
- Yang, X. H., Boateng, K. A., Strittmatter, L., Burgess, R. and Makaroff, C. A.** (2009). Arabidopsis separase functions beyond the removal of sister chromatid cohesion during meiosis. *Plant Physiol.* **151**, 323-333.
- Yeung, E. C. and Meinke, D. W.** (1993). Embryogenesis in angiosperms - development of the suspensor. *Plant Cell* **5**, 1371-1381.
- Yuan, L., Yang, X. H., Ellis, J. L., Fisher, N. M. and Makaroff, C. A.** (2012). The arabidopsis SYN3 cohesin protein is important for early meiotic events. *Plant J.* **71**, 147-160.
- Yuan, L., Yang, X. H., Auman, D. and Makaroff, C. A.** (2014). Expression of epitope-tagged SYN3 cohesin proteins can disrupt meiosis in arabidopsis. *J. Genet. Genomics* **41**, 153-164.
- Zimmermann, P., Hirsch-Hoffmann, M., Hennig, L. and Gruissem, W.** (2004). GENEVESTIGATOR. Arabidopsis microarray database and analysis toolbox. *Plant Physiol.* **136**, 2621-2632.



# EXTRA SPINDLE POLES (Separase) controls anisotropic cell expansion in Norway spruce (*Picea abies*) embryos independently of its role in anaphase progression

Panagiotis N. Moschou<sup>1</sup>, Eugene I. Savenkov<sup>1\*</sup>, Elena A. Minina<sup>1,2\*</sup>, Kazutake Fukada<sup>1\*</sup>, Salim Hossain Reza<sup>1,2</sup>, Emilio Gutierrez-Beltran<sup>1,2</sup>, Victoria Sanchez-Vera<sup>1</sup>, Maria F. Suarez<sup>3</sup>, Patrick J. Hussey<sup>4</sup>, Andrei P. Smertenko<sup>5,6</sup> and Peter V. Bozhkov<sup>1,2</sup>

<sup>1</sup>Department of Plant Biology, Uppsala BioCenter, Swedish University of Agricultural Sciences and Linnean Center for Plant Biology, PO Box 7080, SE-75007 Uppsala, Sweden; <sup>2</sup>Department of Chemistry and Biotechnology, Uppsala BioCenter, Swedish University of Agricultural Sciences and Linnean Center for Plant Biology, PO Box 7015, SE-75007 Uppsala, Sweden;

<sup>3</sup>Departamento de Biología Molecular y Bioquímica, Facultad de Ciencias, Universidad de Málaga, 290071 Málaga, Spain; <sup>4</sup>The Integrative Cell Biology Laboratory, School of Biological and Biomedical Sciences, University of Durham, Durham, DH1 3LE, UK; <sup>5</sup>Institute of Biological Chemistry, Washington State University, Pullman, WA 99164, USA; <sup>6</sup>Institute for Global Food Security, Queen's University Belfast, 18–30 Malone Road, Belfast, BT9 5BN, UK

## Summary

Author for correspondence:

Panagiotis N. Moschou

Tel: +46 700780553

Email: panagiotis.moschou@slu.se

Received: 29 February 2016

Accepted: 7 April 2016

*New Phytologist* (2016) **212**: 232–243

doi: 10.1111/nph.14012

**Key words:** cell cycle, embryogenesis, microtubules, proteases, separase, spruce (*Picea abies*).

- The caspase-related protease separase (*EXTRA SPINDLE POLES*, *ESP*) plays a major role in chromatid disjunction and cell expansion in *Arabidopsis thaliana*. Whether the expansion phenotypes are linked to defects in cell division in *Arabidopsis ESP* mutants remains elusive.
- Here we present the identification, cloning and characterization of the gymnosperm Norway spruce (*Picea abies*, Pa) *ESP*. We used the *P. abies* somatic embryo system and a combination of reverse genetics and microscopy to explore the roles of Pa *ESP* during embryogenesis.
- Pa *ESP* was expressed in the proliferating embryonal mass, while it was absent in the suspensor cells. Pa *ESP* associated with kinetochore microtubules in metaphase and then with anaphase spindle midzone. During cytokinesis, it localized on the phragmoplast microtubules and on the cell plate. Pa *ESP* deficiency perturbed anisotropic expansion and reduced mitotic divisions in cotyledonary embryos. Furthermore, whilst Pa *ESP* can rescue the chromatid nondisjunction phenotype of *Arabidopsis ESP* mutants, it cannot rescue anisotropic cell expansion.
- Our data demonstrate that the roles of *ESP* in daughter chromatid separation and cell expansion are conserved between gymnosperms and angiosperms. However, the mechanisms of *ESP*-mediated regulation of cell expansion seem to be lineage-specific.

## Introduction

Embryonic pattern formation in seed plants involves the establishment of apical–basal and radial polarities resulting in the formation of primary shoot and root meristems (Mayer *et al.*, 1991; Meinke, 1991; Ueda & Laux, 2012). Knowledge about plant embryogenesis has benefited from studies of embryo-defective mutants in the angiosperm model species *Arabidopsis thaliana* (Mayer *et al.*, 1991; Capron *et al.*, 2009; Kanei *et al.*, 2012; Wendrich & Weijers, 2013). However, our understanding of the molecular mechanisms underlying embryogenesis remains limited, owing to the restricted accessibility of zygotic embryos during early developmental stages. Somatic embryogenesis represents a valuable model for studying regulation of embryogenesis, as it

allows synchronized production of a large number of embryos at a specific developmental stage and their life imaging (Pennell *et al.*, 1992; von Arnold *et al.*, 2002; Smertenko & Bozhkov, 2014).

Early embryogenesis in *Arabidopsis* proceeds through highly regular cell division patterns, starting with an asymmetric first division of the zygote, which gives rise to a smaller apical and a larger basal cell. The basal cell divides transversely to form a single file of suspensor cells and a hypophysis cell, while the apical cell undergoes several rounds of divisions to give rise to a globular embryo. This stage is followed by the establishment of bilateral symmetry and differentiation of two cotyledons. In most gymnosperms (e.g. Norway spruce, *Picea abies*), the zygote undergoes several rounds of karyokinesis without cytokinesis (free nuclear stage), followed by cellularization and formation of the lowest and the upper cell tiers (Singh, 1978). The lowest tier will form

\*These authors contributed equally to this work.

the embryonal mass (gymnosperm equivalent of embryo proper), while the upper tier will form the first layer of suspensor. A fully developed suspensor in spruce embryos is composed of several layers of nondividing elongating cells. Unlike *Arabidopsis* embryos, spruce embryos form a crown of multiple cotyledons with radial symmetry surrounding the shoot apical meristem (Singh, 1978). Despite morphological differences in the embryo patterning in different plant lineages, the core regulatory network appears to be conserved (reviewed in Smertenko & Bozhkov, 2014).

Previous studies highlighted the importance of proteases in plant embryogenesis and other developmental processes (van der Hoorn, 2008). For example, in *Arabidopsis* the subtilisin-like serine protease ALE1 is required for cuticle formation in protoderm (Tanaka *et al.*, 2001) and the phytocain DEK1 is essential for embryonic cell fate determination (Johnson *et al.*, 2005). *DEK1* mutant embryos that develop beyond globular stage show aberrant cell division planes in the suspensor and embryo proper (Johnson *et al.*, 2005; Lid *et al.*, 2005). In addition, early embryonic patterning in Norway spruce requires the activity of metacaspase mclI-Pa (Suarez *et al.*, 2004; Minina *et al.*, 2013). Knockdown of *mclI-Pa* suppresses differentiation of the suspensor and abrogates establishment of apical-basal polarity.

Separase (Extra Spindle Poles, ESP) is a caspase-related protease indispensable for embryogenesis in *Arabidopsis* (Liu & Makaroff, 2006) and nonplant species (e.g. Bembek *et al.*, 2010). Initially, ESP was identified as an evolutionary conserved protein that cleaves cohesin to enable disjunction of sister chromatids during metaphase-to-anaphase transition (referred to as the canonical function of ESP; Ciosk *et al.*, 1998). A temperature-sensitive mutant allele of *ESP* from *Arabidopsis* (*At ESP*), *rsw4* (*radially swollen 4*), exhibits a chromosome nondisjunction phenotype (Wu *et al.*, 2010). In addition, *rsw4* causes disorganization of the radial microtubule system in meiocytes (Yang *et al.*, 2011) and defects in anisotropic expansion of root cells associated with radial swelling (Wu *et al.*, 2010).

Previously, we examined the role of *At ESP* in cell polarity and found that *At ESP* controls microtubule-dependent trafficking that is essential for cell plate synthesis during cytokinesis (Moschou *et al.*, 2013). Here we report on the identification and functional characterization of the gymnosperm Norway spruce (*P. abies*) *ESP* homologue Pa *ESP*, and explore the phenotype of spruce embryos depleted of Pa *ESP*.

## Materials and Methods

### Plant material and growth conditions

The *Picea abies* (L.) H. Karst. (Norway spruce) wild-type (WT) embryonic cell lines 95.88.22 and 95.61.21, and Pa *ESP*-RNAi lines were cultured as described previously (Filonova *et al.*, 2000). Embryonal masses were separated from the suspensors of 7-d-old embryos using surgical blades in droplets of culture medium under a binocular microscope.

### Molecular biology

Primers used in this study are listed in Supporting Information Table S1. Full-length cDNA of the Pa *ESP* was obtained by 5'- and 3'-rapid amplification of cDNA ends (RACE) with the SMART RACE cDNA Amplification kit (Clontech, Mountain View, CA, USA) and Advantage 2 PCR kit (Clontech), with primers designed from publicly available sequences of expression sequence tags (<http://congenie.org/>). Amplified PCR products were cloned into pCR4Blunt-Topo (Invitrogen, Carlsbad, CA, USA). The plasmid-carrying *FLAG-PaESP* sequence was constructed by ligating a 5'-FLAG-PaESP fragment digested with *PacI* and *AatII* with the 3'-end fragment digested with *AatII* and *Sse8783I* into the *PacI/Sse8783I*-cleaved vector pAHC25.

The *FLAG-PaESP* plasmid was used as a template to amplify by PCR two overlapping fragments using the primers FWPaESPExp1topo-Se-R3 (5'-fragment) and RvPaESPExpAscI-Se-F2 (3'-fragment). The overlapping region contained a *Clal* restriction site. The 5'-fragment was introduced into the pTOPO/D vector (Invitrogen) giving rise to the pTOPO/D-PaESP 3.0 kb. The pTOPO/D vector contains an *Ascl* site, upstream of the *attR2* site. The remaining part of Pa *ESP* was introduced by digesting the 3'-fragment by *Clal* and *Ascl* and ligating it into pTOPO/D-PaESP 3.0 kb digested with *Clal* and *Ascl*, thus producing pTOPO/D-PaESP 6.9 kb. The Pa *ESP* insert was subcloned into the pGWB15 (3×HA-tagged) vector by the gateway recombination reaction using the LR enzyme (Invitrogen).

A 2423-bp-long C-terminal fragment was amplified with primers Sep-C-terminus CHis-P, Sep-CHis-M1 and Sep-CHis-M2 from pTOPO/D-PaESP 6.9 kb and introduced into a modified pET11a vector (Qiagen, Valencia, CA, USA). The pET11a vector was modified by introducing a part from the polylinker of pKOH122 digested with *NdeI* and *BamHI* (amplified by pKOH122-MCS-P and MCS-reverse-with-*SacI*).

For constructing the Pa *ESP*-RNAi vector, two fragments were amplified using the primers FWPaESPExp1topo, PaESPRN-AiRV1EcoRI and FwPaESPRNaiAscI, PaESPRNaiRV2EcoRI. Primer PaESPRNaiRV2EcoRI anneals 400 bp downstream of the PaESPRNaiRV1EcoRI. This 400 bp region represents the loop between two arms of the hairpin. The first fragment was cloned in a pTOPO/D vector, which was subsequently digested with *EcoRI* and *Ascl* and the second fragment was introduced by ligation producing the pTOPO/D-hpRNAiPaESP vector. The hairpin insert was subcloned into a pGWB2 vector (constitutive silencing; Nakagawa *et al.*, 2007) or the pMDC7 (LexA-VP16-ER (XVE)  $\beta$ -estradiol-inducible promoter, which is derived from the pER8 vector and contains the oestrogen receptor-based transactivator XVE; Brand *et al.*, 2006). The resulting constructs, pGWB2-hpRNAiPaESP and pMDC7-hpRNAiPaESP, were transformed into *Agrobacterium tumefaciens* GV3101 by electroporation. All constructs were verified by sequencing.

### Phylogenetic analysis

Alignments of *ESP* sequences were performed in CLUSTALW. Unrooted trees were constructed using the neighbour-joining

method (Saitou & Nei, 1987) using the yeast homologue as an outgroup. A phylogenetic tree was constructed using PAUP software (<http://paup.csit.fsu.edu>). The bootstrap analysis was performed with 2000 repeats, and branches with bootstrap values over 70% were retained.

### Embryo transformation and transient expression

Norway spruce embryogenic cultures were transformed by *A. tumefaciens* GV3101. Agrobacteria were grown overnight in Luria-Bertani (LB) medium supplemented with 10 mM MgCl<sub>2</sub>, 10 mM 2-(N-morpholino)ethane sulfonic acid (MES), pH 5.5, 40 µM acetosyringone, 50 µg ml<sup>-1</sup> rifampicin and 50 µg ml<sup>-1</sup> kanamycin. Agrobacteria were collected and incubated for 1 h in 10 mM MgCl<sub>2</sub>, 10 mM MES, pH 5.5, and 150 µM acetosyringone at room temperature on a shaker (OD<sub>600</sub> = 10). Ten microlitres of 5-d-old spruce culture (cell line 95.88.22) were collected in a 50 ml tube and the supernatant was discarded. The spruce culture was coincubated with 1 ml *Agrobacterium* in 10 ml of 10 mM MgCl<sub>2</sub>, 10 mM MES, pH 5.5, and 150 µM acetosyringone for 8 h without shaking at 20°C in darkness. Excess liquid was removed and spruce cells were placed on three layers of sterile filter paper. The upper layer was transferred onto half-strength Le Poivre (LP) medium (Filonova *et al.*, 2008). After 48 h, filter paper was transferred onto half-strength LP medium supplemented with 250 µg ml<sup>-1</sup> cefotaxime (Duchefa, Haarlem, the Netherlands), and, after an additional 7 d, onto the same medium containing 15 µg ml<sup>-1</sup> hygromycin B (Duchefa). Filters were transferred onto fresh medium once a week for 6 wk consecutively. Subsequently, cell colonies were transferred onto the medium without filter papers, and grown in the presence of 250 µg ml<sup>-1</sup> cefotaxime, 400 µg ml<sup>-1</sup> timentin (Duchefa) and 15 µg ml<sup>-1</sup> hygromycin B. After colonies were grown to *c.* 2 cm in diameter, suspension cultures were established in half-strength LP without selection agents.

For transient expression of Pa *ESP*-RNAi, Norway spruce embryogenic cultures were transformed by *A. tumefaciens* as described earlier with minor modifications. The cell line 95.61.21 was used and, after cefotaxime treatment for 2 d, cells were fixed and stained with 4',6-diamidino-2-phenylindole (DAPI). As a control, a pMDC32 vector containing the cDNA encoding for monomeric red fluorescent protein (mRFP) was used.

### Absolute quantitative RT-PCR analyses

Quantitative real-time polymerase chain reaction (qRT-PCR) was done as previously described (Moschou *et al.*, 2013). For absolute quantification of cDNA molecules in the qRT-PCR, *At ESP* or Pa *ESP* in pGWB15 vectors were used as standards.

### Preparation of immunogen and antibody

The pET11a-PaESP construct was transformed in BL21-CodonPlus (DE3) RIL (Stratagene, La Jolla, CA, USA) *Escherichia coli* competent cells. Purification of the His-tagged recombinant C-terminal fragment containing the C50 domain (1502–2307

amino acids (aa) of Pa *ESP* was performed according to manufacturer's instructions (Qiagen). Antisera were raised in three mice.

### Western blot analysis

A quantity of 100 mg of plant material was mixed with 200 µl of 2 × Laemmli sample buffer (Laemmli, 1970), kept on ice for 10 min and boiled for 5 min. Samples were centrifuged at 17 000 g for 15 min. Equal amounts of each supernatant were loaded on 9% or 4–15% gradient polyacrylamide gels and blotted on a polyvinylidene fluoride membrane (see also Methods S1). Anti-Pa *ESP* and anti-actin C4 were used at dilutions of 1 : 1000 and 1 : 200, respectively; anti-mouse horseradish peroxidase conjugates (GE Healthcare, Uppsala, Sweden) were used at a dilution 1 : 5000. Blots were developed using the ECL Prime kit (GE Healthcare) and imaged in a LAS-3000 Luminescent Image Analyzer (Fujifilm, Fuji Photo Film, Kleve, Germany).

### Immunocytochemistry and imaging

The immunostaining of embryos was performed using a previously established protocol (Smertenko & Hussey, 2008). Two-day-old early embryos of Norway spruce were fixed in 3.7% (w/v) formaldehyde in microtubule-stabilizing buffer (MTSB; 0.1 M piperazine-N,N'-bis(2-ethane sulfonic acid) (PIPES), pH 6.8, 5 mM EGTA, 2 mM MgCl<sub>2</sub>) supplemented with 1% (v/v) Triton X-100. For methanol fixation, cells were fixed in strainers with 100% (v/v) methanol for 10 min at -20°C, followed by 100% (v/v) acetone for 5 min at -20°C. The cells were then washed three times for 5 min each with phosphate-buffered saline (PBS) at room temperature and allowed to rehydrate in PBS for additional 30 min at room temperature before treatment with cell wall-digesting enzymes. Embryos were blocked with PBS Tween-20 (PBST) supplemented with 5% (w/v) BSA (blocking solution). Subsequently, embryos were incubated overnight with rabbit anti-Pa *ESP*, diluted 1 : 500, and rat anti-tubulin YL1/2 (AbD Serotec, Oxford, UK), diluted 1 : 200 in blocking solution. Specimens were then washed three times for 30 min in PBST and incubated for 3 h with goat anti-rat TRITC (tetramethyl rhodamine isothiocyanate) and anti-rabbit FITC (fluorescein isothiocyanate conjugated) secondary antibodies diluted 1 : 200 in blocking solution. After washing in PBST, specimens were mounted in Vectashield (Vector Laboratories, Burlingame, CA, USA) mounting medium. The samples were examined using a Leica SP5 or Zeiss 710 confocal microscope equipped with oil immersion (×63 with numerical aperture = 1.4) objective.

### Tissue sectioning

Cotyledonary embryos were fixed for 2 h at room temperature under vacuum with 4% (w/v) paraformaldehyde in MTSB supplemented with 0.4% (v/v) Triton X-100. The fixative was washed away with PBST buffer, and embryos were dehydrated on ice by 0.85% (w/v) NaCl (30 min) and an ethanol (EtOH) gradient in 0.85% (w/v) NaCl (50%, 70%, 85%, 95% and

100% for 90 min each, 100% overnight and 100% for 2 h). Samples were treated twice with 100% (v/v) xylene at room temperature for 1 h each, overnight with 50% (v/v) xylene supplemented with 50% (w/v) histowax at 40–50°C, and 100% (w/v) histowax at 60°C, changing twice per day for 3 d consecutively. Samples were stored at 4°C until they were used. Sections of 10 µm thickness were cut using a microtome and placed on poly-lysine-coated slides in water droplets. Water was allowed to evaporate overnight at 45°C. Samples were deparaffinized and rehydrated by two washes, 10 min each, in histoclear, two washes, 2 min each, in 100% (v/v) EtOH, followed by an EtOH gradient (95%, 90%, 80%, 60% and 30%) in PBS for 2 min for each step. Slides were treated for 2 min with H<sub>2</sub>O and 20 min with PBS. Sections were blocked and hybridized with antibodies as described earlier.

### Microtubule and image analysis

The image and pixel analyses were done using IMAGEJ v.1.48 software (<http://rsb.info.nih.gov/ij>). Intensity profile was calculated along an interactively applied line, and data of intensity measurements were exported to Microsoft EXCEL (Microsoft, Redmond, WA, USA) and plotted. Default modules and options were used. Images were prepared using Adobe PHOTOSHOP CS6 (Adobe, San Jose, CA, USA).

### Statistical analysis

Graphs were prepared using EXCEL v.2013 or JMP v.11 (Division of SAS, Cary, NC, USA). Statistical analysis was performed with JMP v.11. Statistical methods used are indicated in the corresponding figure legends.

## Results

### Identification, cloning and sequence analysis of Pa ESP

All known ESP proteins are encoded by single genes, with the sole exception of *Drosophila melanogaster* ESP, which contains two subunits encoded by separate genes (reviewed in Moschou & Bozhkov, 2012). The full-length cDNA for Pa ESP was isolated by RACE, using internal primers that spanned the conserved 3'-end of the gene (Notes S1, S2). The cDNA was sequenced and found to be 7248 bp long and contained an open reading frame encoding a polypeptide of 2308 aa with predicted molecular mass of 259 kDa. We deposited the Pa ESP sequence in GenBank under the accession number HE793991.1. Phylogenetic analysis revealed that Pa ESP together with the ESP homologue from *Klebsormidium* and angiosperms (Fig. 1a; Notes S1). The C-terminus of Pa ESP contains a conserved caspase-related proteolytic domain (Pfam number PF03568; 1673–2187 aa,  $P=7.1e^{-88}$ ; Fig. 1b) with the His and Cys catalytic dyad typical for all members of CD-clan proteases (Aravind & Koonin, 2002). This proteolytic domain is the most conserved region of Pa ESP, showing 30% and 31% identity with the corresponding

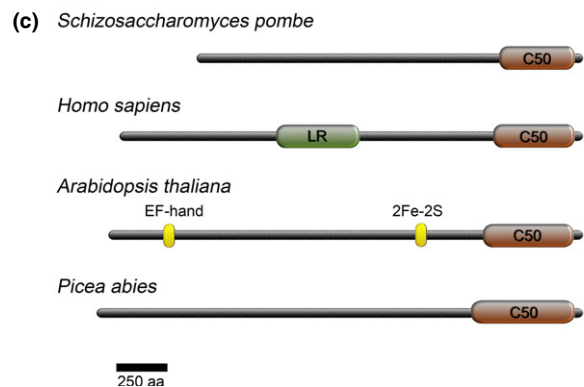
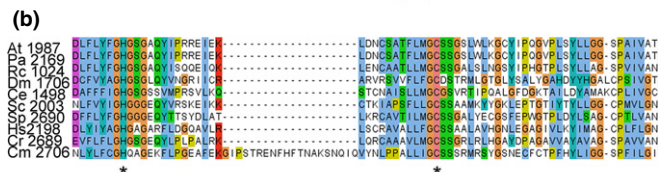
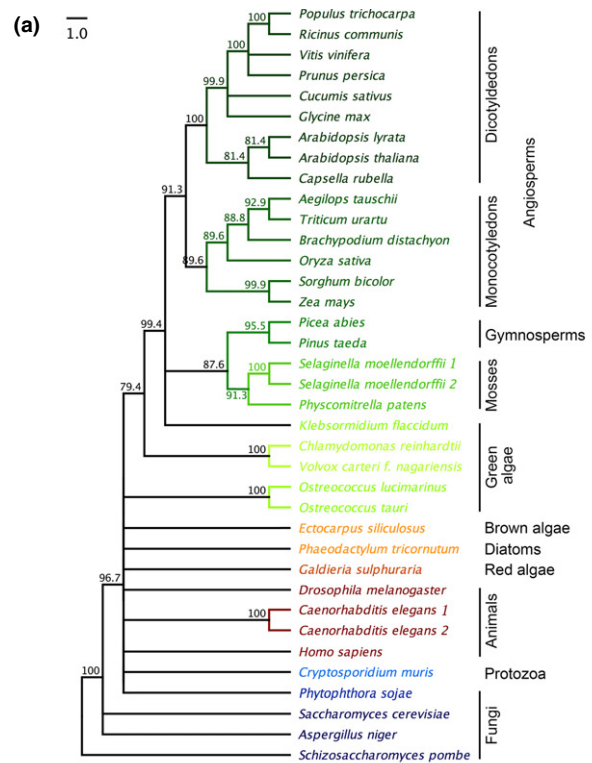


**Fig. 1** Analysis of *Picea abies* EXTRA SPINDLE POLES (Pa ESP) sequence. (a) Phylogenetic tree of ESP protein homologues. The *Saccharomyces cerevisiae* protein sequence was used as an outgroup. The bootstrap values are indicated at the branching points. Accession numbers are indicated in Supporting Information Notes S2. (b) Alignment of amino acid (aa) sequences corresponding to the C50 proteolytic domain of ESP proteins. At, *Arabidopsis thaliana*; Rc, *Ricinus communis*; Dm, *Drosophila melanogaster*; Sc, *Saccharomyces cerevisiae*; Ce, *Caenorhabditis elegans*; Sp, *Schizosaccharomyces pombe*; Hs, *Homo sapiens*; Cr, *Cryptosporidium parvum*; Cm, *Chlamydomonas reinhardtii*; Pa, *Picea abies*. Asterisks denote the conserved His, Cys dyad. Full alignment is shown in Notes S1. (c) Domain organization of selected ESP proteases. C50, proteolytic domain; LR, leucine-rich domain; EF-hand, helix-loop-helix topology with the ability to bind Ca<sup>2+</sup>; 2Fe-2S, iron-sulphur cluster.

domains of human and budding yeast homologues, respectively, and over 50% identity with plant homologues. The rest of the sequence is less conserved, suggesting functional divergence of ESP proteins. In contrast to mammalian homologues, all plant ESP proteins lack a well-defined leucine-rich region, which may be responsible for DNA binding (Fig. 1c; Sun *et al.*, 2009). Furthermore, Pa ESP lacks the Ca<sup>2+</sup>-binding EF-hand and 2Fe-2S motifs identified in the *Arabidopsis* homologue (Fig. 1c). These differences in the primary sequence combined with the monophyletic nature of the phylogenetic tree suggest that ESP functions were fine-tuned in different lineages during evolution.

### Pa ESP protein abundance is developmentally regulated

Early somatic embryos of Norway spruce develop from unorganized multicellular aggregates called proembryogenic masses (PEMs) upon withdrawal of the plant growth regulators (PGRs) auxin and cytokinin (Fig. 2a). The later stages of somatic embryogenesis resemble those of the zygotic pathway and are promoted by abscisic acid (ABA; Filonova *et al.*, 2000). An early spruce embryo is composed of the embryonal

mass, tube cells and the suspensor (Fig. 2a). While the embryonal mass gives rise to the mature embryo, the suspensor is a transient structure undergoing programmed cell death (Filonova *et al.*, 2000). The suspensor cells in Norway spruce embryos are formed via asymmetric cell divisions in the basal-most part of the embryonal mass. Following asymmetric cell division, the upper daughter cell retains its meristematic identity and remains within the embryonal mass, while its sister (lower) cell becomes a terminally differentiated tube cell. The tube cells cease proliferation and expand anisotropically to form suspensor cells. Addition of new tube cells through reiterated cell divisions in the embryonal mass creates long files composed of several suspensor cells at successive stages of programmed cell death along the apical–basal axis. The hollow-walled corpses of suspensor cells are removed from the basal end of the embryo-suspensors (Bozhkov *et al.*, 2005).

To analyse the levels of Pa ESP at successive stages of plant development, we raised an antibody against the C50 catalytic domain of Pa ESP and used it in immunoblotting. The antibody recognized a protein of *c.* 260 kDa that corresponds to the predicted size of Pa ESP (Methods S1). Protein abundance of Pa ESP was high in proliferating PEMs in the presence of PGR (+PGR), but not during differentiation of early embryos (–PGR; Fig. 2b), and in the microsurgically separated embryonal masses of early embryos (Fig. 2c). Neither suspensor cells nor distinct parts of seedlings, including cotyledons, young needles, hypocotyls and roots, contained detectable amounts of Pa ESP protein, demonstrating that high amounts of Pa ESP are associated with actively proliferating tissues. The amount of Pa ESP seems to be regulated at the transcriptional level, as suspensor cells, cotyledons, hypocotyls and roots contained at least five-fold less Pa ESP mRNA than the embryonal mass (Fig. S1a).

### Pa ESP localizes to microtubules and associates with the cell plate during cytokinesis

The intracellular localization of Pa ESP in the meristematic cells of PEMs and early embryos was examined using immunofluorescence microscopy (Figs 3, S2). In nondividing meristematic cells, Pa ESP decorated cortical microtubules (Fig. S2, top images), while during preprophase, Pa ESP was found on the preprophase band and perinuclear basket of microtubules (Fig. 3a,b1). At the beginning of prophase and until the onset of anaphase, Pa ESP was detected around the mitotic spindle, as well as on the kinetochore microtubules (Fig. 3b2). At the onset of anaphase, most Pa ESP was associated with the spindle poles and midzone microtubules (Fig. 3b3,c). This localization was independent of the fixation method as the same staining pattern was observed after more stringent fixation with methanol/acetone, which exposes epitopes masked by protein folding or interaction with other proteins (Fig. 3c). Densitometry profiling of the anaphase spindle revealed three apparent peaks corresponding to both spindle poles and the midzone (Fig. 3c). During telophase, Pa ESP concentrated in the phragmoplast midzone, where the cell plate is assembled (Fig. 3b4). A similar localization was observed after the methanol/acetone fixation and the densitometry profiling

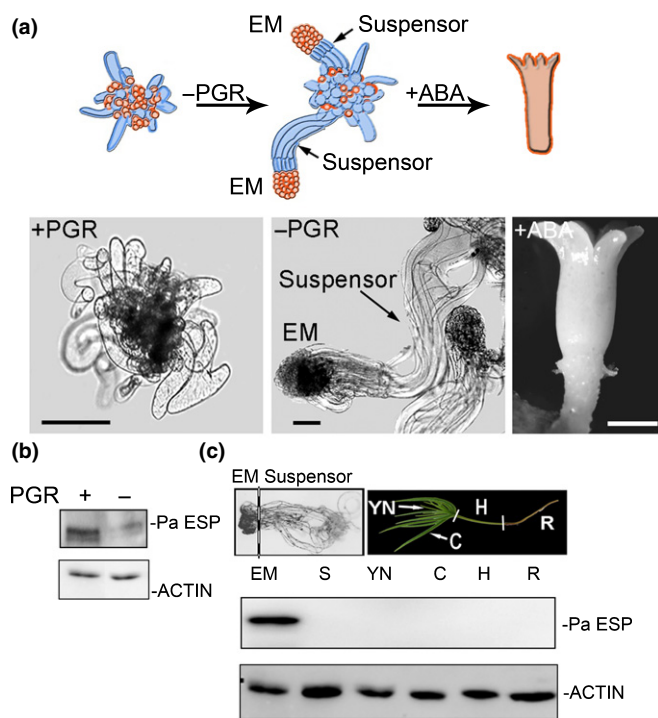


**Fig. 2** *Picea abies* EXTRA SPINDLE POLES (Pa ESP) level is developmentally regulated. (a) A model (adapted from Filonova *et al.*, 2000) and corresponding micrographs of three principal stages of Norway spruce somatic embryogenesis. Red and blue colours denote proliferating and dying cells, respectively. EM, embryonal mass; PGR, plant growth regulators; ABA, abscisic acid. Bars, 100  $\mu$ m. (b) Western blot analysis of Pa ESP in 2-d-old embryogenic culture grown in the presence (+PGR) or absence (–PGR) of PGR. (c) Western blot analysis of Pa ESP in the embryonal masses (EM) and suspensors (S); on the Western blot) of early somatic embryos, as well as in cotyledons (C), young needles (YN), hypocotyls (H) and roots (R) of seedlings. The equal loading was confirmed using anti-actin. The images of representative plant material used for protein extraction are shown above the Western blot.

revealed only one major peak of fluorescence in the phragmoplast midzone (Fig. 3d). Apart from the midzone, Pa ESP colocalized with microtubules at the leading edge of the phragmoplast in all cases examined ( $n = 53$ ; Fig. 3b4, inset). At later stages of phragmoplast development, Pa ESP remained at the cell plate after the depolymerization of microtubules (Fig. 3b5).

We examined localization of Pa ESP in the first layer of anisotropically expanding cells adjacent to the embryonal mass, the tube cells. These cells cease proliferation, becoming committed to programmed cell death. During the subsequent differentiation steps, the tube cells elongate to form stereotypical suspensor cells (Bozhkov *et al.*, 2005; Smertenko & Bozhkov, 2014; Zhu *et al.*, 2014). Pa ESP was absent from these cells (Fig. S2, lower images), consistent with the finding that the Pa *ESP* mRNA level is greatly reduced in the suspensor (Fig. S1a).

### Pa *ESP* deficiency impairs early embryo development

To investigate the role of Pa *ESP* in embryogenesis we produced transgenic lines constitutively expressing a hairpin construct against Pa *ESP* (Pa *ESP*-RNAi; Figs 4, S1b). We could only obtain two viable cell lines (4.1 and 4.2), while the rest of the transgenic lines ceased proliferation following initial selection. Both lines exhibited significantly lower levels of Pa *ESP* (Figs 4a, S1b). Knockdown of Pa *ESP* inhibited the development of early embryos from PEMs upon withdrawal of PGR (Fig. 4b). WT cultures contained embryos with compact embryonal masses and several files of anisotropically expanding suspensor cells. By contrast, Pa *ESP*-RNAi lines contained irregularly formed embryonal masses connected to a suspensor-like structure composed of supernumerary cells showing impaired anisotropic expansion (Figs 4c, S3a,b). These cells were not part of the embryonal masses, which could be easily distinguished by bright fluorescein diacetate staining (Fig. S4a; Methods S2). This implies that Pa *ESP* deficiency does not affect specification of the tube or suspensor cells, but rather inhibits their elongation (Fig. S3a). Consistently, these cells did not show high mRNA levels of the cell division-related genes Pa *CYCB1* (CyclinB-Like 1) and Pa *RBRL* (Retinoblastoma Like; Fig. S4b,c; Zhu *et al.*, 2014). We noticed that some suspensor-like cells at the basal pole of the RNAi embryos showed apparent signs of cell death (staining with Evans blue; Fig. S5). However, these cells lacked any signs of proper anisotropic expansion.

To exclude the possibility that observed phenotype was a consequence of pleiotropic effects of the constitutive depletion of Pa *ESP*, we generated estradiol-inducible Pa *ESP* RNAi lines (Pa *ESP*-XVE > RNAi; Fig. S1a). Depletion of Pa *ESP* induced by estradiol (induction was done from early embryogenesis onwards) resulted in similar developmental defects as described for constitutive RNAi lines (Fig. S3a–c). No alteration in embryo morphology was observed in the noninduced Pa *ESP*-XVE > RNAi (data not shown).

### Pa *ESP* is required for chromosome disjunction

To investigate the role of Pa *ESP* in sister chromatid separation, we stained Pa *ESP*-RNAi or Pa *ESP*-XVE > RNAi cells with

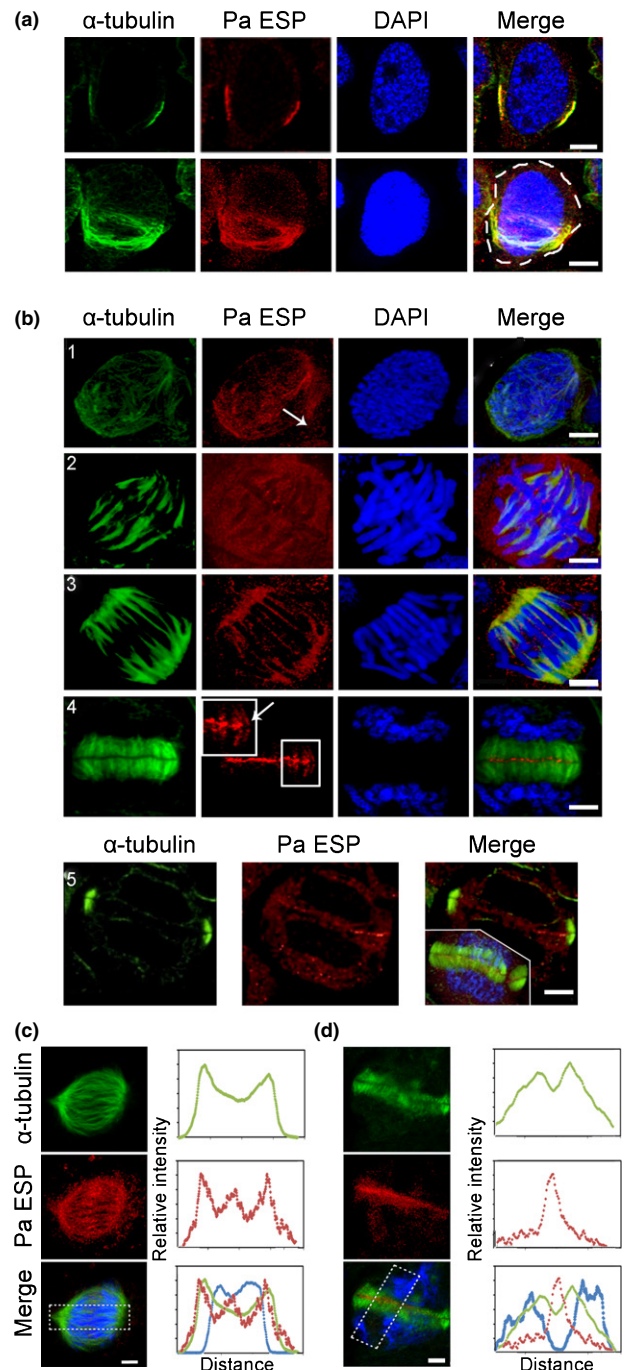


**Fig. 3** Intracellular localization of *Picea abies* EXTRA SPINDLE POLES (Pa *ESP*). (a, b) Staining of Pa *ESP* (red), tubulin (green) and DNA (blue; 4',6-diamidino-2-phenylindole, DAPI) in the embryonic Norway spruce cells fixed with formaldehyde during (a) early prophase, (b1) prophase, (b2) metaphase, (b3) anaphase, (b4) telophase and (b5) late cytokinesis. In (a) upper images are from a single Z-axis optical section and lower images are maximal projection. The cell boundaries are denoted by the dotted line (lower). In (b1) the arrow denotes the peripheral preprophase band. The inset in (b4) shows a higher magnification of the phragmoplast leading edge. The arrow denotes association of Pa *ESP* with microtubules. The inset in (b5) shows the maximum projection image with DNA staining. Bars, 5  $\mu$ m. (c, d) Staining of Pa *ESP*, tubulin and DNA in the embryonic cells fixed with methanol during anaphase (c) and telophase (d). Density scans were performed in the framed areas. Different colours indicate Pa *ESP* (red), tubulin (green) and DNA (blue) intensities. Bars, 5  $\mu$ m.

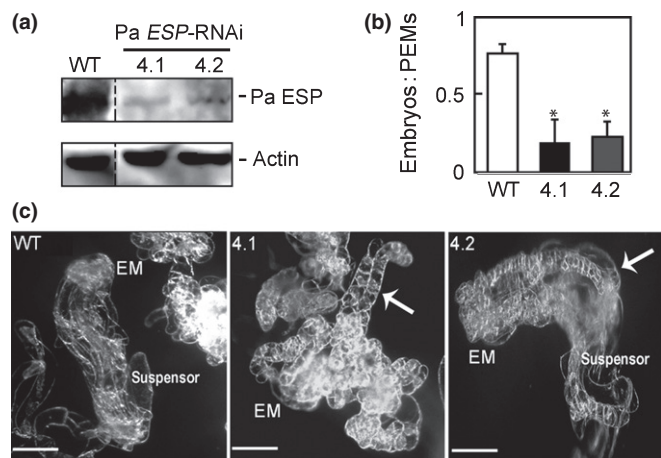


**Fig. 4** Effect of *Picea abies* EXTRA SPINDLE POLES (*Pa ESP*) knockdown on early embryogenesis. (a) Western blot analysis of *Pa ESP* in wild-type (WT) and *Pa ESP*-RNAi cell lines of Norway spruce. The equal loading was confirmed using anti-actin. (b) Ratio of early embryos to proembryogenic masses (PEMs) in WT and *Pa ESP*-RNAi lines grown for 7 d without plant growth regulators (PGR). The data show means  $\pm$  SD of triplicate experiments. \*,  $P < 0.01$  (vs WT, Student's *t*-test). (c) Representative dark field microscopy images of early embryos from WT and *Pa ESP*-RNAi lines grown for 7 d without PGR. Arrows indicate formation of ectopic files of small cells instead of elongated suspensor cells. EM, embryonal mass. Bars, 100  $\mu$ m.

DAPI (Fig. 5a). We failed to identify discernible chromosomal aberrations, suggesting that during the selection process we most likely counter-selected for lines that had sufficient levels of *Pa ESP* to sustain cell division. In fact, neither constitutive nor inducible expression of the *Pa ESP*-RNAi construct led to the reduction of the *Pa ESP* mRNA level to  $< 50\%$  of control values (WT or noninduced, respectively) (Fig. S1).

We have overcome this limitation by the transient expression of the *Pa ESP*-RNAi construct mediated by *A. tumefaciens* (as detailed in the Materials and Methods section). We used a control vector expressing mRFP to estimate the percentage of cells transformed following *A. tumefaciens* transfection. Approximately 80% of cells showed detectable mRFP fluorescence under a confocal microscope. Transient depletion of *Pa ESP* resulted in over 90% reduction of *Pa ESP* levels, when compared with mRFP transfected cells (determined by qRT-PCR; see also the Materials and Methods section). We assume that some cells should have even higher suppression of *Pa ESP*, considering that *c.* 20% of cells remained untransformed. Analysis of the transformed cells revealed a chromosome nondisjunction phenotype (Fig. 5a; 12 of 56 cells examined vs none of 67 in mRFP control) resembling the *Arabidopsis rsw4* allele (Moschou *et al.*, 2013). Complementation experiments of the *Arabidopsis rsw4* phenotype with *Pa ESP* showed that *Pa ESP* could rescue the chromatid nondisjunction phenotype of *rsw4* (Liu & Makaroff, 2006; Fig. 5b), but failed to rescue the root-swelling phenotype (Fig. S6). On the other hand, a point mutant of *Pa ESP* with a catalytic cysteine-to-glycine (C<sup>2147</sup>G) mutation failed to rescue chromatid nondisjunction (data not shown). Thus, *Pa ESP* performs the canonical role of ESP proteins in anaphase progression.

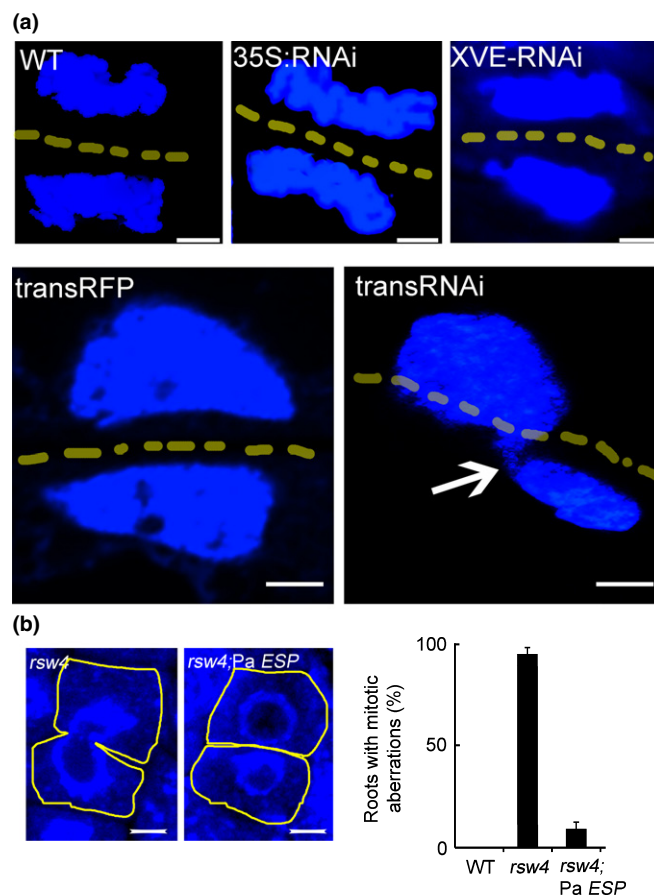


**Fig. 5** Chromosomal aberrations in cells with transiently diminished *Picea abies* EXTRA SPINDLE POLES (*Pa ESP*) and complementation of *rsw4* chromatid nondisjunction phenotype. (a) For detection of chromosomal aberrations, cells of Norway spruce were fixed and stained with 4',6-diamidino-2-phenylindole (DAPI). Images are from a single representative experiment repeated twice. As a control in transient assays, lines transiently expressing monomeric red fluorescent protein (mRFP) under a 35S promoter were used. Aberrations were never observed in these transformants. The arrow indicates chromosomal aberration. Yellow dotted lines demarcate the cell wall between chromosomes of daughter cells. trans, transient. Bars, 5  $\mu$ m. (b) Complementation of nondisjunction phenotype in *Arabidopsis rsw4* line p1 expressing *Pa ESP* (left) and the frequencies of roots with chromosomal aberrations (right). In *rsw4*, chromatid nondisjunction results in chromosomal bridges and improper karyokinesis, leading to the formation of nuclei dissected by a cell wall (similarly to what was reported by Moschou *et al.*, 2013). Note that under our experimental conditions we did not observe chromosomal aberrations in wild-type (WT) plants. Yellow lines demarcate the cell periphery. The data shown in the chart are means  $\pm$  SD of triplicate experiments with 10–12 roots each. Bars, 2.5  $\mu$ m.

### *Pa ESP* is essential for late embryogenesis

We next compared the later stages of embryogenesis in WT and *Pa ESP*-deficient lines (Figs 6, S7). Whereas normally the cotyledonary embryos could be detected following 2 wk after transfer to the maturation medium containing ABA, the cotyledonary embryos in *Pa ESP*-RNAi or *Pa ESP*-XVE > RNAi lines formed only after 10 wk (Figs 6a, S7a,b). Notably, the cotyledonary embryos eventually formed in the RNAi lines, but exhibited a range of morphological abnormalities, including misshapen and

missing cotyledons, short hypocotyls, and split embryos (Fig. 6b, c). Histological examination revealed that cells in the hypocotyls of the cotyledonary embryos were enlarged and showed reduced anisotropy (Figs 6d,e, S8).

In order to examine whether these phenotypes are associated with chromatid nondisjunction or other mitotic aberrations, we performed microscopic examination of the DNA after staining with DAPI. We checked sections of the WT and mutant lines and examined 1848 DAPI-stained nuclei (of these, 653 in WT, 595 in *Pa ESP*-RNAi and 600 in *Pa ESP-XVE > RNAi*). None of these nuclei revealed discernible nondisjunction phenotype. From these cells, only 20 cells (*c.* 0.1%) were at the metaphase stage (nine in WT, six in *Pa ESP*-RNAi, and four in the *Pa ESP-XVE > RNAi*). Such a limited dataset precludes us from drawing conclusions regarding mitotic aberrations other than chromatid nondisjunction.

To overcome this limitation, we examined the shoot apical meristem region of cotyledonary embryos where *c.* 2% of WT

cells showed mitotic features (51 out of 2550 cells). In *Pa ESP*-RNAi and in *Pa ESP-XVE > RNAi*, only 0.5% of the cells had mitotic features (17 out of 3528 cells for *Pa ESP*-RNAi; 21 out of 3540 cells for *Pa ESP-XVE > RNAi*). However, no discernible mitotic abnormalities were observed. In the WT we identified 14 cells (out of 51), while in *Pa ESP*-RNAi we identified three and in *Pa ESP-XVE > RNAi* we identified four (out of 27 and 21 cells, respectively) that were in anaphase. Taken together, these observations suggest that mitotic cells are less frequent in the mutant lines and their developmental defects are not caused by chromosomal aberrations.

### Pa ESP deficiency affects microtubule stability

As polarized development depends on cell expansion, which is in turn controlled by microtubules, we examined microtubule organization in early and cotyledonary embryos. The microtubules in elongating suspensor cells evaded analyses owing to their highly

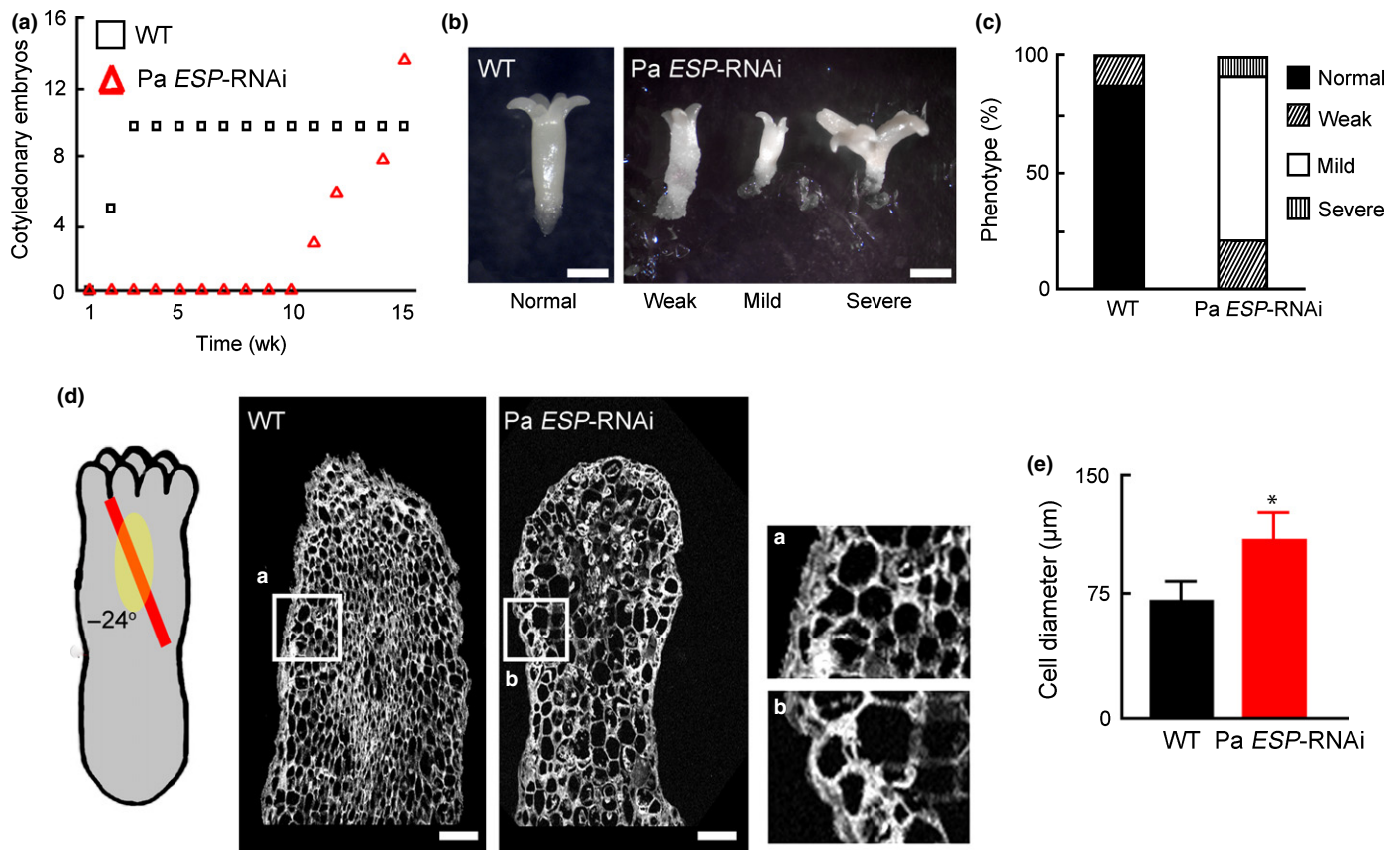


**Fig. 6** Effect of *Picea abies* EXTRA SPINDLE POLES (*Pa ESP*) knockdown on the development of cotyledonary embryos. (a) Time course analysis of Norway spruce cotyledonary embryo formation in wild-type (WT) and *Pa ESP*-RNAi line 4.1. Numbers on the y-axis are absolute numbers (embryos formed). Data are from a single representative experiment, which was repeated three times with similar results. (b) Classes of cotyledonary embryo phenotypes observed in the WT and *Pa ESP*-RNAi line 4.1. Normal, cotyledonary embryos showing radial symmetry and average size; weak, cotyledonary embryos with disturbed radial symmetry and decreased size; severe, cotyledonary embryos showing scission and/or loss of radial symmetry and/or size aberrations; mild, in between the weak and severe classes. Bars, 5 mm. (c) Frequency distribution of distinct phenotypes of cotyledonary embryos in WT and *Pa ESP*-RNAi line 4.1. Note the absence of normal embryos in the RNAi line. Data are from a single representative experiment, which was repeated three times with similar results. (d) Sections of hypocotyls from cotyledonary embryos of WT and *Pa ESP*-RNAi line 4.1 (severe class). The red line on the cartoon illustrates orientation of the section, and the faint yellow ellipse indicates the region of the shoot apical meristem. Shown on the right are the enlarged boxed areas. Bars, 300 µm. (e) Diameter of hypocotyl cells of cotyledonary embryos from WT and *Pa ESP*-RNAi lines. The data show means  $\pm$  SD of triplicate experiments, each containing at least 10 tissue sections. \*,  $P < 0.01$  (vs WT, Student's *t*-test).

fragmented nature (see also Smertenko *et al.*, 2003). Knockdown of Pa *ESP* caused no significant alterations in the random organization of cortical microtubules in the embryonal mass cells (Fig. 7a; Smertenko *et al.*, 2003). By contrast, cortical microtubule bundles in the tube cells of Pa *ESP*-RNAi showed reduced density (Fig. 7a,b). Similarly, the density of cortical microtubule bundles in the hypocotyl cells of Pa *ESP*-RNAi cotyledonary embryos was reduced (Fig. 7a,b). Furthermore, while the majority (*c.* 70%) of microtubules in the hypocotyl cells of cotyledonary WT embryos were transverse, in the Pa *ESP*-RNAi lines they were predominantly oblique or longitudinal (Fig. 7c). Taken together, these results demonstrate that despite a significant reduction of Pa *ESP* expression during cell differentiation, its activity remains critical for regulation of both microtubule organization and cell elongation.

## Discussion

### Diversification of ESP proteins

All ESP proteins identified so far share a caspase-haemoglobinase fold characteristic for the CD clan of cysteine proteases, which includes clostripains, legumains, gingipains, caspases, paracaspases and metacaspases (Aravind & Koonin, 2002). Apart from this conserved fold, the primary structure of ESP lacks a significant conservation (Notes S1). For example, Pa *ESP* is devoid of

the Ca<sup>2+</sup>-binding EF-hand and 2Fe-2S motifs found in At *ESP*. However, whether these motifs serve any function remains unclear.

Phylogenetic analysis reveals that *ESP* homologues of green, brown, diatom algae and land plants form independent clades (Fig. 1a). This pattern suggests that besides the role in daughter chromatid disjunction, *ESP* evolved specific functions in each lineage. The monophyletic nature of the land plant clade indicates that structure and functions of *ESP* coevolved with increased complexity of plant morphology and life cycle. The primary structure of *ESP* in Streptophyta appears to have undergone significant alterations with development of the multicellular body plan in *Klebsormidium*, and then with evolution of the phragmoplast and colonization of land in Embryophytes (Leliaert *et al.*, 2011). Another round of substantial modifications of the *ESP* structure has happened with the evolution of angiosperms.

### Role of Pa *ESP* in cell division and microtubule organization

Extra Spindle Poles from different lineages reveal variable intracellular localization pattern. Yeast *ESP* associates with spindle poles and microtubules of anaphase spindle, whereas human *ESP* was found only on the metaphase spindle poles and then became cytoplasmic in anaphase (Jensen *et al.*, 2001; Chestukhin *et al.*, 2003). *Arabidopsis* *ESP* associates with microtubules of the

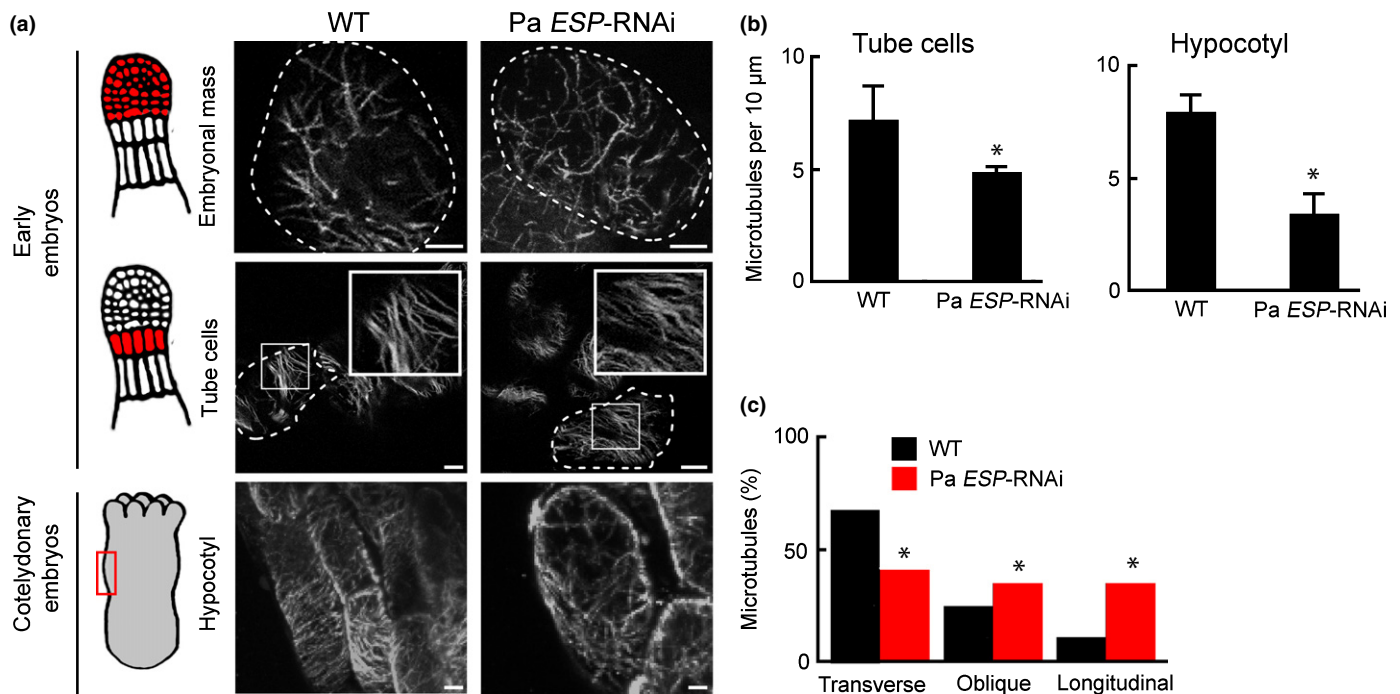


**Fig. 7** Effect of *Picea abies* EXTRA SPINDLE POLES (Pa *ESP*) knockdown on the organization of cortical microtubules. (a) Cortical microtubules in embryonal mass and tube cells of early embryos and hypocotyl cells of cotyledonary embryos from wild-type (WT) and Pa *ESP*-RNAi line 4.1 of Norway spruce. Insets show higher magnification of boxed areas. Bars, 10 μm. (b) Microtubule density (number of microtubules per 10 μm) in the embryonal tube cells and hypocotyl cells from WT and Pa *ESP*-RNAi line 4.1. The data show means ± SD of triplicate experiments, each including 60 cells analysed. \*,  $P < 0.05$  (vs WT, two-sided Dunnett's test). (c) Orientation of microtubules (percentage of microtubules in each particular orientation) in the hypocotyl cells from WT and Pa *ESP*-RNAi line 4.1. Data are from a single representative experiment, which was repeated twice, each time including 60 cells. \*,  $P < 0.05$  (vs WT, Fisher's exact test).

prophase, metaphase and anaphase spindle, as well as phragmoplast microtubules and cell plate (Moschou *et al.*, 2013).

Similar to At ESP, Pa ESP associates with microtubules during the interphase, prophase, metaphase and anaphase, and then associates with the phragmoplast microtubules, midzone and cell plate during telophase. Pa ESP remains associated with the cell plate after disassembly of the phragmoplast microtubules, suggesting that it might be required for vesicle trafficking to the maturing cell plate. Consistent with this conclusion, At ESP was found to temporally colocalize with RabA2a-specific endosomes (Moschou *et al.*, 2013).

In our experiments, constitutive down-regulation of Pa ESP did not result in chromosome nondisjunction and cytokinetic defects observed in other species, including *Arabidopsis* (Fig. 5; Liu & Makaroff, 2006; Wu *et al.*, 2010; Moschou *et al.*, 2013). Furthermore, despite association of Pa ESP with mitotic microtubule arrays, no discernible abnormalities in their organization were observed in the Pa *ESP*-RNAi lines. The most likely explanation for normal cell divisions in the Pa *ESP*-RNAi lines is the incomplete gene silencing still allowing production of a sufficient amount of protein (Fig. 4a) that sustains anaphase transition. Accordingly, a more efficient reduction of Pa ESP using the transient transformation method that we established here revealed the requirement of Pa ESP for chromosome disjunction. Therefore, Pa ESP plays a canonical role in the metaphase–anaphase transition. Although in constitutive RNAi lines the abundance of Pa ESP was sufficient to ensure a normal anaphase progression, the reduced number of meristematic cells in the hypocotyls of Pa ESP-deficient embryos may suggest that Pa ESP is required for the regulation of meristem size, independently of its role in anaphase. Alternatively, the reduced meristem size could be a pleiotropic effect of the retarded embryo development in the Pa ESP-deficient lines.

Consistent with the specific functions of ESP in different lineages, Pa ESP failed to rescue the root-swelling phenotype of *Arabidopsis rsw4*, although previously this phenotype could be complemented by At ESP (Fig. 5b; Moschou *et al.*, 2013). Considering that Pa ESP could complement the chromatid nondisjunction phenotype of *rsw4* and its knockdown in *P. abies* results in chromatid nondisjunction, Pa ESP appears to be a functional homologue of canonical ESP proteins. These findings suggest different effector mechanisms underlying the functions of ESP in anaphase progression and in controlling anisotropic cell expansion.

In contrast to the unaltered microtubule arrays in the embryonal masses, the cortical microtubules in tube cells, and especially in epidermis and cortex cells of cotyledonary embryos of Pa *ESP*-RNAi lines, exhibited reduced density and length, as well as altered orientation (Fig. 7). The hypocotyl cells in the Pa ESP-deficient embryos were bigger than in the WT, indicating that abnormal microtubule organization was associated with irregular cell expansion (Baskin, 2001; Wasteneys, 2004; Baskin & Gu, 2012). This implies that regulation of microtubule dynamics in cells engaged in anisotropic growth are more sensitive to the loss of Pa ESP function than proliferating cells of early embryos, which can tolerate a reduced abundance of Pa ESP protein.

Therefore, Pa ESP could facilitate stabilization of microtubules which define the elongation axis. Pa ESP may not function directly in microtubule regulation, but instead may regulate cell wall functions that affect microtubule orientation and dynamics. We assume that Pa ESP function in the regulation of microtubules or cell wall could be noncell-autonomous, involving mobile signals produced in meristematic cells. Furthermore, we cannot exclude the possibility that morphological defects observed in Pa *ESP*-RNAi lines directly impact the flux of mobile signals such as auxin. This function of Pa ESP is consistent with our findings that elongating cells with undetectable Pa ESP (e.g. tube cells) are affected when Pa ESP is depleted in proximal meristematic cells (e.g. embryonal mass cells).

### Pa ESP is required for elongation of the suspensor

Norway spruce embryos at the early embryogeny stage undergo polarization and forms two domains with distinct developmental fates: proliferating embryonal mass and terminally differentiated suspensor, including the uppermost layer of tube cells (Fig. 2a; Bozhkov *et al.*, 2005). Pa ESP protein could be detected using antibody only in the embryonal masses, while the degree of protein accumulation in the elongating embryo-suspensors, tube cells and seedlings was below detection limits. In accordance with the western blotting data, qRT-PCR demonstrated significant down-regulation of ESP in all organs or tissues but embryonal mass.

Our reverse genetics experiments suggest that Pa ESP is critically required to sustain cell elongation during embryogeny. Developmental defects induced by Pa ESP deficiency resemble the phenotype of spruce embryos grown in the presence of polar auxin transport inhibitor, 1-N-naphthylphthalamic acid (Larsson *et al.*, 2008). For example, in both cases, the fate of suspensor cells was affected and supernumerary suspensor-like cells could be detected instead of normally elongating cells. It is plausible that, as in *Arabidopsis* root cells (Moschou *et al.*, 2013), inhibition of Pa ESP perturbs auxin signalling and in this way interferes with the cell expansion.

### Conclusion

Here, we were able to dissect two functions of ESP by showing that a gymnosperm homologue could complement the chromosome nondisjunction phenotype of *rsw4*, but not the root-swelling phenotype. This cell division-unrelated function of ESP could be attributed to the regulation of polarized vesicular trafficking. So far, no robust molecular markers of cell polarity have been established for gymnosperms. However, recent advances in gymnosperm genomics and an increasing number of fully sequenced gymnosperm genomes should help to overcome these limitations (Birol *et al.*, 2013; Nystedt *et al.*, 2013; Zimin *et al.*, 2014).

### Acknowledgements

The authors are grateful to Tsuyoshi Nakagawa for sharing published research materials and Alison Ritchie for the assistance in preparation of anti-Pa ESP. This work was supported by grants

from the VR Swedish Research Council (to P.N.M. and P.V.B.), Pehrsson's Fund (to P.V.B.), the Swedish Foundation for Strategic Research (to P.V.B.), the Olle Engkvist Foundation (to P.V.B.), the Knut and Alice Wallenberg Foundation (to P.V.B.), the August T. Larsson Foundation (to A.P.S. and P.V.B.), Hatch Grant WNP00826 (to A.P.S.), and a Spanish Ministry of Science and Innovation grant (AGL2010-15684 to M.F.S.). V.S.-V. was recipient of a FPI fellowship from the Spanish Ministry of Science and Innovation (BES-2008-003592).

## Author contributions

P.N.M., E.I.S., E.A.M., K.F., S.H.R., E.G.-B., A.P.S. and V.S.-V., performed the research; P.N.M., A.P.S., P.V.B., designed the research; P.N.M., A.P.S., P.V.B. wrote the article; M.F.S. and P.J.H. offered materials/analytical methods. All authors approved the final version of the manuscript.

## References

- Aravind L, Koonin EV. 2002. Classification of the caspase-hemoglobinase fold: detection of new families and implications for the origin of the eukaryotic separins. *Proteins* 46: 355–367.
- von Arnold S, Sabala I, Bozhkov P, Dyachok J, Filonova L. 2002. Developmental pathways of somatic embryogenesis. *Plant Cell Tissue and Organ Culture* 69: 233–249.
- Baskin TI. 2001. On the alignment of cellulose microfibrils by cortical microtubules: a review and a model. *Protoplasma* 215: 150–171.
- Baskin TI, Gu Y. 2012. Making parallel lines meet: transferring information from microtubules to extracellular matrix. *Cell Adhesion and Migration* 6: 404–408.
- Bembenek JN, White JG, Zheng YX. 2010. A role for separase in the regulation of RAB-11-positive vesicles at the cleavage furrow and midbody. *Current Biology* 20: 259–264.
- Birol I, Raymond A, Jackman SD, Pleasance S, Coope R, Taylor GA, Saint Yuen MM, Keeling CI, Brand D, Vandervalk BP *et al.* 2013. Assembling the 20 Gb white spruce (*Picea glauca*) genome from whole-genome shotgun sequencing data. *Bioinformatics* 29: 1492–1497.
- Bozhkov PV, Filonova LH, Suarez MF. 2005. Programmed cell death in plant embryogenesis. *Current Topics in Developmental Biology* 67: 135–179.
- Brand L, Horler M, Nuesch E, Vassalli S, Barrell P, Yang W, Jefferson RA, Grossniklaus U, Curtis MD. 2006. A versatile and reliable two-component system for tissue-specific gene induction in *Arabidopsis*. *Plant Physiology* 141: 1194–1204.
- Capron A, Chatfield S, Provart N, Berleth T. 2009. Embryogenesis: pattern formation from a single cell. *Arabidopsis Book* 7: e0126.
- Chestukhin A, Pfeffer C, Milligan S, DeCaprio JA, Pellman D. 2003. Processing, localization, and requirement of human separase for normal anaphase progression. *Proceedings of the National Academy of Sciences, USA* 100: 4574–4579.
- Ciosk R, Zachariae W, Michaelis C, Shevchenko A, Mann M, Nasmyth K. 1998. An ESP1/PDS1 complex regulates loss of sister chromatid cohesion at the metaphase to anaphase transition in yeast. *Cell* 93: 1067–1076.
- Filonova LH, Bozhkov PV, Brukhin VB, Daniel G, Zhivotovsky B, von Arnold S. 2000. Two waves of programmed cell death occur during formation and development of somatic embryos in the gymnosperm, Norway spruce. *Journal of Cell Science* 24: 4399–4411.
- Filonova LH, Suarez MF, Bozhkov PV. 2008. Detection of programmed cell death in plant embryos. *Methods in Molecular Biology* 427: 173–179.
- van der Hoorn RAL. 2008. Plant proteases: from phenotypes to molecular mechanisms. *Annual Review of Plant Biology* 59: 191–223.
- Jensen S, Segal M, Clarke DJ, Reed SI. 2001. A novel role of the budding yeast separin Esp1 in anaphase spindle elongation: evidence that proper spindle association of Esp1 is regulated by Pds1. *Journal of Cell Biology* 152: 27–40.
- Johnson KL, Degnan KA, Walker JR, Ingram GC. 2005. *AtDEK1* is essential for specification of embryonic epidermal cell fate. *Plant Journal* 44: 114–127.
- Kanei M, Horiguchi G, Tsukaya H. 2012. Stable establishment of cotyledon identity during embryogenesis in *Arabidopsis* by *ANGUSTIFOLIA3* and *HANABA TARANU*. *Development* 139: 2436–2446.
- Laemmli UK. 1970. Cleavage of structural proteins during the assembly of the head of bacteriophage T4. *Nature* 227: 680–685.
- Larsson E, Sitbon F, Ljung K, von Arnold S. 2008. Inhibited polar auxin transport results in aberrant embryo development in Norway spruce. *New Phytologist* 177: 356–366.
- Leliaert F, Verbruggen H, Zechman FW. 2011. Into the deep: new discoveries at the base of the green plant phylogeny. *BioEssays* 33: 683–692.
- Lid SE, Olsen L, Nestestog R, Aukerman M, Brown RC, Lemmon B, Mucha M, Opsahl-Sorteberg HG, Olsen OA. 2005. Mutation in the *Arabidopsis thaliana* *DEK1* calpain gene perturbs endosperm and embryo development while over-expression affects organ development globally. *Planta* 221: 339–351.
- Liu Z, Makaroff CA. 2006. *Arabidopsis* separase *AESP* is essential for embryo development and the release of cohesin during meiosis. *Plant Cell* 18: 1213–1225.
- Mayer U, Ruiz RAT, Berleth T, Misera S, Jurgens G. 1991. Mutations affecting body organization in the *Arabidopsis* embryo. *Nature* 353: 402–407.
- Meinke DW. 1991. Perspectives on genetic-analysis of plant embryogenesis. *Plant Cell* 3: 857–866.
- Minina EA, Filonova LH, Fukada K, Savenkov EI, Gogvadze V, Clapham D, Sanchez-Vera V, Suarez MF, Zhivotovsky B, Daniel G *et al.* 2013. Autophagy and metacaspase determine the mode of cell death in plants. *Journal of Cell Biology* 203: 917–927.
- Moschou PN, Bozhkov PV. 2012. Separases: biochemistry and function. *Physiologia Plantarum* 145: 67–76.
- Moschou PN, Smertenko AP, Minina EA, Fukada K, Savenkov EI, Robert S, Hussey PJ, Bozhkov PV. 2013. The caspase-related protease separase (*EXTRA SPINDLE POLES*) regulates cell polarity and cytokinesis in *Arabidopsis*. *Plant Cell* 25: 2171–2186.
- Nakagawa T, Kurose T, Hino T, Tanaka K, Kawamukai M, Niwa Y, Toyooka K, Matsuoka K, Jinbo T, Kimura T. 2007. Development of series of gateway binary vectors, pGWBs, for realizing efficient construction of fusion genes for plant transformation. *Journal of Biosciences and Bioengineering* 104: 34–41.
- Nystedt B, Street NR, Wetterbom A, Zuccolo A, Lin YC, Scofield DG, Vezzi F, Delhomme N, Giacomello S, Alexeyenko A *et al.* 2013. The Norway spruce genome sequence and conifer genome evolution. *Nature* 497: 579–584.
- Pennell RI, Janniche L, Scofield GN, Booj H, Devries SC, Roberts K. 1992. Identification of a transitional cell state in the developmental pathway to carrot somatic embryogenesis. *Journal of Cell Biology* 119: 1371–1380.
- Saitou N, Nei M. 1987. The neighbor-joining method – a new method for reconstructing phylogenetic trees. *Molecular Biology and Evolution* 4: 406–425.
- Singh HE. 1978. *Embryology of gymnosperms*. *Handbuch der Pflanzenanatomie*. Berlin, Germany: Gebruder Borntraeger.
- Smertenko A, Bozhkov PV. 2014. Somatic embryogenesis: life and death processes during apical–basal patterning. *Journal of Experimental Botany* 65: 1343–1360.
- Smertenko AP, Bozhkov PV, Filonova LH, von Arnold S, Hussey PJ. 2003. Re-organisation of the cytoskeleton during developmental programmed cell death in *Picea abies* embryos. *Plant Journal* 33: 813–824.
- Smertenko AP, Hussey PJ. 2008. Immunolocalization of proteins in somatic embryos – applications for studies on the cytoskeleton. *Methods in Molecular Biology* 427: 157–171.
- Suarez MF, Filonova LH, Smertenko A, Savenkov EI, Clapham DH, von Arnold S, Zhivotovsky B, Bozhkov PV. 2004. Metacaspase-dependent programmed cell death is essential for plant embryogenesis. *Current Biology* 14: R339–R340.
- Sun YX, Kucej M, Fan HY, Yu H, Sun QY, Zou H. 2009. Separase is recruited to mitotic chromosomes to dissolve sister chromatid cohesion in a DNA-dependent manner. *Cell* 137: 123–132.
- Tanaka H, Onouchi H, Kondo M, Hara-Nishimura I, Nishimura M, Machida C, Machida Y. 2001. A subtilisin-like serine protease is required for epidermal

- surface formation in *Arabidopsis* embryos and juvenile plants. *Development* 128: 4681–4689.
- Ueda M, Laux T. 2012. The origin of the plant body axis. *Current Opinion in Plant Biology* 15: 578–584.
- Wasteneys GO. 2004. Progress in understanding the role of microtubules in plant cells. *Current Opinion in Plant Biology* 7: 651–660.
- Wendrich JR, Weijers D. 2013. The *Arabidopsis* embryo as a miniature morphogenesis model. *New Phytologist* 199: 14–25.
- Wu S, Scheible WR, Schindelasch D, Van Den Daele H, De Veylder L, Baskin TI. 2010. A conditional mutation in *Arabidopsis thaliana* separase induces chromosome non-disjunction, aberrant morphogenesis and cyclin B1;1 stability. *Development* 137: 953–961.
- Yang XH, Boateng KA, Yuan L, Wu S, Baskin TI, Makaroff CA. 2011. The *Radially Swollen 4* separase mutation of *Arabidopsis thaliana* blocks chromosome disjunction and disrupts the radial microtubule system in meiocytes. *PLoS One* 6: e19459.
- Zhu T, Moschou PN, Alvarez JM, Sohlberg JJ, von Arnold S. 2014. *Wuschel-related homeobox 8/9* is important for proper embryo patterning in the gymnosperm Norway spruce. *Journal of Experimental Botany* 65: 6543–6552.
- Zimin A, Stevens KA, Crepeau M, Holtz-Morris A, Koriabine M, Marçais G, Puiu D, Roberts M, Wegrzyn JL, de Jong PJ *et al.* 2014. Sequencing and assembly of the 22-Gb loblolly pine genome. *Genetics* 196: 875–890.

## Supporting Information

Additional Supporting Information may be found online in the Supporting Information tab for this article:

**Fig. S1** Relative expression levels of Pa *ESP* in WT, Pa *ESP*-RNAi or Pa *ESPXVE*> RNAi lines.

**Fig. S2** Intracellular localization of Pa *ESP* in interphase embryonal mass cells and differentiated tube cells.

**Fig. S3** Width, length and number of tube and suspensor cells and potency for embryo formation, as affected by Pa *ESP* deficiency.

**Fig. S4** Staining of the embryonal mass with fluorescein diacetate and suspensor cells with Evans blue and Sytox orange of Pa *ESP*-RNAi and relative expression levels of Pa *CYCBL1* and Pa *RBRL* in WT and Pa *ESP*-RNAi.

**Fig. S5** Evans blue staining of suspensor cells in the WT and Pa *ESP*-RNAi.

**Fig. S6** Pa *ESP* does not complement the *rsw4* root-swelling phenotype.

**Fig. S7** Effect of inducible Pa *ESP* knockdown on the morphology of cotyledonary embryos.

**Fig. S8** Width and length of embryos hypocotyl cells, as affected by Pa *ESP* deficiency.

**Table S1** List of primers

**Methods S1** Western blot analysis of Pa *ESP* protein.

**Methods S2** Fluorescein diacetate staining of embryonal mass.

**Notes S1** Alignment of *ESP* proteins.

**Notes S2** Accession numbers.

Please note: Wiley Blackwell are not responsible for the content or functionality of any supporting information supplied by the authors. Any queries (other than missing material) should be directed to the *New Phytologist* Central Office.



## About New Phytologist

- *New Phytologist* is an electronic (online-only) journal owned by the New Phytologist Trust, a **not-for-profit organization** dedicated to the promotion of plant science, facilitating projects from symposia to free access for our Tansley reviews.
- Regular papers, Letters, Research reviews, Rapid reports and both Modelling/Theory and Methods papers are encouraged. We are committed to rapid processing, from online submission through to publication 'as ready' via *Early View* – our average time to decision is <28 days. There are **no page or colour charges** and a PDF version will be provided for each article.
- The journal is available online at Wiley Online Library. Visit [www.newphytologist.com](http://www.newphytologist.com) to search the articles and register for table of contents email alerts.
- If you have any questions, do get in touch with Central Office ([np-centraloffice@lancaster.ac.uk](mailto:np-centraloffice@lancaster.ac.uk)) or, if it is more convenient, our USA Office ([np-usaoffice@lancaster.ac.uk](mailto:np-usaoffice@lancaster.ac.uk))
- For submission instructions, subscription and all the latest information visit [www.newphytologist.com](http://www.newphytologist.com)